UNIVERSITY OF CAMBRIDGE

The Biogenesis of Terrestrial and Marine Polycyclic Ethers

Andrew Robert Gallimore

St. John's College, Cambridge

Submitted in partial fulfilment of the requirements for the degree of Doctor of Philosophy at the University of Cambridge

July 2006

Preface

This dissertation describes the results of experiments carried out in the Department of Chemistry, University of Cambridge, between October 2002 and January 2006. It is entirely the result of my own work and includes nothing that is the outcome of collaboration, except where specifically indicated in the text. This dissertation has not been submitted, in whole or in part, for any other degree, diploma or qualification at this or any other institution. It does not exceed 60,000 words.

Andrew Robert Gallimore
St. John's College, Cambridge

July 2006

FOR MUM AND DAD

XXX

Acknowledgements

First and foremost, I would like to thank my supervisor, Dr. Joe Spencer, for his advice and support throughout my research, as well as for allowing me to direct my PhD in the way that has satisfied me to the fullest. His non-dictatorial and flexible approach to my research, as well as his humility in consideration of my thoughts, ideas and opinions, has permitted me to produce a thesis that I can be proud of. I am also thankful for the occasional beer (or two).

I would also like to thank Prof. Peter Leadlay, my official university PhD mentor and unofficial co-supervisor, for many helpful, and occasionally heated, discussions regarding my work and opinions, as well as allowing me to use and abuse his labs without restriction. Further, his somewhat eclectic vocabulary has exposed me to words and idioms I didn't know existed, many of which I am still unsure do.

The legendary Prof. Emeritus Jim Staunton has followed my work continuously, with great interest and enthusiasm, and has humbly expressed his privilege in being allowed to do so. However, I'd like to suggest to Jim that the privilege is rightly mine. Respect.

My primary colleague and fellow PhD student in the monensin project, Barbara Harvey, has been invaluable in her guidance through her molecular biology expertise, and for this I am most grateful.

Regarding the technical staff of the chemistry department, Duncan Howe has been priceless in taking the time to carry out the NMR analyses of my, often, almost invisible samples. Paul Skelton, of the mass spectrometry facility, has cheerfully spent several afternoons kicking the **** out of my poor molecules, in an attempt to force them to fall apart. It is only through his tenacity that they eventually acquiesced.

It is only fair that I thank *all* members of the Spencer-Leadlay group for help and advice, and for putting up with me for over three years (thus far!).

Finally, I must be grateful to the EPSRC for funding my PhD here at Cambridge. I can only hope that they don't live to regret it.

Abbreviations used in the Text

FAS	Fatty Acid Synthase
PKS	Polyketide Synthase
AT	Acyltransferase
KS	Ketosynthase
ACP	Acyl Carrier Protein
KR	Ketoreductase
DH	Dehydratase
ER	Enoylreductase
DEBS	Deoxyerythronolide B Synthase
HPLC	High-performance Liquid Chromatography
LCMS	Liquid Chromatography [coupled with] Mass Spectrometry
FAB	Fast-Atom Bombardment
NMR	Nuclear Magnetic Resonance
NOE	Nuclear Overhauser Effect
NOESY	NOE Spectroscopy
COSY	Correlation Spectroscopy
HSQC	Heteronuclear Single Quantum Correlation
HMQC	Heteronuclear Multiple Quantum Correlation
3D-PFG	3D-Pulsed-Field Gradient
BTX (PbTx)	Brevetoxin (*Ptychodiscus brevis* toxin)
CTX	Ciguatoxin
YTX	Yessotoxin
MTX	Maitotoxin
VSSC	Voltage-Sensitive Sodium Channel

Summary

Polycyclic ethers, or polyethers, represent a major family of polyketide natural products. Terrestrial polyethers generally act as ionophoric antibiotics, disrupting ionic gradients across bacterial cell membranes. The widely accepted hypothetical model for their biosynthesis involves a polyene intermediate that undergoes an oxidative cyclisation via the corresponding polyepoxide. Recently, a triene shunt metabolite from monensin-producing *Streptomyces cinnamonensis* lent great support to this model. Sequencing of the gene cluster also supported this model. However, the role of two novel genes, *monBI* and *monBII*, was unclear. Deletion of these genes resulted in the production of a number of apparent monensin analogues, whilst abolishing monensin production itself. By isolating and characterising novel epimers of monensin, from one of these mutants, a role of the monB genes in the cyclisation of the final monensin intermediate is proposed. Acid-catalysed cyclisation of surmised cyclisation intermediates from this mutant serves to confirm this proposal. An approach to trapping a triepoxide intermediate analogue that is unable to spontaneously cyclise is then explored. The preliminary results suggest that such an approach might lead to the isolation and characterisation of such a triepoxide.

The closest marine relatives of the terrestrial polyethers are the ladder polyethers, such as brevetoxin and ciguatoxin. Analogous to the polyepoxide biosynthetic model proposed for monensin, a similar model has been proposed for the marine structures. By extrapolating the polyepoxide model to all known marine ladder polyethers, a simple biosynthetic model is proposed, based on the development and justification of the "*stereochemical uniformity rule*". Interestingly, application of this model and rule to the largest known ladder polyether, maitotoxin, reveals a stereochemical discrepancy at one of the ring junctions. It is thus suggested that this new rule may have uncovered an error in the established structure of this molecule, as well as being a potentially useful rule in the assignment of new ladder polyether ladder structures.

Contents

The Biogenesis of Terrestrial and Marine Polycyclic Ethers

Chapter One

General introduction to polycyclic ethers and their biosynthetic origin.

Maitotoxin[1] (Fig.1.1) is the largest known non-polymeric natural product that has been characterised thus far. It also belongs to the extensive family of natural structures known as the polycyclic ethers (or more often simply "polyethers"). These universally bioactive molecules are produced by both terrestrial and marine microorganisms and, although those of the former class are characteristically distinct from those of the latter, they share the common structural feature by which they are known, namely, all contain a number of ether rings ranging from the 5-membered to the 9-membered. The most fundamental feature of both the terrestrial and the marine polyethers is their biosynthetic origin, that is, all of these molecules are derived from the polyketide biosynthetic pathway. The family of polyketide natural products is immeasurably vast, displaying remarkable structural diversity and biological activity. Despite this, the polyketide biosynthetic pathway is, at its most basic level, both a straightforward and logical one – almost deceptively so. The pathway may be considered, at a conceptual level at least, as a natural deviation from the fatty acid biosynthetic pathway. Indeed, it is this deviation from, or corruption of, fatty acid biosynthesis that affords the polyketide pathway its diverse natural products.

Fatty Acid Biosynthesis.

A brief, but essential, discussion of the biosynthetic pathway to the saturated fatty acids will suffice before the polyketide pathway naturally follows. The processes of fatty acid biosynthesis are very well established and are known to be catalysed by the, appropriately named, fatty acid synthase (FAS)[2]. In animals, this enzyme is a single multifunctional protein that carries all the necessary catalytic activities for fatty acid biosynthesis (Type I). In contrast, plants and bacteria utilise an assembly of discrete and separable proteins, each with a single catalytic role (Type II). In either context, the mechanism of fatty acid construction is the same (Figure 1.2).

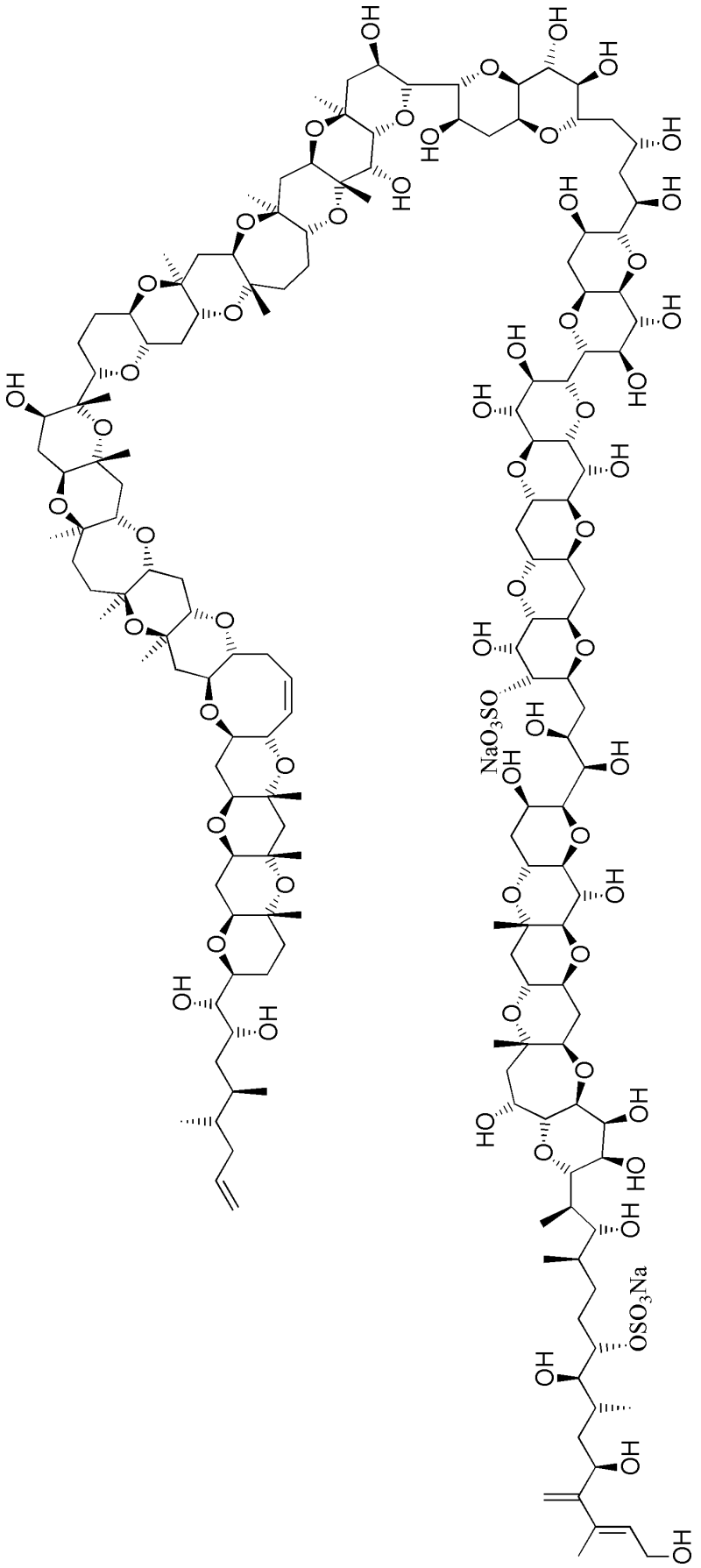

Figure 1.1 Maitotoxin.

Construction of the fatty acid chain is initiated by the condensation of an acetate 'starter unit' with a malonate 'extender unit'. Acetyl-CoA and malonyl-CoA are first converted into enzyme-bound thioesters. The acetyl-CoA starter unit is loaded onto a specific cysteine residue on the β-ketoacyl synthase (KS). Similarly, the malonyl-CoA extender unit, catalysed by malonyl acetyl transferase, is loaded onto a thiol of the acyl carrier protein (ACP). However, in this case, the thiol is not part of the primary protein chain, but is the terminus of a phosphopantetheine chain added in a post-translational modification step. This chain acts as a 'swinging arm' and has the role of delivering the growing chain to the relevant catalytic activities necessary for chain extension. The fundamental chain extension step is catalysed by the ketosynthase and is a Claisen-like condensation facilitated by decarboxylation of the malonyl-ACP. This gives the acetoacetyl-ACP. Subsequently, the ketoester is reduced by a ketoreductase (KR), dehydrated by a dehydratase (DH) and, finally, reduced further by an enoyl reductase (ER) (see Figure 1.3). This completes the first round of chain extension, after which the chain is transferred from the ACP onto the ketosynthase (translocation), freeing up the ACP for the loading of the next extender unit (Figure 1.3). The extension process is repeated, two carbon units at a time, until the specific chain length is obtained. At this point, the enzyme-bound thioester is off-loaded from the FAS, by means of a thioesterase, to give the free fatty acid (see Figure 1.4). The length of this chain may be determined by the specificity of the thioesterase.

Polyketide Biosynthesis.

The polyketides are constructed on large enzymes very similar to the fatty acid synthase, namely polyketide synthases (PKS)[3]. Indeed, the cycle of chain extension is directly analogous. However, the crucial difference lies in the fact that the ketoester may be left unprocessed, by an absent or inactive ketoreductase, or reduced to varying degrees by the absence or presence of the subsequent catalytic steps. Thus, each extension cycle may afford either a keto-, hydroxyl, enoyl functionality or the fully saturated C_2-extension product. This is the basis for the variety of polyketide chain structures generated by this pathway. Further structural diversity may be obtained by the utilisation of alternative starter units[4],[5] or extender units, other than malonate, in each cycle of chain extension (e.g. methylmalonate). Further structural and functional modifications of this chain, whether these occur whilst the chain is still attached to the

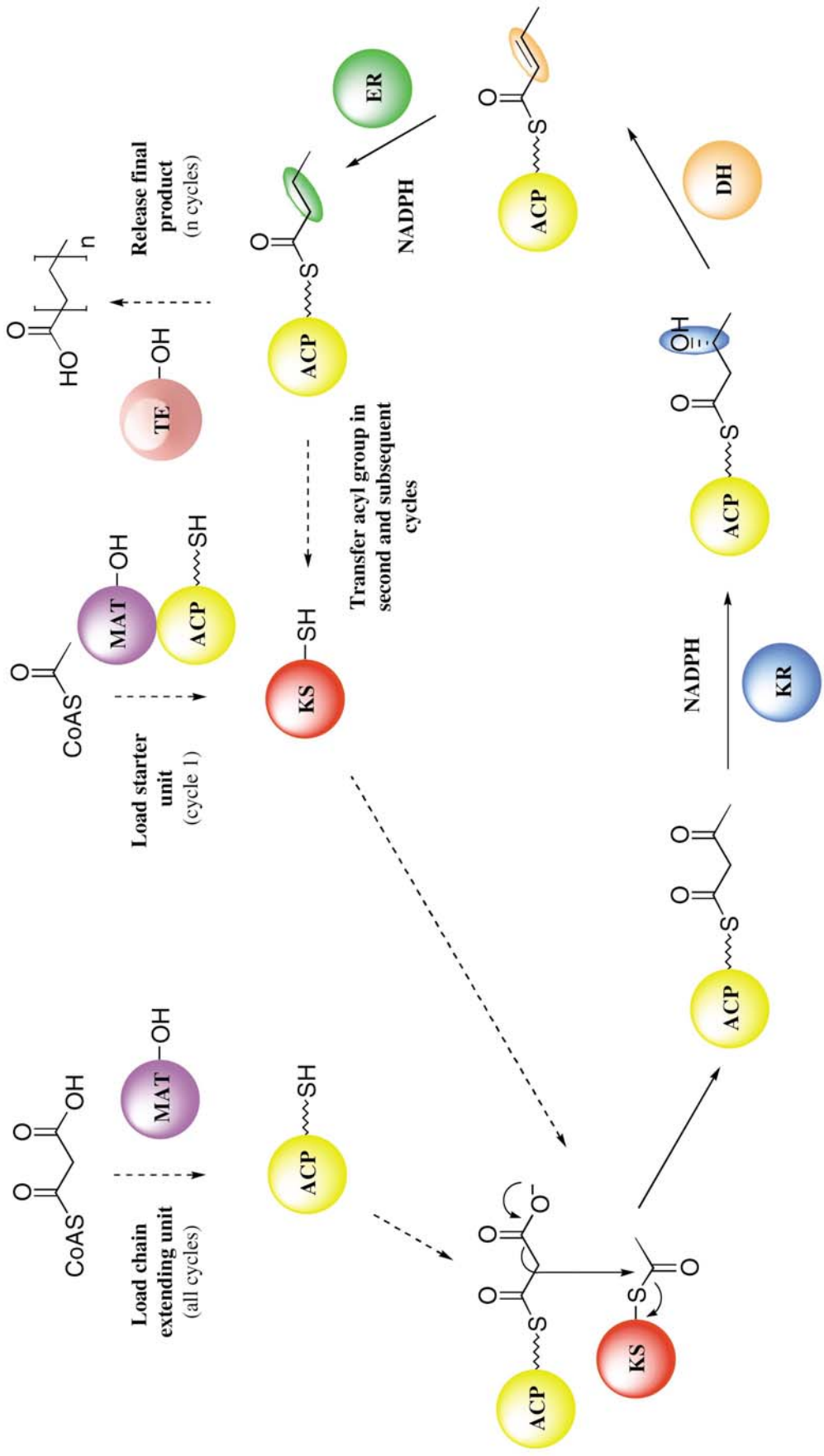

Figure 1.2 Cycle of fatty acid biosynthesis

PKS or has been off-loaded, or even if occurring during chain extension (the timing is *very* often unclear), afford the final natural product – the polyketide.

The Type I modular polyketide synthases are large multifunctional enzymes organised into discrete modules. Each module contains the necessary catalytic activities for a single round of chain extension (the '*minimal PKS*', consisting of ketosynthase, acyltransferase and acyl carrier protein), together with varying capacity for reductive activity (the '*reductive loop*', consisting of ketoreductase, dehydratase and enoyl reductase, as appropriate). Members of the actinomycetes genera are responsible for the production of the terrestrial polyethers and utilise the Type I PKS system.

The most comprehensively understood of the Type I PKS systems is that responsible for the production of the macrolide antibiotic, erythromycin, produced by *Saccharopolyspora erythraea.* Indeed, the gene cluster encoding this enzyme was the first to be sequenced and represents the single most important breakthrough in polyketide biosynthesis research to date[6]. The PKS itself assembles the backbone precursor of erythromycin, deoxyerythronolide B macrolactone (Figure 1.4). Post PKS modifications then afford the antibiotic. The deoxyerythronolide synthase (DEBS) consists of a single loading module, six chain extension modules and a thioesterase catalysing off-loading from the enzyme. Offloading occurs by ring closure of the macrolactone to form deoxyerythronolide B. The DEBS synthase is not actually a single protein, but consists of three large proteins (DEBS 1, 2 and 3) that interact to form the fully functioning system. The DEBS paradigm has shaped the foundation for all subsequent studies of Type I polyketide synthases and indeed the polyketide products themselves. Such is the logical, systematic methodology employed by these PKS systems (often dubbed 'production-lines') that it is usually quite straightforward to predict, by visual inspection alone, the structure of the backbone polyketide chains they construct. As with the DEBS system, the deoxyerythronolide B product constitutes the complete macrolide nucleus of erythromycin, and only awaits minor post-PKS modifications to yield the complete antibiotic. In many cases, however, modifications of the PKS-derived polyketide chain are more numerous and complex. This may render the final structure profoundly transformed from its parent polyketide chain. Polyethers represent such an example, whereby the polycyclic structures do not immediately suggest an obvious route along the polyketide biosynthetic pathway.

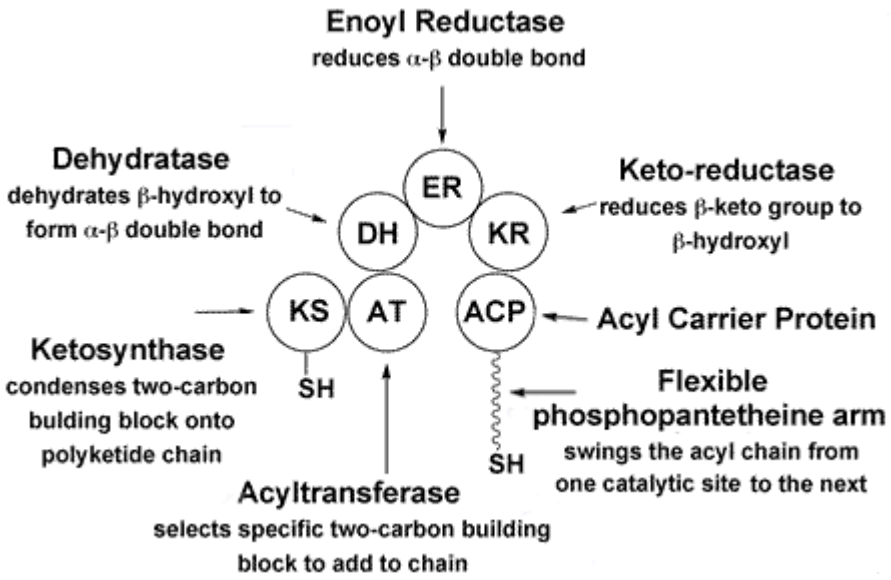

Figure 1.3 Enzymes of the FAS/PKS. (J. Staunton, *used with permission*)

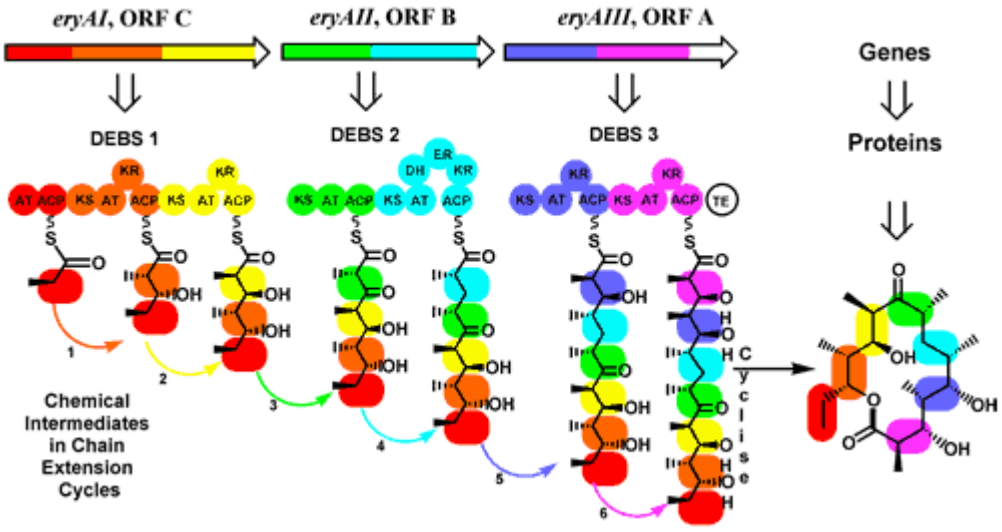

Figure 1.4 Structure of the erythromycin PKS, showing construction of the deoxyerythronolide B macrolide precursor. (J. Staunton, *used with permission*)

Chapter Two

Introduction to Terrestrial Polyethers and their Biosynthesis.

Without exception, all known terrestrial polycyclic ethers are produced by actinomycetes. In particular, the vast majority are derived from the genus *Streptomyces*, and, so far, over 120 such polyethers have been isolated and characterised[7]. The polyethers that will be the focus of this discussion, the ionophore antibiotics, share both structural characteristics and biological activities in common. From a structural perspective, all contain ether rings that are 5 or 6-membered and saturated. No larger ring sizes have been observed. Rings are either connected as a spiroketal system (2-3 rings , di- or tri-oxaspiro-cycloalkanes), or, otherwise, each ring is always separated by at least one single bond, with fused rings being absent from these structures. This will become significant when considering their biosynthesis, and not least so when considering their marine cousins. In addition to this general architecture, the terrestrial polyethers may contain a range of other structural features and functionalities, including hydroxyl, methoxy, halo, phenyl, and, often unusual, heterocyclic systems, some of which may be important for biological activity. Although not covalently cyclised, most exhibit a carboxyl at one terminus that interacts through hydrogen bonding with one or two hydroxyls at the other (Figure 2.1)[8].

Biological Activity of Carboxylic Polyether Ionophores

All known terrestrial polyethers act as ionophores, which are compounds that form lipid soluble, dynamically reversible, complexes with cations, enabling these to be transported across biological membranes. The results of this are changes in transmembrane ion gradients and electrical potentials, causing a variety of effects on cellular function.

There are two major subclasses of ionophores: (a) neutral ionophores, such as valinomycin, that contain no ionisable groups, and form charged complexes with cations and transport them down their electrochemical gradient (not discussed here); (b) carboxylic ionophores, such as monensin, that form neutral zwitterionic complexes, and promote an electrically neutral exchange of cations across membranes. All of this class are also capable of transporting H^+ as their protonated

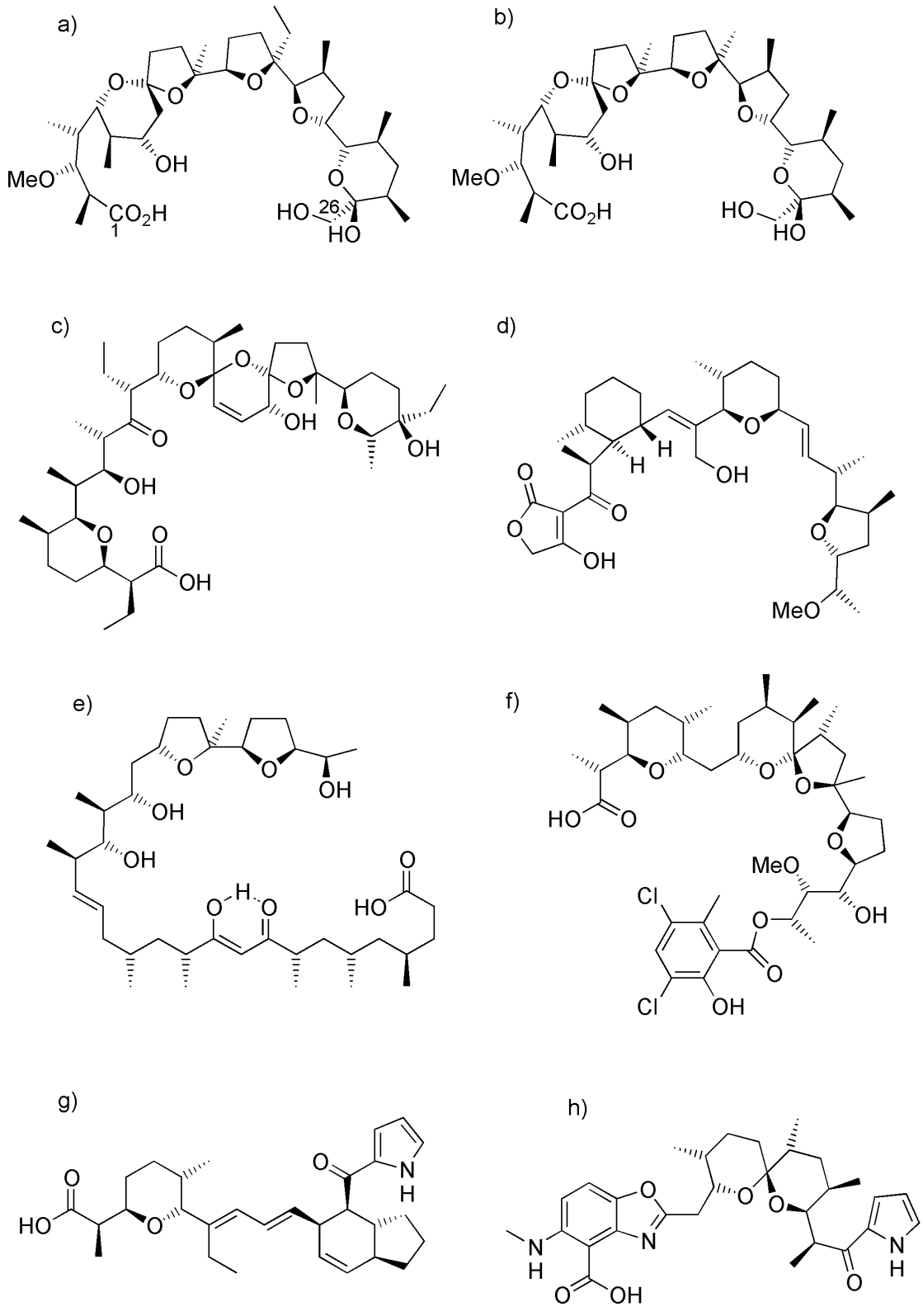

Figure 2.1 Polyether ionophores. a) Monensin A; b) Monensin B; c) Salinomycin; d) Tetronasin; e) Ionomycin; f) CP-54883; g) Cafamycin; h) Calcimycin

carboxylic forms. Biologically, the most important cations transported are Na^+, K^+, Ca^{2+} and Mg^{2+}.

The carboxylic ionophores form complexes by enveloping cations and displacing their solvation shell. This is done by strategically placed oxygens, which may be etheric, hydroxyl, carboxyl or carbonyl, that coordinate to the central cation by means of ionic-dipole interactions as the backbone assumes the critical conformation to surround it. Thus, the cation and the polar interior of the ionophore are shielded, whilst the hydrophobic exterior gives the ionophore its essential lipid solubility. Because of the length and limited flexibility of the polyether backbone, the size of the cavity is well-defined and provides a means of selectivity for particular cations. Monensin, for example, is 10 times selective for sodium over potassium, and forms a cage-like structure tightly around the ion[9] (Figure 2.2).

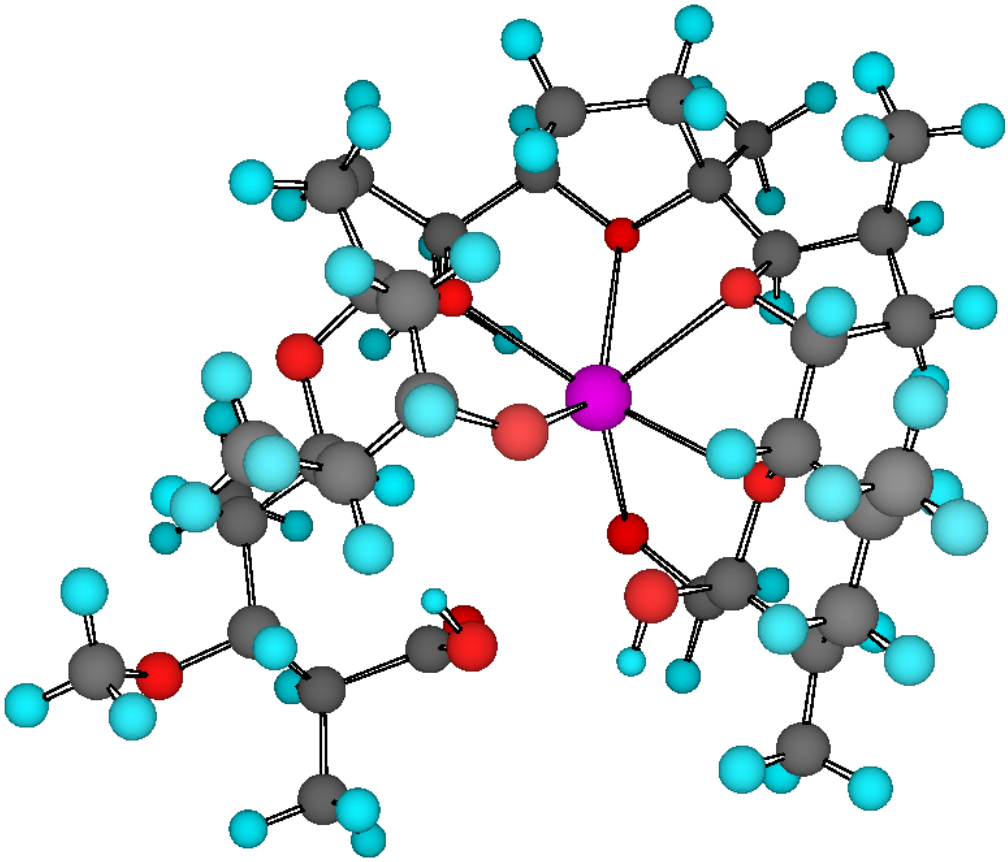

Figure 2.2 Crystal structure of monensin A sodium salt. Na, purple; O, red.

In order for transport to be efficient, the complexation affinity must be carefully balanced, and must be strong enough to favour complexation in the first place and, yet, not so strong as to disfavour the release of the cation once transported across the membrane. In other words, the complexation-decomplexation kinetics must be rapid[10].

The mechanism of transport can be broken down into several steps:

1. The protonated ionophore within a membrane diffuses to one interface, exposing it to the bulk solvent. At this point, the carboxyl is deprotonated and the molecule becomes trapped at this position, with the hydrophobic backbone buried in the membrane, whilst the polar and charged surface faces the bulk solvent.
2. As a complexable cation approaches, the oxygen ligands of the ionophores concertedly coordinate the cation and displace its water of solvation. The now neutral complex may diffuse back into the membrane, transporting the cation across to the opposite interface, where the cation is released, coincident with its resolvation.
3. The charged ionophore is now trapped at the opposite interface, where it may be protonated and diffuse back into the membrane for another cycle of cation-proton exchange, or complex another cation. The balance between proton and cation transport will thus be dependent both on the pH of the bulk solvent and the cation concentration.

The antibiotic activity of the ionophores lies in their inherent ability to disrupt the carefully controlled, energetically demanding, balance of ions across bacterial membranes. Generally, cells maintain a higher intracellular concentration of potassium than extracellular, and expel sodium and protons. Dissipation of these gradients by ionophores has two major effects: Firstly, the cell will attempt to counter the ion flux by activating membrane ATPases and transporters, leading ultimately to complete de-energisation. Ion influx, unabated, may then cause a massive increase in osmotic pressure and the water influx may, literally, cause the bacterium to burst[11].

The biological activity of these molecules is not limited to bacteria, but extends to higher animals, including humans. In particular, excitable cells, such as neurons, must maintain precise membrane potentials in order to function. This is achieved

through the control of transmembrane ionic gradients. It is thus clear why polyether ionophores tend to be highly toxic to humans[12] and are generally regarded as being of little therapeutic value. More recently, however, this attitude is changing, as monensin, for example, has been found to inhibit the growth of certain tumour cell-lines[13] and potentiate the effects of anticancer agents[14].

The Biosynthesis of Monensin

The polyether ionophore that has been most extensively studied is the aforementioned monensin, and it is thus appropriate that the majority of the research reported and discussed surrounding terrestrial polyether biosynthesis will be centred around this particular ionophore. There are, in fact, two natural monensins, both produced by the same actinomycetes, *Streptomyces cinnamonensis*. Monensin A and monensin B differ only, however, in the presence of an ethyl group in monensin A that is represented by a methyl group in monensin B (see Figure 2.1).

Monensin A was first isolated and characterised in 1967 by Agtarap *et al*.[15] Initial hypotheses attempting to explicate its biosynthesis can be traced back over thirty years. Classical feeding studies firmly established the polyketide nature of the ionophore; feeding of C^{14}-labelled precursors demonstrated that the monensin backbone was constructed from five acetate, seven propionate units and a single butyrate unit.[16] Utilising deuterium-labelled propionate, Robinson *et al* demonstrated that propionyl-CoA is converted *in vivo* to methylmalonyl-CoA with a specific stereochemistry at the pendant methyl group. Subsequent decarboxylation and condensation, with inversion of configuration, thus establishes the requisite stereochemistry of these methyl groups in the final monensin structure[17]. Further studies, utilising $^{18}O_2$, revealed that three of the ether ring oxygens and the terminal C26-hydroxyl were derived from molecular oxygen (Figure 2.3)[18]. However, prior to this, back in 1974, Westley proposed the formation of the terminal ether ring of a related ionophore, lasalocid, as resulting from the opening of an alkene-derived epoxide intermediate.[19] This idea was specifically applied to the monensin structure in 1983 by Cane, Celmer and Westley (Figure 2.4).[20] This model, however, involved three epoxide-derived ether rings. Also, two of the ether rings are joined as a spiroketal, and it was proposed that these might initially be derived from a carbonyl.

Both the feeding studies and this purely hypothetical model were without conflict. Encouraged to some extent by these feeding studies, this model was both a rational and an attractive one. Indeed, this simple model has remained the foremost right up to the present, although variations on the theme have been proposed, as will be discussed. An important feature of the Cane-Celmer-Westley (CCW) model is the requisite stereochemistry of the three double-bonds, which must all have the *trans* configuration. Two alternative models have been proposed, both of which involve a triepoxide intermediate. However, each requires a different set of double-bond configurations.

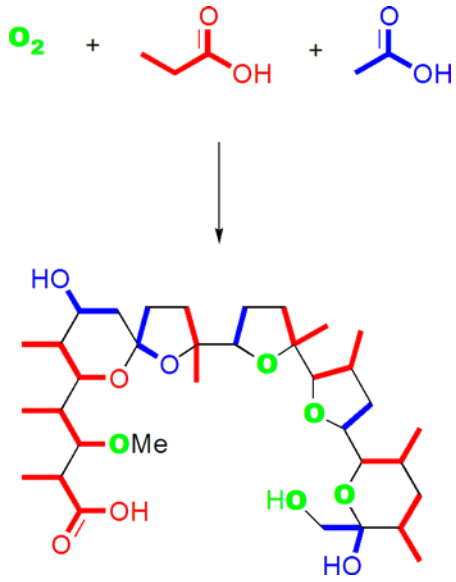

Figure 2.3 Biosynthetic origin of carbon and oxygen units of monensin.

The first model to be proposed that was distinct from the CCW model was the Townsend-Basak model. This model invoked a series of [2+2] oxidative cyclisations utilising iron and necessitates a Z,Z,Z-triene.[21] The only model to follow was that proposed by Staunton and Leadlay (Figure 2.4), and although similar in principle to the CCW model, was a modified version that addressed possible concerns over the mechanistic aspects of the CCW model. The cyclisation mechanism involves two successive S_N2 inversions at tertiary centres, generally regarded as highly chemically disfavoured. However, this alternative model overcame this concern by invoking S_N1 attack at these centres with retention of stereochemistry. Whereas the CCW mechanism appears to be a cascade initiated by the S_N2 opening of the first epoxide, this alternative mechanism appears to be initiated from the terminal end. In what appears to be a concerted (or almost so) process, the disubstituted epoxide is opened (S_N2 with inversion) by the second trisubstituted epoxide acting as a nucleophile as it itself opens to form the stabilised tertiary carbocation. This process could be assisted by activation of the terminal carbonyl, which may help activate the disubstituted epoxide towards the S_N2 reaction. The resulting carbocation is then quenched, with

retention, by the opening of the first trisubstituted epoxide to yield a second tertiary carbocation, which is finally quenched by the hydroxyl. Overall, distinct from the CCW mechanism, this requires two trisubstituted *cis* epoxides and thus *cis* double-bonds in the precursor – a Z,Z,E-triene. Although the three models all feature a triene intermediate, it is noteworthy that each involves a different set of double-bond configurations. Thus, it is clear that if indeed a triene intermediate precedes monensin, the stereochemistry is decisive in supporting any one of the hypotheses. Hughes-Thomas *et al* have utilised the terminal thioesterase of the DEBS cluster to off-load both tetra- and pentaketide intermediates from the monensin PKS; each containing the third double bond of the hypothetical premonensin triene. The configuration of this double bond was determined as being *trans* and thus the opposite to what would be required for the Townsend-Basak model, whilst still allowing the Staunton-Leadlay model to be feasible[22].

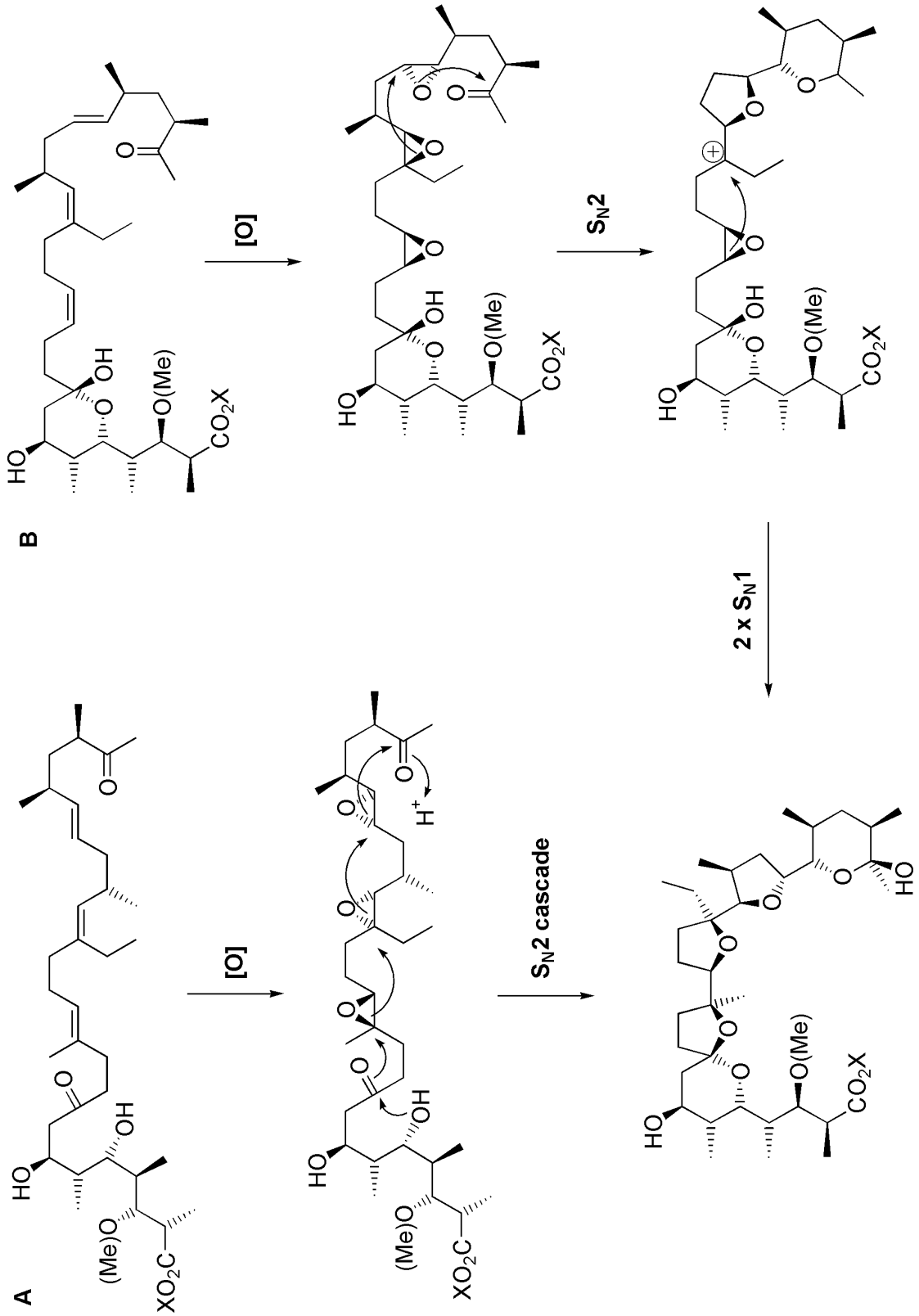

Figure 2.4 Cane-Celmer-Westley (A) and Staunton-Leadlay (B) mechanisms of monensin cyclisation.

The Monensin Biosynthetic Gene Cluster.

The overall organisation of the monensin gene cluster has been established by sequence analysis of cosmid fragments from a monensin-producing strain of *S. cinnamonensis*[23]. Conforming to the DEBS paradigm, the cluster is organised into twelve modules, distributed over eight open-reading frames (labelled *monAI* to *monAVIII*), and each responsible for one cycle of chain extension (Figures 2.5 and 2.6). This would be predicted from the structure of monensin. Two additional ORFs (*monAIX* and *monAX*), the function of which was initially unclear, have recently been shown to encode two discrete 'editing' thioesterases that have the role of offloading erroneous intermediates from the PKS and thus avoid its obstruction[24]. Additional genes, most likely governing methylation of the C3-hydroxyl (*monD*) and hydroxylation of the terminal C26 methyl (*monE*) reactions are also present. The further presence of four *novel* genes, not previously found in any complex polyketide gene cluster aroused the most attention – *monBI, monBII, monCI* and *monCII*. The *monCI* gene product shows considerable sequence homology to authentic non-haem epoxidases (specifically to the squalene epoxidase of *Candida albicans*) and thus it has been inferred that it is this gene that governs the epoxidation of the triene intermediate. The MonCI protein has been cloned, expressed and purified and binds FAD. It has also been shown active in utilising NADH to reduce its flavin co-factor[25]. Preliminary experiments *in vivo* have supported its role as an epoxidase, whereas *in vitro* experiments have, thus far, proved inconclusive[26]. Based on its sequence similarity to known epoxide hydrolases, *monCII* was assigned as such and given the role of managing the cyclisation of the final triepoxide intermediate. MonBI and MonBII, display a low but significant peptide sequence homology to known *ketosteroid isomerase* enzymes from *Commononas testeroni* and *Pseudomonas putida*. MonBI, for example, is 46.3% identical to the isomerase from *Commononas* and 37% to that of *Pseudomonas*. MonBI is, however, only 48% identical to MonBII[27]. The ketosteroid isomerase is one of the most proficient enzymes catalysing the allylic isomerisation of Δ^4-3-ketosteroids to Δ^5-3-ketosteroids (Figure 2.7a)[28]. The protein exists as a homodimer with the two independently-folded monomers packing together by means of extensive hydrophobic and electrostatic interactions. Each monomer contains three α-helices and a β-pleated sheet arranged to form a deep hydrophobic cavity that constitutes the active site. The high resolution crystal structure of the enzyme from *Pseudomonas* has been solved[29]. These studies

confirmed earlier site-directed mutagenesis studies[30], where the active site was found to include Asp38, which acts as a base to abstract the proton from the C4 of the steroid, as well as Tyr14, which acts to stabilise the dienolate intermediate. More recent NMR studies, however, also indicated the involvement of an Asp99 residue adjacent to Tyr14 and also thought to contribute to stabilisation of the intermediate, both through short, strong hydrogen bonds, acting as charge buffers to stabilise the build up of negative charge on the dienolate intermediate[31]. The MonBII protein also contains the Tyr14 and Asp38 active site residues, whereas, in MonBI, the Tyr14 residue is replaced by histidine. It has been suggested, however, that at physiological pH, this may be protonated and thus able to function as a Lewis acid[27]. Formation of an extended enolate in any acyclic α,β-unsaturated carbonyl has the potential of resulting in isomerisation of the double-bond, owing to the potential for free rotation about the α-β bond of the enolate (Figure 2.7b). During the β-oxidation of unsaturated fatty acids, mitochondrial 3,2-*trans*-enoyl-CoA isomerase converts 3-*cis* and 3-*trans*-enoyl-CoA intermediates into their 2-*trans* isomers[32]. If indeed the *monB* genes did encode isomerase enzymes, their presence could be neatly explained by the Leadlay-Staunton cyclisation model. The conjecture was that as each α,β-unsaturated double-bond of the growing polyketide chain is formed, this transiently activated bond could be isomerised, *in trans*, by a MonB enzyme via an extended enolate. More specifically, if each of the trisubstituted double-bonds is isomerised from a *trans* configuration to *cis*, the result is effectively the conversion of an all *trans* (i.e. *E,E,E*) *pre*monensin to a *Z,Z,E* configuration. This is precisely the configuration required by the above model. Further, if each 'isomerase' is responsible for only one double-bond, then the presence of two such enzymes is explained. However, the only precedent involving a discrete enzyme modulating a polyketide chain as it is formed on the PKS (*in trans*), comes from lovastatin biosynthesis; a separate enoyl reductase, LovC, is necessary for the correct processing of the growing chain to form the nonaketide lovastatin precursor, dihydromonacolin L[33].

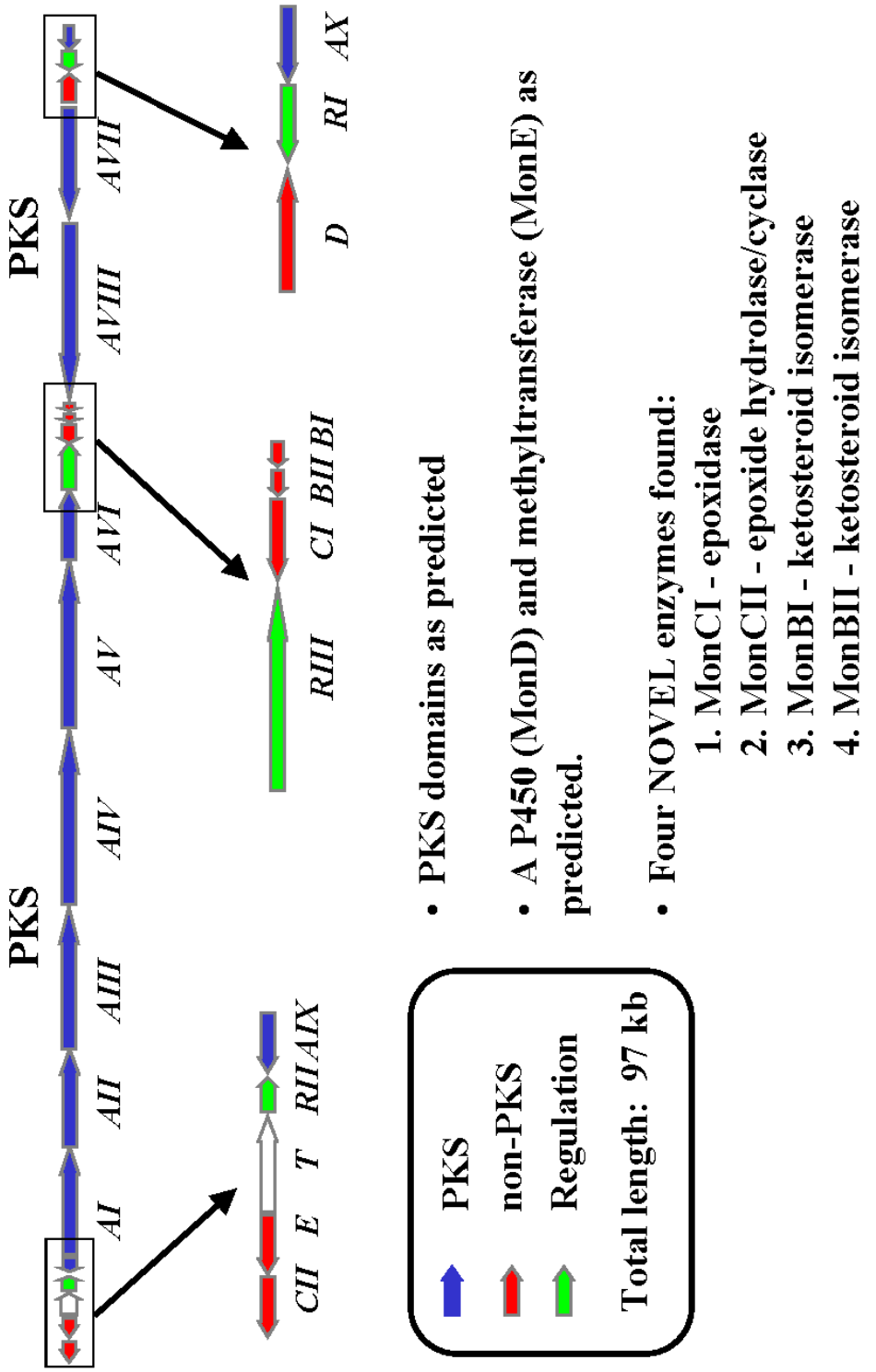

Figure 2.5 Organisation of the monensin biosynthetic gene cluster.

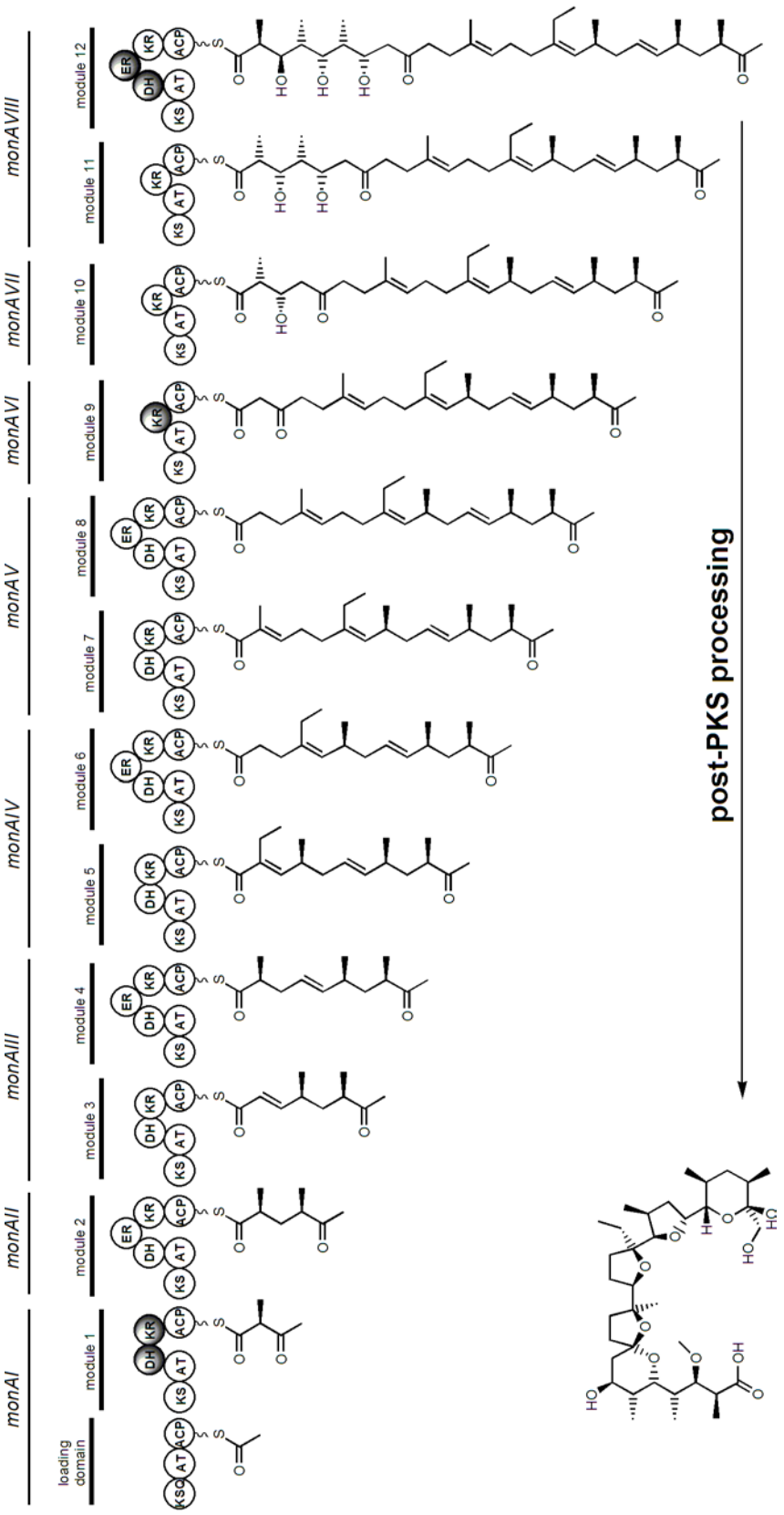

Figure 2.6 Proposed formation of the 'premonensin' polyketide chain on the monensin PKS. Shaded enzymes are inactive.

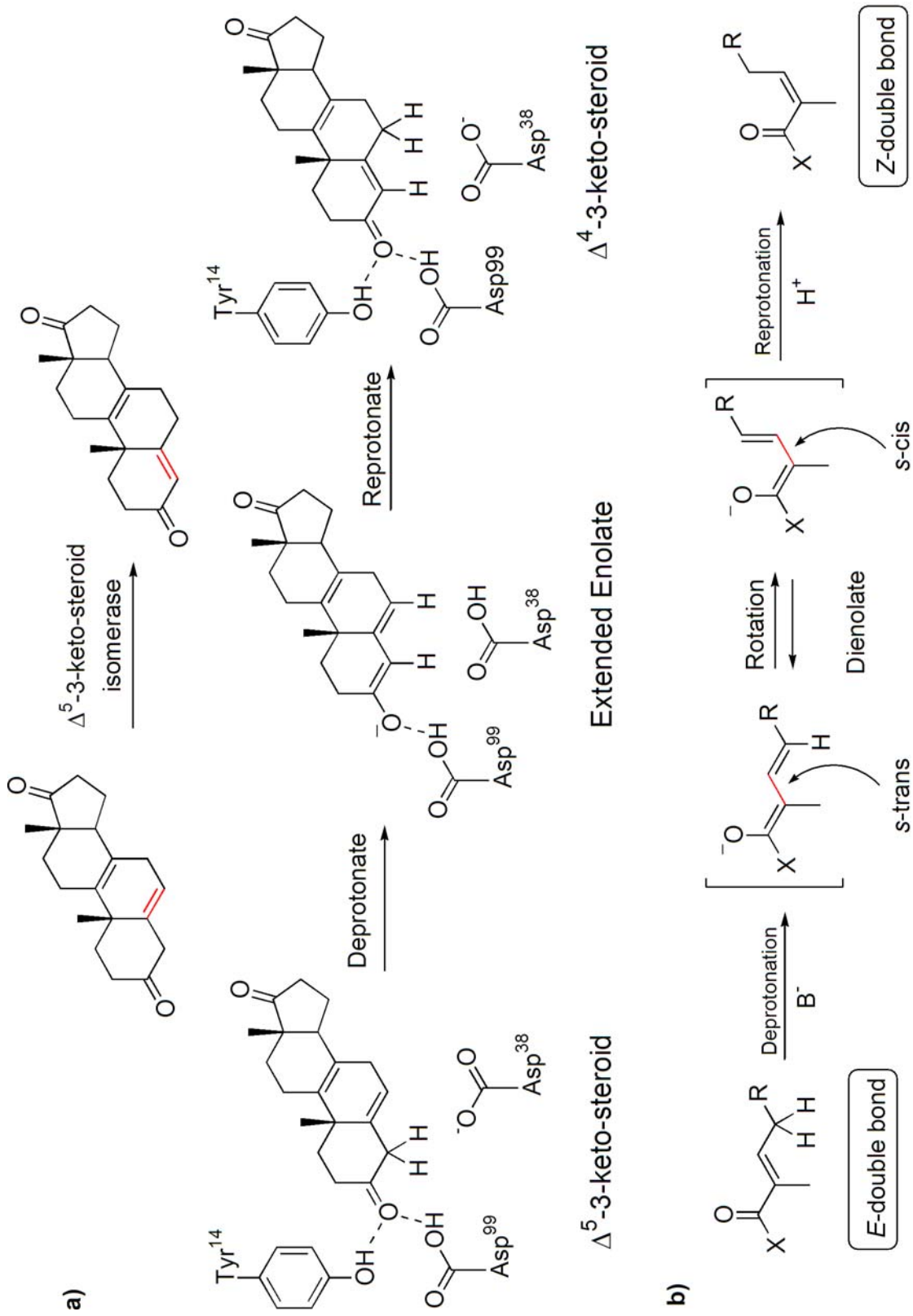

Figure 2.7 a) Mechanism of Δ^4-3-ketosteroid isomerase; b) Proposed mechanism of double-bond isomerisation via extended enolate

All of the four novel enzymes had thus been assigned possible roles in the monensin biosynthetic pathway. This was, however, based almost entirely on sequence homology and informed reasoning, with no experimental evidence, barring the preliminary studies with MonCI. Although *monBI* was cloned and the protein expressed and purified, experiments with model substrates failed to show any isomerase-like activity[27].

At this point, gene-disruption/deletion experiments were seen as the route forward. One particular choice for such an experiment was the *monCI* gene. Its disruption should, in theory, close down the epoxidation of the triene intermediate, possibly leading to its accumulation and isolation. This would prove the role of MonCI in the epoxidation of the triene intermediate, whilst obviously confirming beyond reasonable doubt, the general triene-triepoxide model that had remained, although plausible, only a hypothesis for over twenty years. Also, as noted earlier, the double-bond configuration of the triene intermediate would be decisive when considering the three distinct mechanistic models that have been proposed and discussed. It was thus clear that this could well be an *experiment crucis***.** It should be noted, however, that labelled analogues of this *E,E,E-pre*monensin triene have been synthesised for classical feeding studies, but no incorporation of this hypothetical intermediate into monensin has ever been observed[34].

Disruption of the *monCI* gene did indeed lead to the isolation and characterisation of a triene shunt metabolite, confirming its role as an epoxidase[35]. However, all three of the double bonds were assigned as having *trans* geometry (Figure 2.8). This, of course, made both the Townsend-Basak and the Leadlay-Staunton cyclisation models appear less likely to be correct. Concerning the latter model, the role of the *monB* genes was no longer such a straightforward issue. Further to this, disruption of the *monCI* gene *together* with either or both of the *monB* genes had no effect on the triene produced. Their role as double-bond isomerases was thus beginning to look unlikely, although could not be discounted; it is not totally unreasonable to question whether elimination of the MonCI enzyme could have an effect on the MonB enzymes, since so little is known concerning the exact coordination of events leading to the final monensin product.

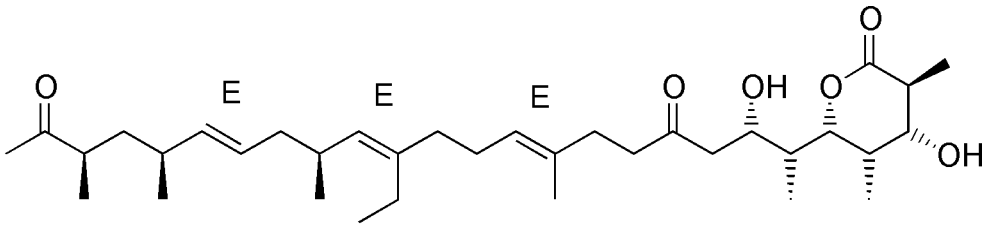

Figure 2.8 Triene shunt-metabolite isolated from *S.cinnamonensis ΔmonCI* mutant.

Chapter Three

Isolation of a Novel Epimer of Monensin A

Following isolation of the triene shunt-metabolite from the *monCI*-disrupted (as well as the *monCI-monBI/monBII*) strain of *S. cinnamonensis*, the most obvious experiment was disruption of the monBI genes alone. Initially, this was carried out by Dr. A. Bhatt of this group[36], by deletion of the genes in-frame. Thus, three mutants were obtained – the single *monBI* and *monBII*-deficient mutants as well as the double mutant (Δ*monBI*, Δ*monBII* and Δ*monBI-BII,* respectively).

These mutants were cultured and extracted with ethyl acetate, as for the wild-type strain. None of these mutants, however, produced either monensin A or monensin B. Thus, it was clear at this initial stage, that the *monB* genes were essential for monensin biosynthesis. However, the most fascinating and, for some time, the most baffling feature of these mutants, was the metabolites that they *did* generate. Firstly, all three mutants displayed the same metabolite profile, which consisted of a number of early-eluting, polar species coincident with the masses of the protonated sodium salts of monensin A ($M+Na^+ = 693.5$), monensin B ($M+Na^+ = 679.5$), C3-O-demethylmonensin A ($M+Na^+ = 679.5$) and C3-O-demethylmonensin B ($M+Na^+ = 665.5$). These metabolites eluted between around 4-12 minutes, and varied in number and elution time from culture to culture. However, the most prominent of these metabolites eluted at ~9 and ~11 minutes, with masses of 665.5 and 679.5, respectively. Notably, these retention times are identical to those of C3-O-demethylmonensin A and B, respectively, which suggested that these might be authentic monensin analogues (Figures 3.1 to 3.4).

In addition to these early eluting species, two other metabolites were striking. These possessed the same mass as monensin A (693.5), but eluted at ~12 minutes and ~16 mins (rarely visible, but see Figure 3.9). As monensin A, itself, elutes under a minute later than the latter species, the extract was spiked with authentic monensin A to confirm it as distinct. These species were named isomonensin A12 and isomonensin A16.

It was clear that to attempt the isolation and characterisation of one or more of these unusual metabolites was the direction in which to move. A major concern in this regard, however, was the unpredictable and erratic manner in which the production of

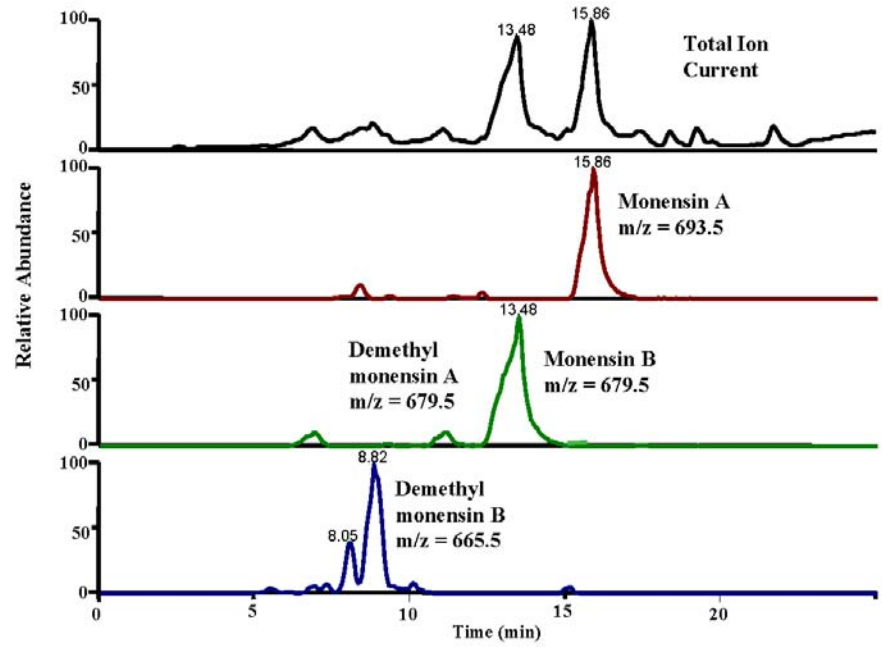

Figure 3.1 LCMS trace of crude extract of *S. cinnamonensis* wild-type

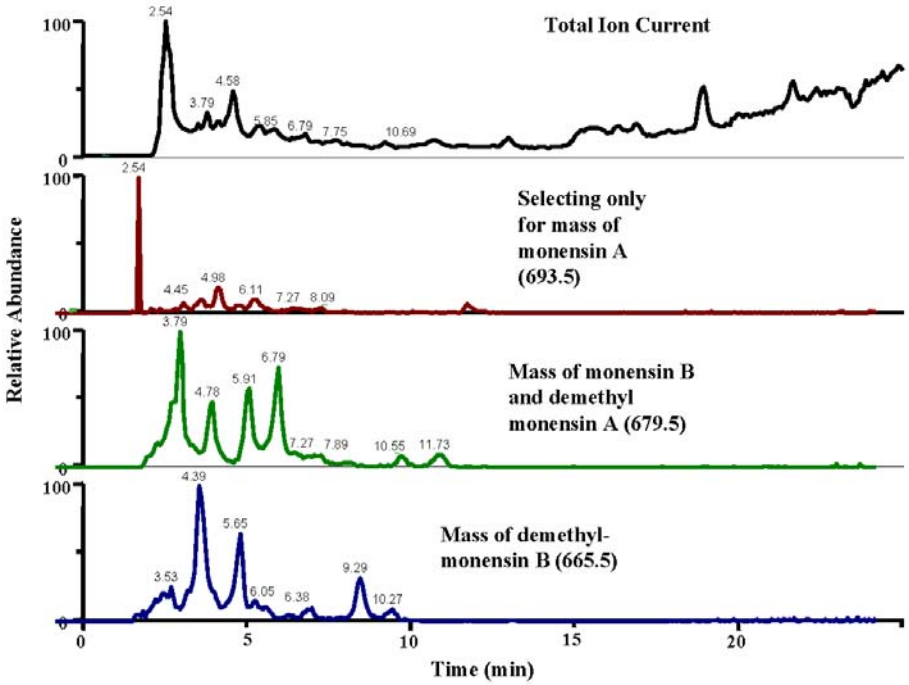

Figure 3.2 LCMS trace of crude extract of *S. cinnamonensis* Δ*monBI*

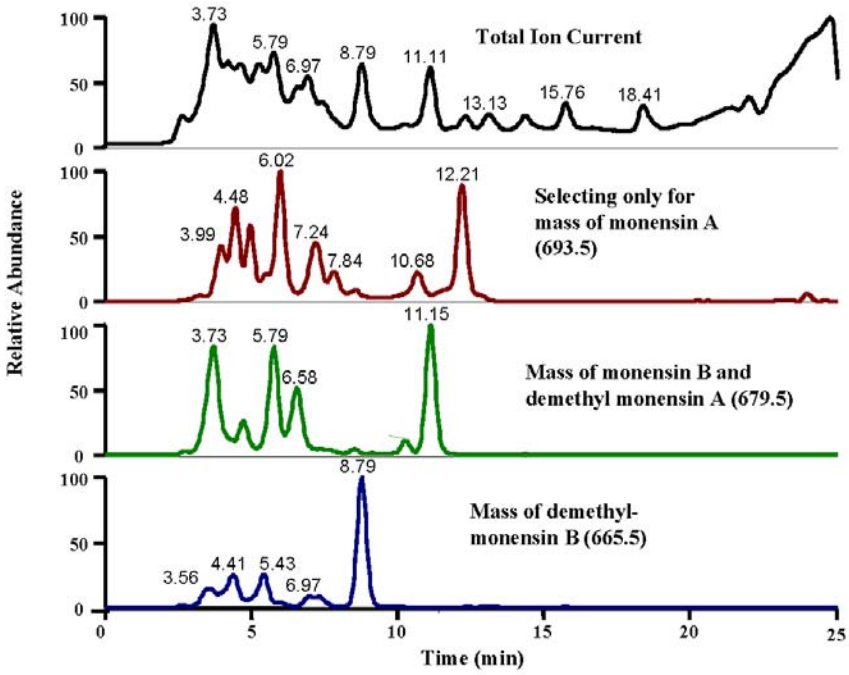

Figure 3.3 LCMS trace of crude extract of S. cinnamonensis Δ*monBII*

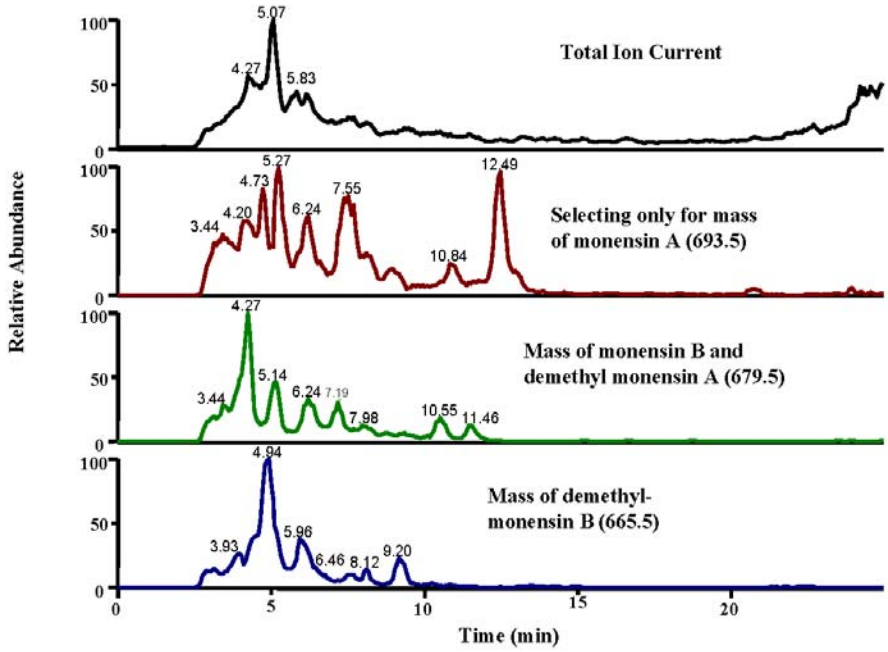

Figure 3.4 LCMS trace of crude extract of *S. cinnamonensis* Δ*monBIBII*

these species varied from culture to culture. The very early eluting metabolites often manifested in a messy cluster, and it was not possible to identify any particular species to target. Also, the production of isomonensins A12 and A16 was similarly unpredictable; their appearance was no more foreseeable than their absence. Further to this, the quantities of these metabolites appeared to be very low. However, it wasn't until the initial isolation of isomonensin A12 that this very low-level production became disappointingly clear. Although the metabolite profiles of all the mutants were identical, the LCMS traces suggested that the ΔBII mutant, for some unknown reason, was more consistent in its production levels. For this reason, the ΔBII mutant was used for the majority of work.

Isolation of Isomonensin A12

Unlike the early-eluting species, isomonensin A12, when it was present in the extracts, eluted in a predictable manner and separate enough from the other metabolites to make it a more attractive target for isolation and characterisation.

Cultures of the ΔBII mutant were scaled up to several litres and the ethyl acetate extracts purified, firstly by silica-column chromatography and finally by preparative HPLC, to yield isomonensin A12 as being very pure by LCMS. Unfortunately, the amount of material was, by weight, immeasurably miniscule and could not be analysed by NMR. Also, subsequent analysis by LCMS indicated that isomonensin A12 was gradually converting to isomonensin A16, suggesting that these were related by some form of chemical lability. One guess as to the nature of this was the terminal hemiacetal, being the only decidedly labile moiety in the monensin structure. However, such conjecture was of no value at this stage.

Mass Spectral Fragmentation Studies of Isomonensins A12 and A16.

Although the amount of material was diminutive, the sensitivity of mass spectrometry made the isomonensins amenable to analysis by this method. The fragmentation of authentic monensins A and B has been thoroughly studied by ESI tandem mass spectrometry[37], so it was thought rational to attempt such analysis of these isomeric species.

Both monensin A and B exhibit identical fragmentation patterns in their MS/MS spectra, and fragment through three distinct pathways. In all three pathways,

fragmentation occurs exclusively at the termini of the polyether structure, with the three central rings, B, C and D, remaining intact. This is also the case with the isomonensins. Figure 3.5B follows the monensin A pathway, with fragmentation initially occurring at the carboxyl terminus. Initial loss of water breaks open the first ring (ring A), and subsequent neutral elimination of mass 174 yields the conjugated diene species 1. Further loss of water, at the other terminus (ring E), yields fragment 2, which then undergoes a pericyclic rearrangement to yield fragment 3.

Whilst the fragmentation of isomonensins A12 and A16 follows this same pathway, a striking feature of the MS/MS spectrum (Figure 3.6), in both, is the occurrence of what appears to be an intermediary fragment (m/z=587) not seen in that of monensin A (Figure 3.5A). This species appears to result from fragmentation at the carboxyl terminus itself. Reference to the fragmentation of C3-O-demethylmonensin A is helpful in explaining this unusual peak.

C3-O-demethylmonensin A was separated directly from a commercial sample of monensin, as it is naturally present in small amounts (~1%)[38], presumably as an intermediate that was not processed by the methyltransferase responsible for methylation at this position. The absence of this methyl group facilitates a straightforward reverse aldol fragmentation with neutral loss of propanoic acid. Additional water-loss yields the aldehyde (m/z=587). An analogous fragmentation may be used to explain the 587-peak in the MS/MS spectra of isomonensins A12 and A16[39], but would involve a retro-ene type mechanism. The significance of this fragment will be discussed in reference to C9-*epi*-monensin A. The prominent peak, m/z=605, is formed if water-loss across the E-ring occurs after fragmentation at the carboxyl terminus, but is analogous to the 587-fragment. This is also the case with fragments m/z=483 and m/z=501.

Isolation of Authentic C3-O-demethylmonensin A

Although the fragmentation studies confirmed that isomonensins A12 and A16 were both structurally analogous to and yet distinct from monensin A, the results provided no further information. Attempts at scaling up culture fermentation and combining extracts in order to obtain enough material for NMR analysis were unsuccessful. At

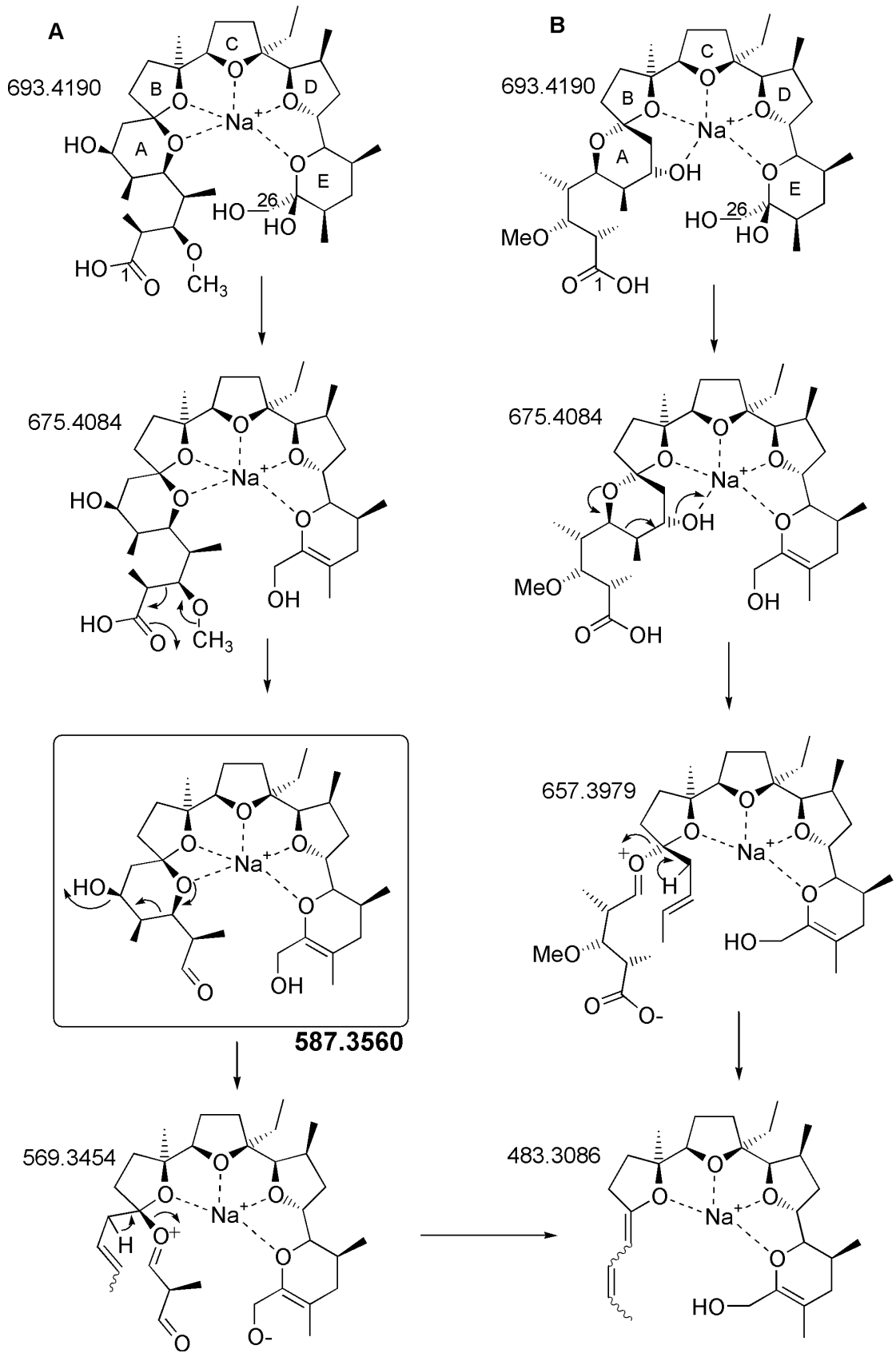

Figure 3.5 Partial fragmentation of isomonensin A12/16 (A) and that of authentic monensin A (B).

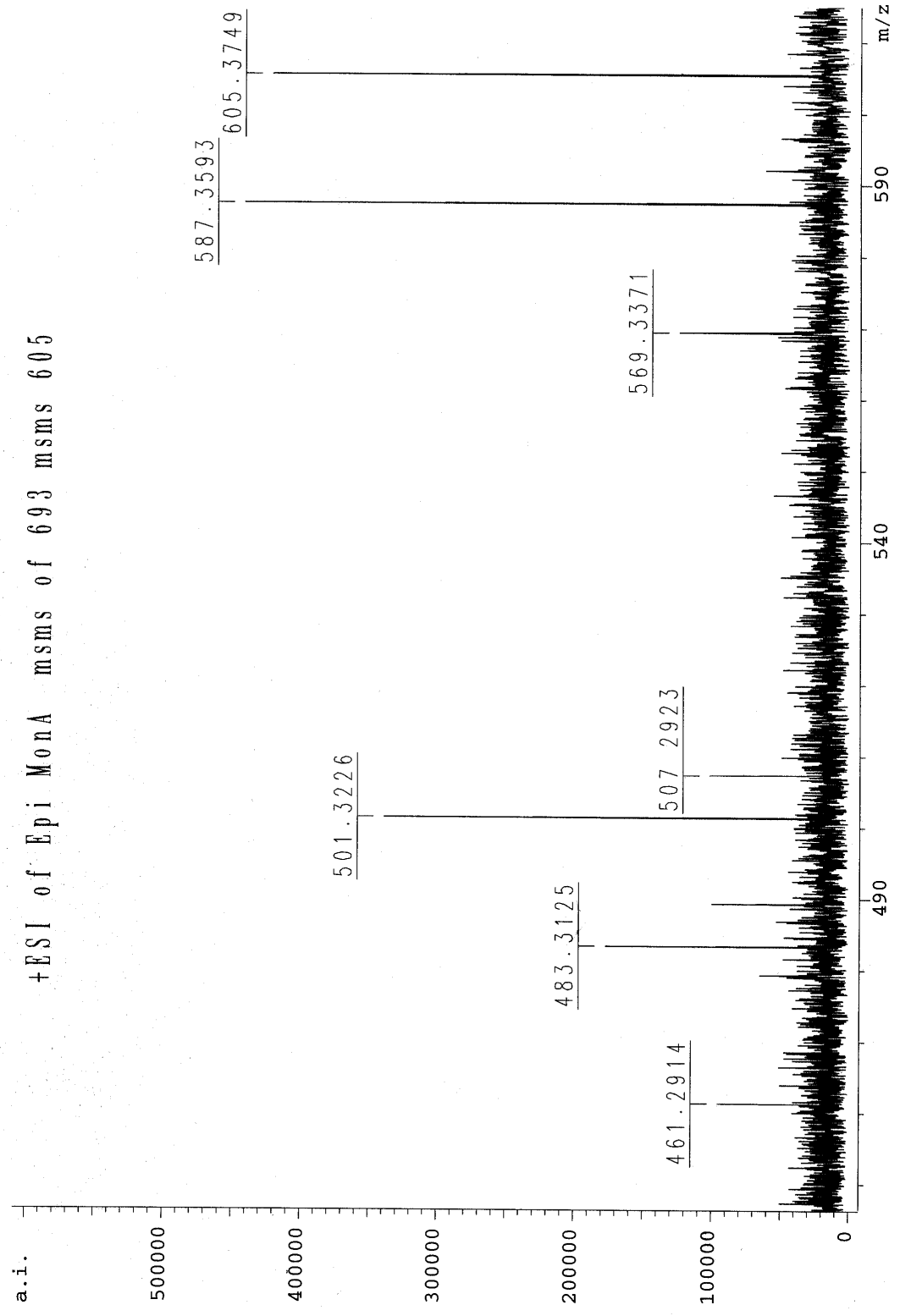

Figure 3.6 High resolution MS/MS spectrum of isomonensin A16

this point, this aspect of the project appeared to hit a dead-end. However, the procurement of a Bulgarian industrial strain of *S. cinnamonensis* (A519) proved to be the decisive acquisition that changed this.

The proprietary culture medium used to grow this strain was a heavily oil-based one and unlike the SM16-1 medium that had been used prior. Whereas the *S. cinnamonensis* strain used previously produces on the order of ~100mg/litre of monensin, the Bulgarian strain produces closer to 100g/litre in ideal growing conditions – three orders of magnitude higher. When grown in SM16-1 medium, however, the Bulgarian strain's production is not significantly higher than that of the original strain. This suggests that the remarkably high production level of the Bulgarian strain is heavily reliant on the culture medium. When the original strain was grown in this oily medium, monensin production was increased dramatically, but only by approximately a single order of magnitude. It is unclear why the oily medium appears to be conducive to monensin over-production outright, but it is possible that beta-oxidation of the fatty acids[40] in the medium provides a massive excess of the polyketide precursors (acetate, propionate, etc.) and stimulates biosynthesis in this manner.

As the original strain produced substantially higher quantities of monensin in the oily medium, the Δ*monBII* mutant was grown in this medium and under the same conditions as specified by the proprietors, in the hope of isolating enough of either isomonensin A12 or A16 (or both) for NMR analysis. Although this was straightforward, the extraction and purification process had to be modified in order to achieve a clean product. Culture supernatants from SM16-1 medium were simply extracted with ethyl acetate. However, ethyl acetate tended to pull out most of the oils together with the desired metabolites. The resulting thick oily residue was difficult to purify further using silica column chromatography. By resuspending the residue in hexane and back-extracting with a methanol:water (3:1) mixture, however, most of the oil was removed and the extract could then be purified as usual.

The LCMS traces of the extracts from this medium were a little messier than those obtained from the SM16-1 medium and production of isomonensins A12 and A16 appeared very low (Figures 3.7 and 3.8). However, the species that, by far, dominated the traces were those eluting at around 9 and 11 minutes, with

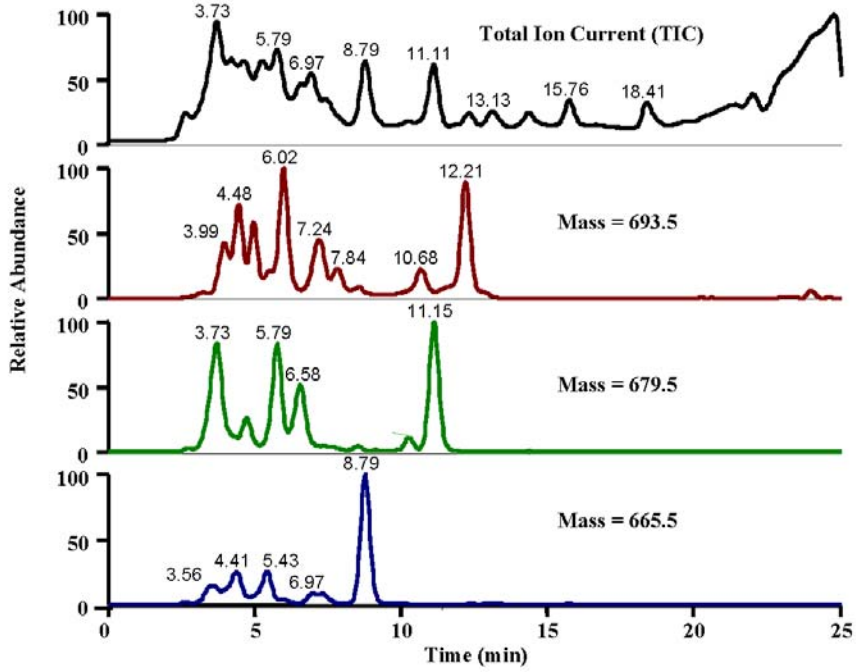

Figure 3.7 *S. cinnamonensis* Δ*monBII* grown in SM16-1 medium.

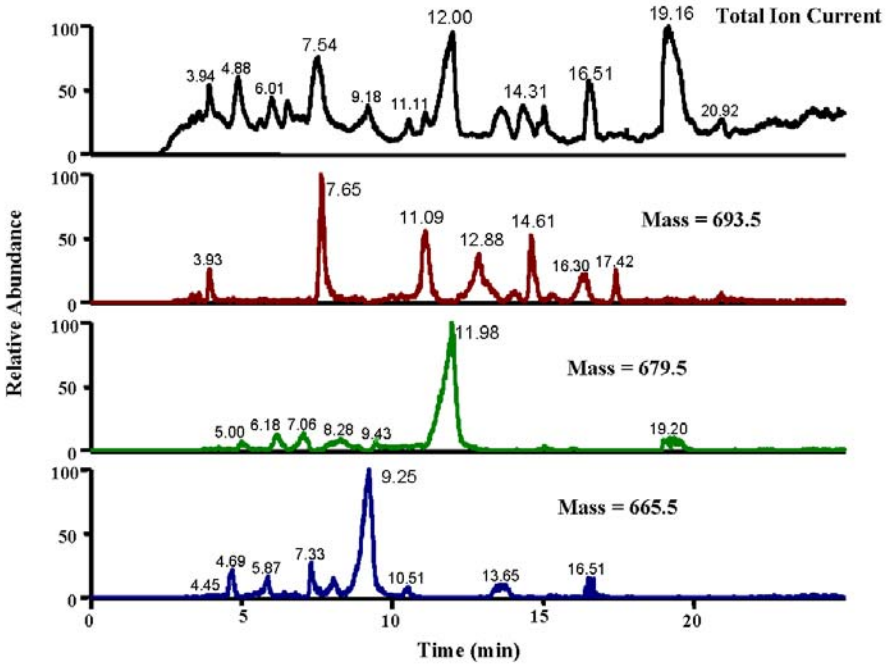

Figure 3.8 *S. cinnamonensis* Δ*monBII* grown in oily medium.

masses of 665.5 and 679.5, respectively. It was thus decided that these would be targeted for isolation, in the first instance. The crude extract was initially flushed through a silica column to remove very polar components and then fractionated by means of silica column chromatography and the fractions analysed by LCMS. Those containing the desired metabolites were further purified in a similar manner to yield the partially purified extract, which was finally purified by preparative HPLC. This yielded both of the desired metabolites in a very pure form as analysed by LCMS, but the yield was very low, on the order of less than 500μg. However, this was adequate for NMR analysis. The ^{1}H- and ^{13}C-NMR is well established[37], and it proved straightforward to confirm that the metabolite obtained was C3-O-demethylmonensin A.

Isolation of C9-epi-Monensin A

Clearly, the isolation of the C3-O-demethylated analogues of both monensin A and B demonstrated the ability of *S. cinnamonensis* to produce the authentic monensin polycyclic structures in the absence of the MonB enzymes, though at much lower levels. However, the mutants appear unable to produce the fully methylated, authentic monensins, whilst producing a range of apparent monensin variants, both methylated and not. Whilst providing valuable information, this also appeared to cause greater confusion, rather than clarifying the role of the MonB enzymes. It was at this point that isolation and characterisation of isomonensins A12 and/or A16 became the prime target. As the original *monB* mutants appeared unable, in reasonable size cultures, to produce enough of these metabolites for NMR analysis, the Δ*monBII* mutant was created in the Bulgarian over-producing strain, A519, in the hope of achieving this. This was straightforward, as A. Bhatt, who produced the original mutants, had created the relevant constructs for in-frame deletion of the *monB* genes utilising the temperature-sensitive pKC1139 vector. Indeed, extracts from this new mutant appeared identical to those of the original.

The proprietary conditions dictated that only small cultures be grown, individually around 40ml. Thus, many small cultures were grown, to achieve a total volume of around a litre; the obvious aim being to maximise the chance of acquiring enough material for NMR analysis. The cultures were extracted using the modified method, developed for the oily medium, and yielded ~80g of a very thick, viscous,

almost black oily residue. This had to be flushed twice through a silica column with ethyl acetate:methanol (95:5), and the later eluting metabolites separated as best possible, before enough of this oil had been removed to enable flash column chromatography to satisfactorily further the purification , as described for the isolation of C3-O-demethylmonensins A and B. Following final purification of the extract by preparatory HPLC, both isomonensin A12 and A16 were obtained as pure white powders, both in amounts less than 500μg. Notably, both C3-O-demethylmonensins A and B were obtained in quantities approaching 100g – at least two orders of magnitude higher than obtained from the original mutants. It is quite clear that without access to the Bulgarian over-producing strain and media, isolation of enough of isomonensins A12 and A16 would have been practically impossible, barring access to fermentation and extraction apparatus that would allow the culturing of 500+ litres of the original mutants in SM16-1 medium.

LCMS analysis showed the isomonensins to be very pure and suitable for NMR analysis (Figure 3.9). Unfortunately, but not that surprisingly, the initial 1D-^{1}H-NMR of isomonensin A12 clearly showed the presence of two distinct compounds. Analysis by LCMS revealed, as seen previously, that isomonensin A12 was converting to A16. However, the ^{1}H-NMR of isomonensin A16 showed only one compound (see Appendix).

It is important to note that there are only a limited number of positions in the monensin structure at which the stereochemistry is not established on the PKS (Figure 3.10). This somewhat simplified the task of identifying stereochemical differences between the authentic and isomeric forms of monensin, as most of the positions can effectively be ruled out as being potentially isomeric. Usefully all of these positions are carbons attached to a single oxygen, barring the disubstituted C9 spiroketal, and thus the corresponding protons are suitably downfield and removed from the backbone protons to allow their clear distinction. The C9 spiroketal and carbons C12 and C15, however, possess no protons, whilst being potentially isomeric. The established structure of authentic monensin A, based on NMR and crystallography, enabled one to confidently justify the NOESY correlations that were examined in detail. Such was this, that any change in the stereochemistry at the positions that were possibly isomeric would be reflected in the NOESY spectra (Figure 3.11). The lack of

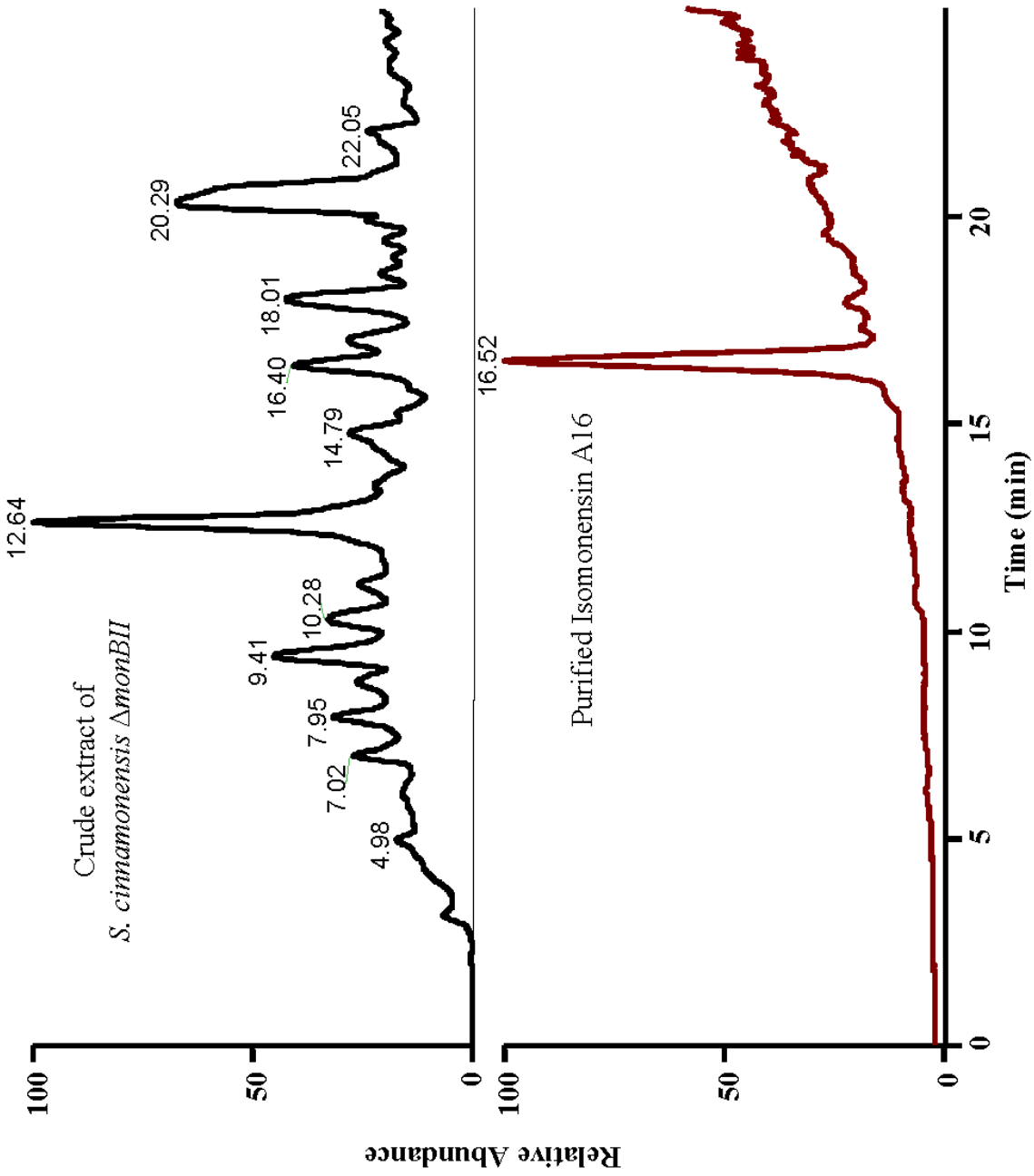

Figure 3.9 Purification of isomonensin A16 from crude extract of *S. cinnamonensis* [Bulg.] Δ*monBII*.

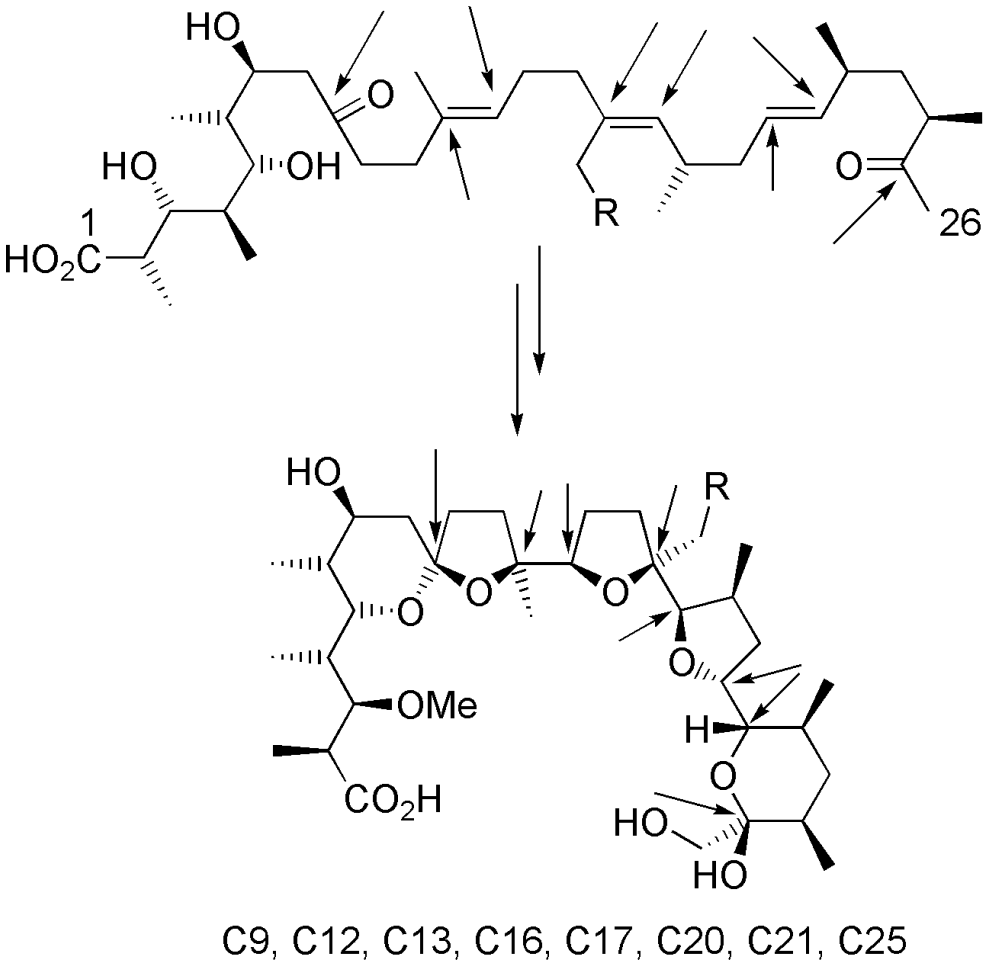

Figure 3.10 Stereogenic centres in monensin that are not established by the PKS.

protons at C12 and C15 posed no concern in this regard, as the methyl and ethyl groups, respectively, have clear NOESY correlations that confirm the stereochemistry at these positions. Likewise, the stereochemistry of the C25 hemiacetal is clear from its NOESY correlations, although this may be regarded as a moot point, considering the lability of this position and thus its natural tendency to equilibrate to its most stable configuration. The C9 spiroketal, however, possessed no such correlations and was thus a potential concern, should it be isomeric. The important NOESY correlations of both monensin A and isomonensin A16 are shown in Figure 3.12. As shown, no variation in NOESY correlations was observed in any of these important positions. However, what *was* noted, was a reorganisation of the NOESY correlations along the carboxyl tail and around the A-ring of the molecule in isomonensin A16. As all of these positions are known to have their stereochemistry established on the PKS, the only explanation was a change in the conformation of this region. As mentioned, the C9 spiroketal was potentially a problematic position should it be isomeric, owing to its lack of characteristic NOESY correlations. By a process of elimination, however, this was the only position that could be isomeric, having ruled out the others. A change in this position would also explain the conformational changes observed at the carboxyl end of the molecule. Notably, two distinct NOESY alterations were observed in isomonensin A16. Firstly, an additional NOE was observed between the C5 proton and the C3 proton. Secondly, the NOE between the C5 proton and the C4' methyl protons, observed in monensin A, was missing from isomonensin A16.

In addition to the changes in the NOESY spectra, the 1D ^{1}H-NMR also displayed a telling feature (Figures 3.13 and 3.14). In monensin A, the C5 proton is observed as a doublet of doublets, coupled to the C4 and C6 protons, at 4.02ppm. However, in isomonensin A16, the C5 proton was shifted significantly downfield to 4.67ppm and appeared as a singlet. A change in configuration at the C9 spiroketal would flip the A-ring and bring the C7 hydroxyl out of coordination with the central sodium ion, whilst moving the A-ring ether oxygen towards it. This oxygen may well then take up the role of the C7 hydroxyl to some degree and coordinate itself. As the ether oxygen is attached to the C5 position, this would deshield the C5 proton and cause the observed downfield shift. Also, the change in dihedral angles between the

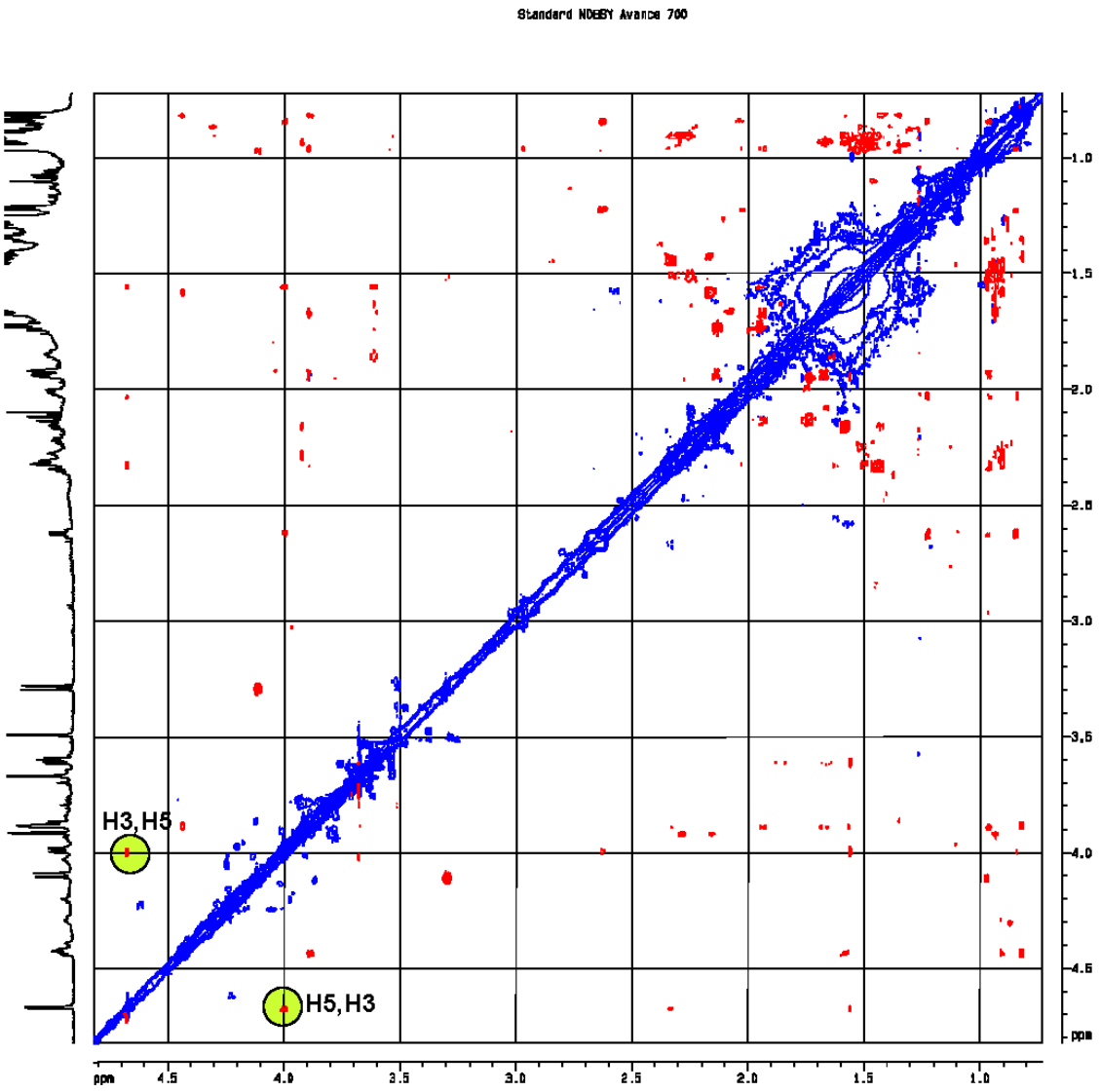

Figure 3.11 Isomonensin A16 NOESY spectrum, highlighting NOE correlation not present in authentic monensin A.

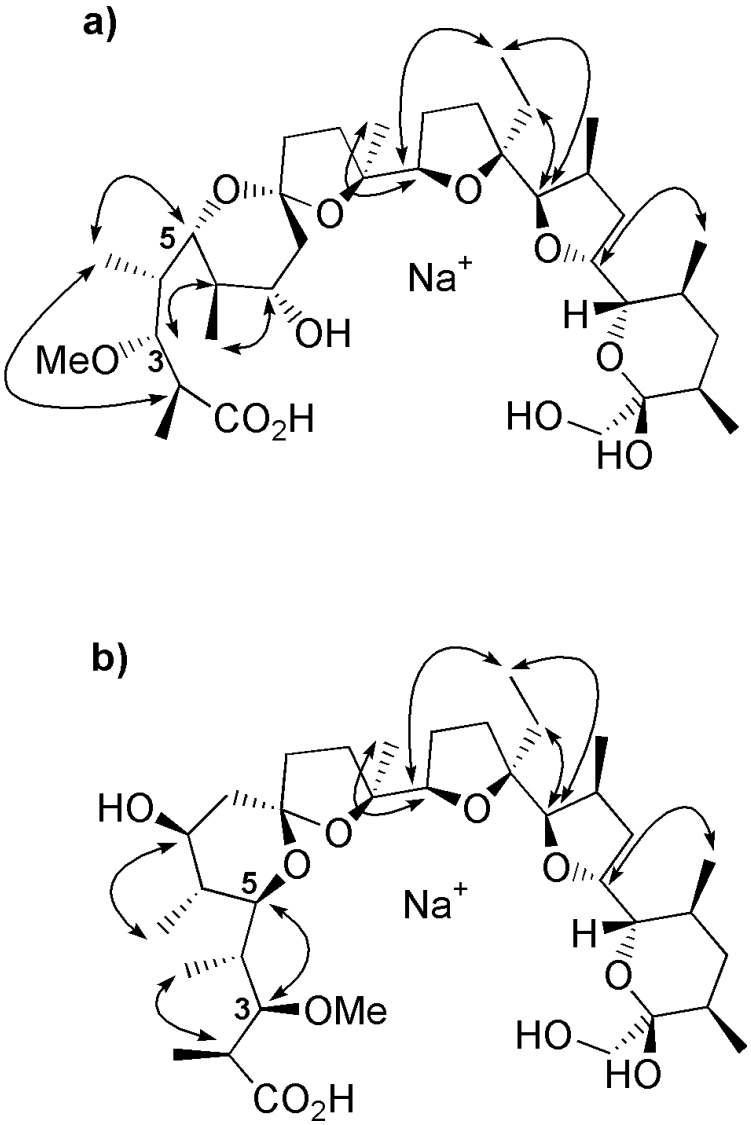

Figure 3.12 Important NOE correlations of a) Monensin A; b) Isomonensin A16

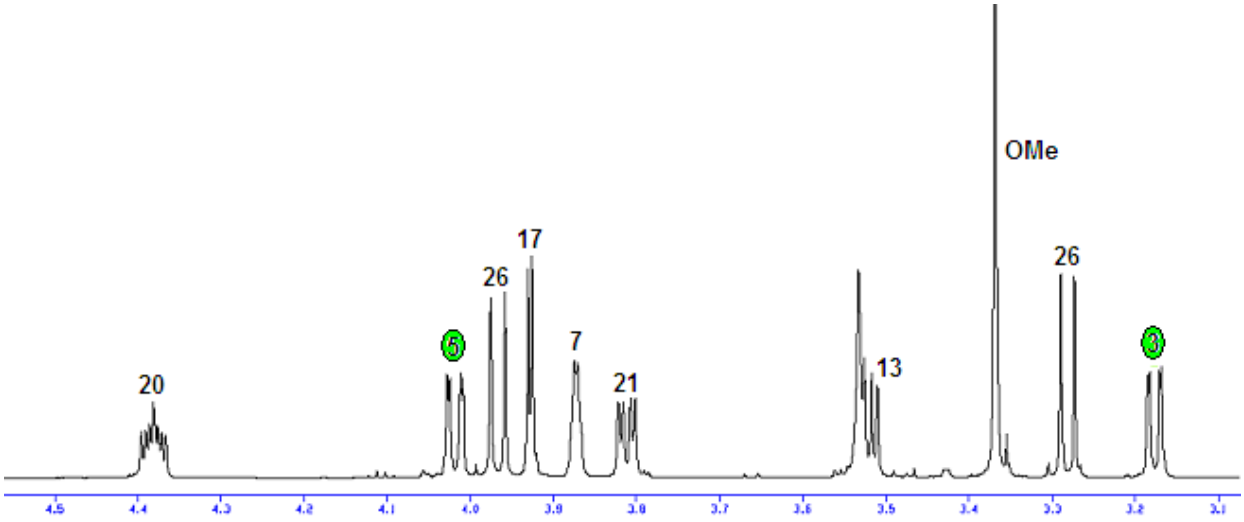

Figure 3.13 Zoomed in region of monensin A ^{1}H-NMR. Notable protons are highlighted.

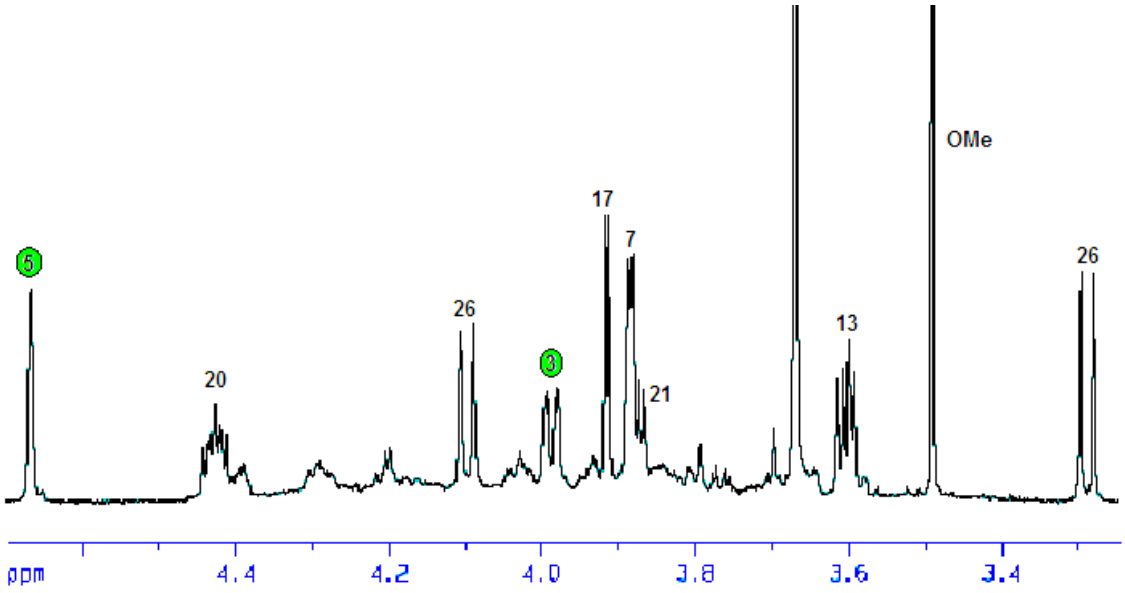

Figure 3.14 Zoomed in region of isomonensin A16 ^{1}H-NMR. Notable protons are highlighted.

C5 proton and the C4 and C6 protons may cause the doublet of doublets to coalesce, according to the Karplus equation, and appear as a singlet. Thus, both changes in the manifestation of the C5 proton can be explained by a change in configuration at the C9 spiroketal. The C3 proton also displayed a downfield shift, which might be explained as a result of the C3 hydroxyl coordinating to the central sodium, or hydrogen bonding across to the C26 hydroxyl and thus taking up the role of the carboxyl in this regard.

Finally, the unusual MS fragment, described earlier, may be explained if one considers the potential effect of a change in the orientation of the carboxyl tail; a 'freeing-up' of the carboxyl group, from its natural hydrogen bonding to the C25 and C26 hydroxyls, might facilitate the additional fragmentation observed at this position. Taking into consideration all of this spectral evidence, it was surmised that isomonensin A16 could be identified as C9-*epi*-monensin A (Figure 3.15).

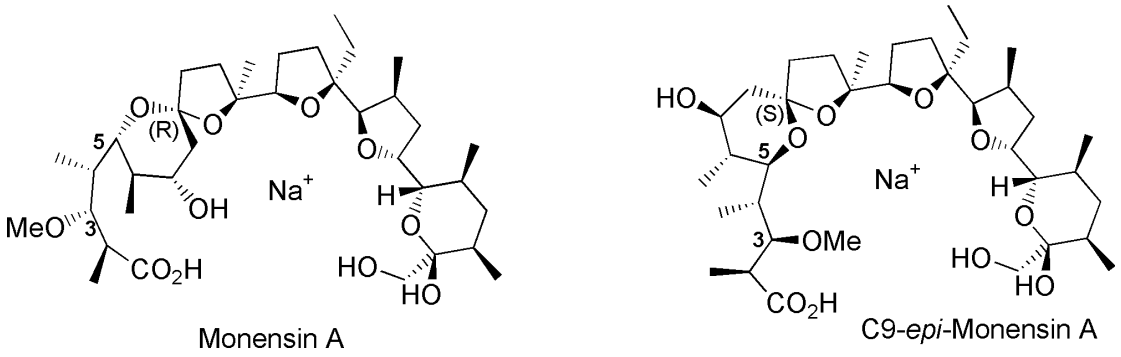

Figure 3.15 Monensin A and its novel C9 epimer.

Epimerisation of the Spiroketal of C9-*epi*-monensin A

The C9 spiroketal of authentic monensin A, is of the general system 1,6-dioxaspiro[4,5]decane, and is in the favoured, most thermodynamically stable configuration. For metabolites containing spiroketal systems, it has generally been assumed that these centres *would* naturally exist in their most thermodynamically stable configuration. Synthetic studies have usually shown this to be a valid assumption[41]. Specifically, in protonated monensin, both the C6 methyl and the C7 hydroxyl are axially disposed. This is stabilised by an intramolecular hydrogen bond between the C7 hydroxyl and the axial spiroketal (B-ring) oxygen (see diagram left).

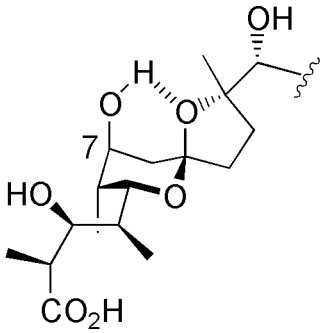

This is confirmed by a sharp absorption at 3560cm^{-1} in the IR spectrum[42]. This provided the rationale for an elegant experiment to further confirm the structure of isomonensin A16 as being monensin A's C9 spiroketal epimer. Treatment of isomonensin A16 with acid should revert the spiroketal to its most stable configuration and thus to authentic monensin A. Usefully, the characteristic LCMS retention times and distinct fragmentation patterns of these would enable such a conversion to be easily detected. Upon treatment with hydrofluoric acid, complete and clean conversion of isomonensin A16 to monensin A was observed (Figure 3.16), thus confirming the identification of isomonensin A16 as C9-*epi*-monensin A. Initially, this was attempted with hydrochloric acid[43] and was also successful in the conversion. However, dehydration, and other unidentified, products dominated a messy LCMS trace.

Isolation of an Open E-ring Analogue of C9-*epi*-26-deoxy-Monensin A

Following isolation and characterisation of the C9-epimer of monensin A, attention was turned to a late eluting metabolite (~20mins, see figure 3.8) with a mass of 677.5 that was present in several of the flash column fractions. This appeared to be present in some considerable quantity, so, initially out of curiosity, this was separated by HPLC and yielded ~5mg of a white powder. Its late elution time suggested that it was a less polar compound than the other monensins. Owing to the sizeable quantity of C3-O-demethylmonensin A isolated from this culture broth, it was thought that this may be the oxidised form, in which the C3-hydroxy had somehow been oxidised to form deoxy-3-oxo-monensin A. This would explain both its mass and lower polarity. The compound was treated with borohydride, in an attempt to reduce down the carbonyl to the hydroxyl, and this appeared to be successful. As would be expected, two compounds with mass 679.5, corresponding to both reduction diastereomers, were identified by LCMS (Figure 3.17).

Monensin A has a single carbonyl group, which is, of course, that of the carboxyl (178.96ppm). As there was more than ample compound available for analysis, a 1D-^{13}C-NMR was carried out to look for the presence of an additional carbonyl (Figure 3.18). Indeed, the ^{13}C-NMR spectrum clearly showed two carbonyls – the additional one downfield in the ketone region (208.72). However, the ^{1}H-NMR

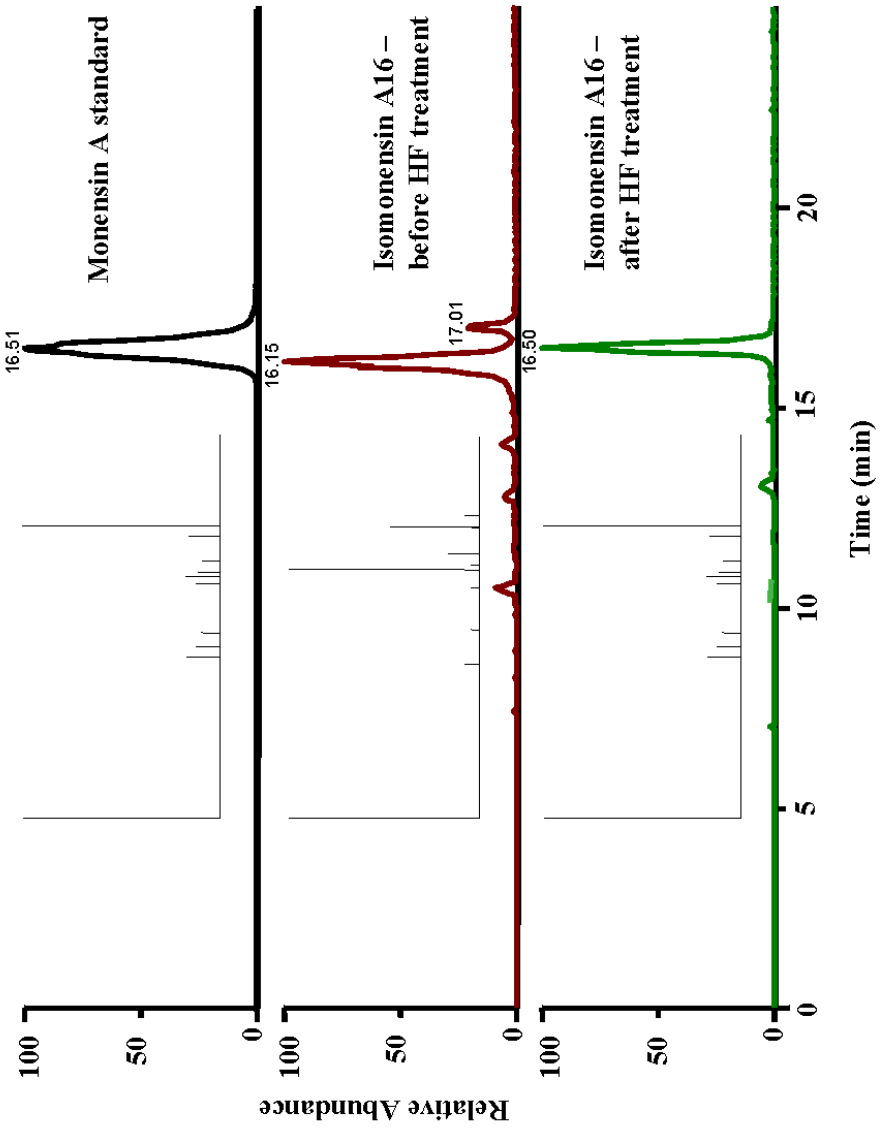

Figure 3.16 Epimerisation of *epi*monensin A to monensin A with HF. The MS^3 spectra are only intended to illustrate the differing patterns of fragmentation and thus contain no detail.

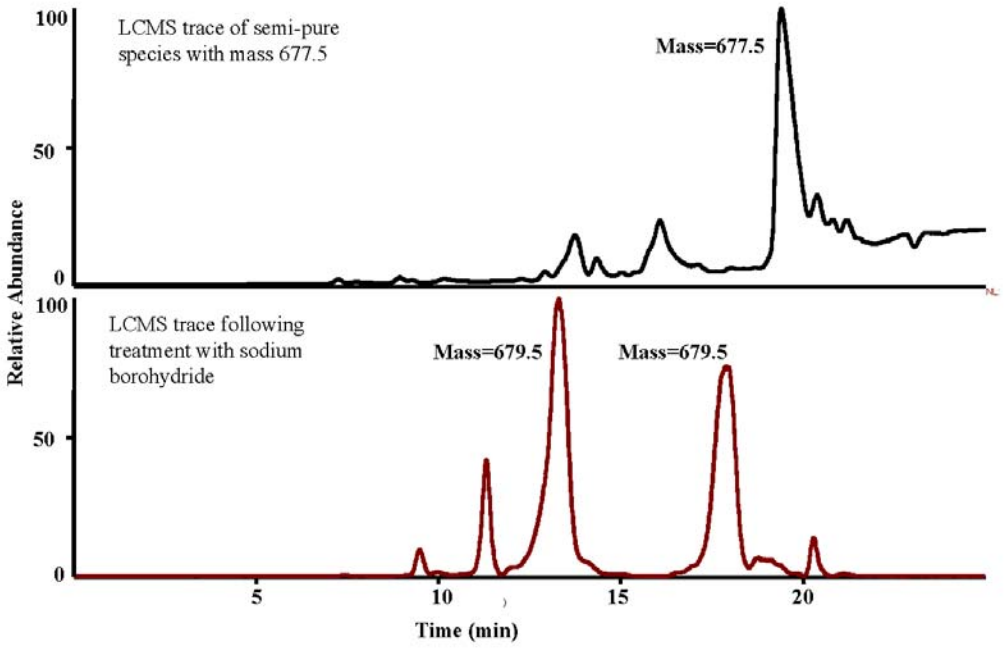

Figure 3.17 Borohydride reduction of late-eluting species with mass 677.5

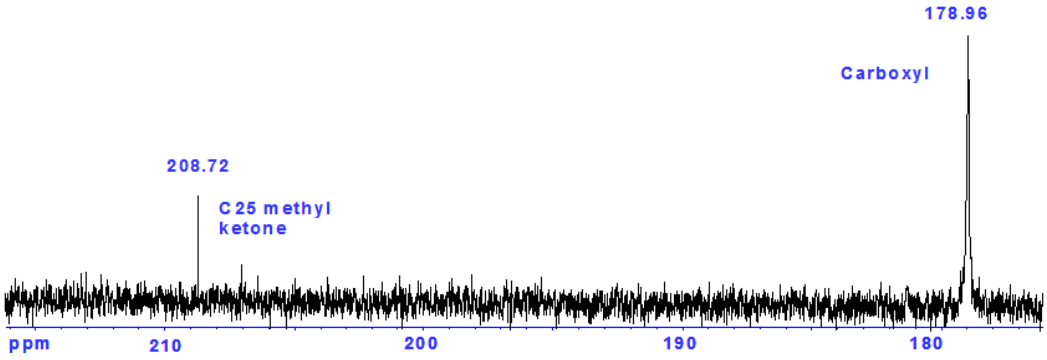

Figure 3.18 Zoomed in region of ^{13}C-NMR showing the presence of the two carbonyls in the 677.5 monensin analogue.

was surprising, as it did not support the original structural proposal based on the evidence so far. The identity of this compound was soon clarified, however. The most notable feature of the ^{1}H-NMR was the apparent disappearance of the two diastereotopic C26 protons from the 4-5ppm region of the spectrum (Figure 3.19). A correlation between the ketone and the C26 protons in the HMBC spectrum revealed these protons shifted to the methyl ketone region of the spectrum, at 2.18ppm. Further to this, as in C9-*epi*-monensin A, the C5 proton displayed the same striking downfield shift. It was thus becoming clear that this compound was, in fact, the C26-deoxy analogue of C9-*epi*-monensin A. The presence of the methyl ketone suggested that the E-ring was not closed to form the lactol, although it is possible that the open and closed form are in equilibrium. However, it is possible that the open form might be stabilised by coordination of the C21-hydroxyl to the central sodium, thus precluding its attack at the C25-carbonyl.

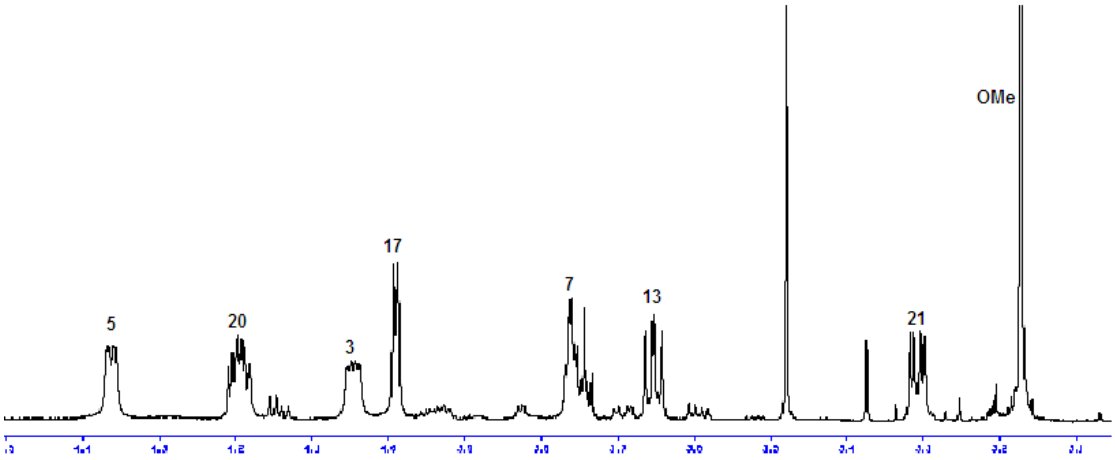

Figure 3.19 Zoomed in region of 1H-NMR of C9-*epi*-C26-deoxy-monensin A, below:

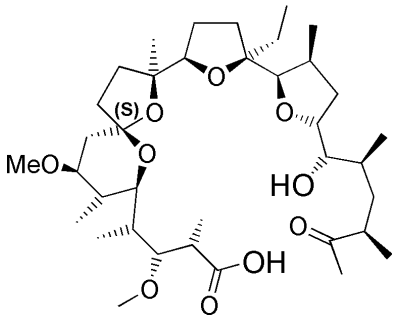

Chapter Four

Implications of C9-*epi*-Monensin A Regarding the Role of the *monB* Genes in Monensin Biosynthesis

Before considering how the isolation of the metabolites, described in the previous chapter, might aid in elucidating the role of the MonB enzymes in monensin biosynthesis, it was necessary to explain the formation of the novel epimers from a mechanistic standpoint. This was accomplished by considering, in detail, the process of cyclisation of the putative triepoxide intermediate.

The first step in the cyclisation process is the attack of the C5 hydroxyl at the C9 carbonyl to form the first hemiacetal intermediate and closing the A-ring. Significantly, this can occur on either face – the *Re* or the *Si* face. This hemiacetal forms the C9 spiroketal as the first epoxide is opened and the B-ring is closed. The spiroketal in authentic monensin has the (R) absolute configuration. This results when the C9 carbonyl is attacked from the *Si* face. Alternatively, if the C9 carbonyl is attacked from the *Re* face, the resulting spiroketal has the (S) absolute configuration and C9-*epi*-monensin A is formed (Figure 4.1). The *monB*-null mutants of *S. cinnamonensis* produce a mixture of monensin analogues – those with the natural (R) configuration, and the epimers with the unnatural (S) configuration at the C9 spiroketal. This implies that the stereochemistry of the spiroketal is not controlled in the absence of the MonB enzymes, and immediately suggested that these enzymes might have a role in the cyclisation of the putative triepoxide intermediate, or, possibly, be entirely responsible for this process. Further consideration of the metabolites produced by the *monB*-null mutants supports this view.

Non-enzymatic Cyclisation of Triepoxide Intermediates

If MonBI and MonBII *had* been correctly identified as the enzymes that control the conversion of a triepoxide intermediate into the final polyether structure, then, in their absence, one could expect such an intermediate to accumulate. However, the issue was complicated by the C3-O-methyl transferase and C26-hydroxylase enzymes that are present as part of the monensin biosynthetic pathway. Nothing is known regarding the specificity of their action; it is not known whether they act upon the open triepoxide intermediate or the cyclised polyether, or whether they act whilst the

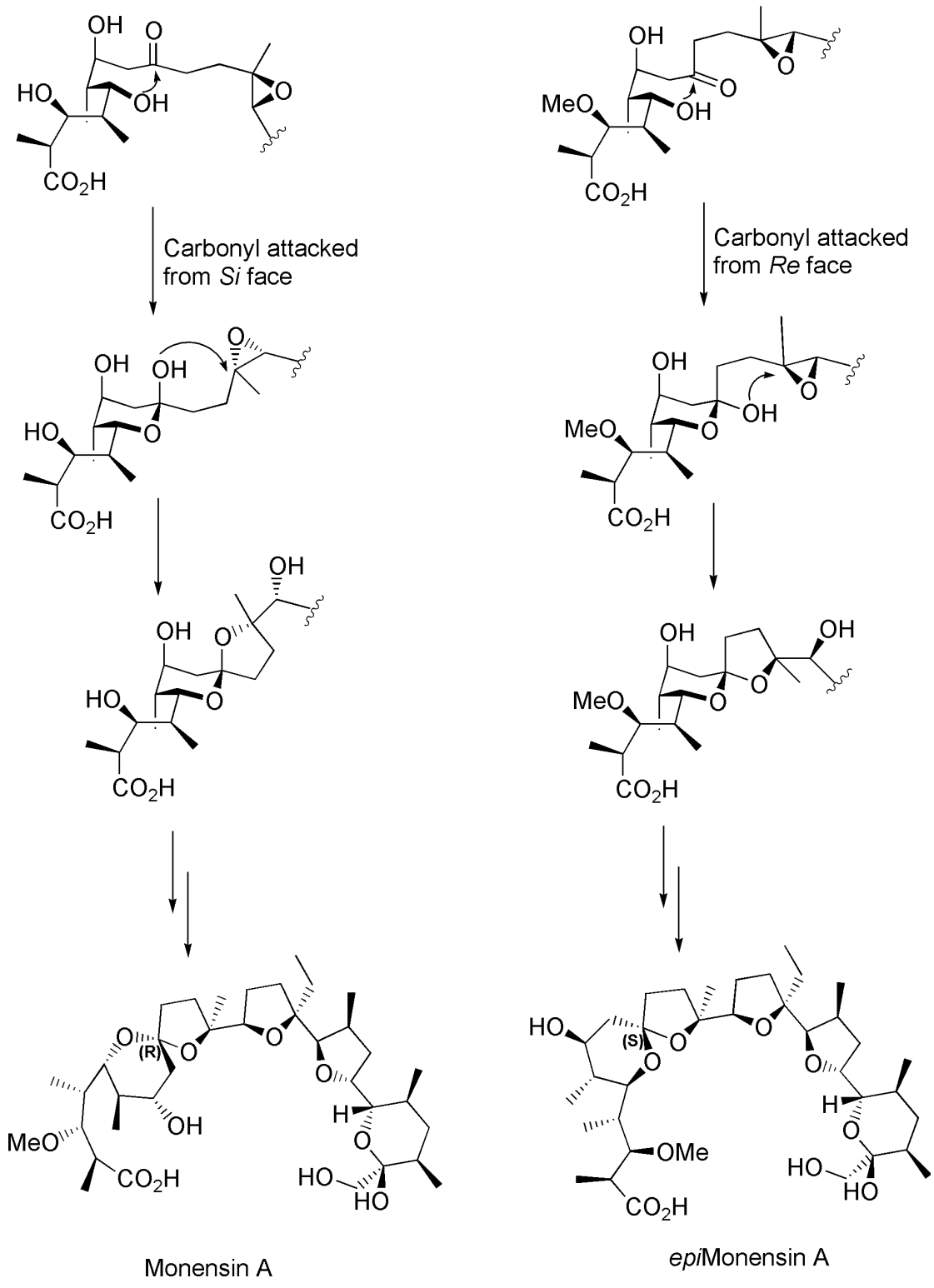

Figure 4.1 Modes of cyclisation leading to authentic monensin A and its C9 epimer.

former or latter is bound to the PKS or not. The products isolated from fermentation extracts of *monB*-null mutants ought then to reflect a balance between the chemical degradation or modification of such species, their chemical or enzymatic release if they are protein-bound, and the specificity of the methyltransferase and hydroxylase. The isolation of C3-O-demethylmonensin A and B as the major products from all *monB* mutant strains suggested that epoxide ring opening and formation of the polyether rings with the correct regio- and stereochemistry is a chemically favoured process that occurs spontaneously in the absence of the MonB enzymes. Also, this suggested that O-methylation at C3 occurs either before polyether ring formation or before release of the monensin product from a protein, or both; the free C3-O-demethylmonensins are not processed by the methyltransferase. Further, it seems that in the absence of methylation at the C3 hydroxyl, nucleophilic attack by the C5 hydroxyl group at the C9 carbonyl is kinetically favoured at the *Si* face, to form the *natural* epimer of the hemiacetal. The subsequent cyclisation gives C3-O-demethylmonensins with the correct configuration at the C9 spiroketal.

Once the A-ring has formed, the resulting hemiacetal hydroxyl opens the first epoxide to form the B-ring, by nucleophilic attack at the more hindered carbon and with inversion at this centre. This chemical preference can be rationalised on the basis that the alternative attack at the less hindered carbon would be a disfavoured *6-endo-tet* cyclisation in violation of Baldwin's rules[44] (Figure 4.2). Also, inversion at the tertiary centre can be understood if acid catalysis promotes partial opening of the epoxide in the transition state, allowing the developing tertiary carbocation to be captured by the incoming hydroxyl nucleophile. This "loose S_N2" mechanism avoids the sterically disfavoured S_N2 mechanism, while ensuring stereochemical inversion. Such a mechanism has been exploited in the construction of synthetic cyclic polyethers[45]. The closure of the C, D and E rings can be explained analogously.

The occurrence of C9-epi-monensin A and its C26-deoxy analogue can also be explained by a spontaneous cyclisation model. It appears that, if the C3 hydroxyl is methylated prior to initiation of cyclisation, then attack by the C5 hydroxyl at the C9 carbonyl's *Re* face is *kinetically* favoured to form the unnatural hemiacetal epimer. Subsequent cyclisation then 'traps' this epimer as the spiroketal and the C9-*epi*-monensin structure is formed. This may then compromise the action of the C26-hydroxylase, of which the unnatural epimer is a poor substrate. Further, closure of the E-ring and hydroxylation of the C26 position might be a closely coordinated process;

for instance, if the hydroxylation occurs as the E-ring closes to form the hemiacetal, or, if the hydroxylase promotes cyclisation as it binds, then disruption of the activity of the hydroxylase would not only result in the C26-deoxy analogue, but also in the open E-ring form, as is observed. Interestingly, *Streptomyces albus*, which produces the ionophore salinomycin[46], also produces its C17 spiroketal epimer. It is notable that this has only been isolated as C20-deoxy-C17-*epi*-salinomycin[47],in which the C20 position, normally hydroxylated in salinomycin, is left unprocessed. It seems that the alternative epimer is a poor substrate for the hydroxylase responsible for oxidation at this position, akin to what is seen with the unnatural epimer of monensin (Figure 4.3).

Overall, the major products of this spontaneous cyclisation process are *either* natural C3-O-demethylmonensins *or* C26-deoxy-*epi*-monensins. Indeed, these are the major metabolites observed. C9-*epi*-monensin A is an almost negligible product, in which C26-hydroxylation has taken place despite the unnatural configuration of the spiroketal. The correct spontaneous cyclisation of the B, C and D rings can be explained quite simply in terms of Baldwin's rules, as resulting from a series of three favoured *exo-tet* ring formations.

Cyclisation Intermediates in monB-null Mutant Extracts

If the above scenario is correct, then one might expect to see intermediates in the extracts, in which the triepoxides have only partially cyclised, since this is a non-enzymatic and, thus, relatively slow process (Figure 4.4). Referring to the original LCMS traces of the *monB*-null mutants, a number of fast-eluting metabolites were noted as minor components of the extracts. The nature of these more polar metabolites is crucial for the proposal that the MonB enzymes govern polyether ring formation from the putative triepoxides. These species have molecular ions coincident with those of monensin A (693.5), monensin B and demethylmonensin A (679.5) and demethylmonensin B (665.5), but were present in quantities too small to allow direct structural determination. However, it was predicted that if these do indeed represent partially cyclised triepoxides, then their cyclisation should be accelerated by acid catalysis to form the natural monensins. These minor components, eluting between ~3-8 minutes, were separated by HPLC and treated with hydrofluoric acid. Complete conversion to the fully cyclised monensins was observed; C3-O-demethylmonensin A and B and monensin A and B were all detected (Figure 4.5).

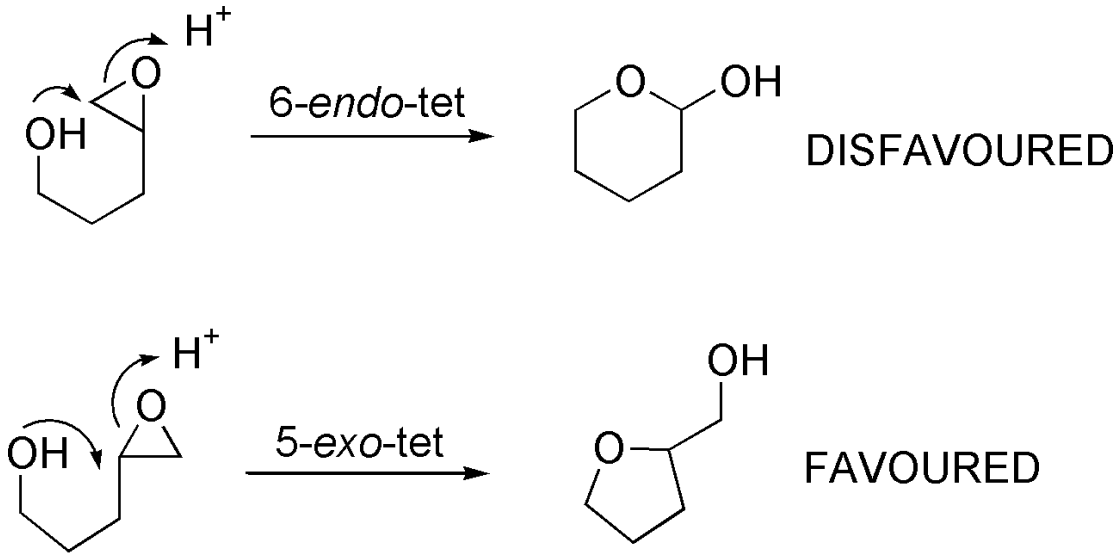

Figure 4.2 Baldwin's Rules applied to epoxide opening/cyclisation

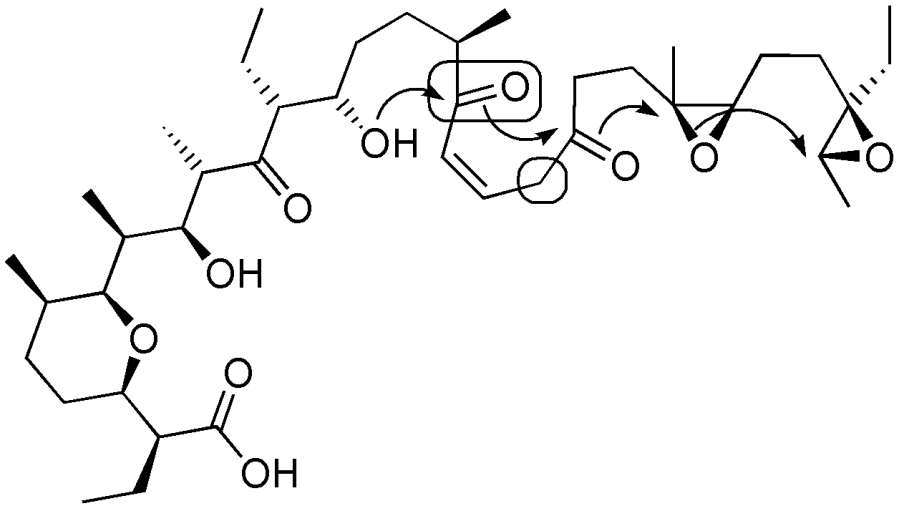

Figure 4.3 Proposed cyclisation of salinomycin. Boxed areas indicate ambiguous attack at carbonyl and site of hydroxylation affected by spiroketal stereochemistry.

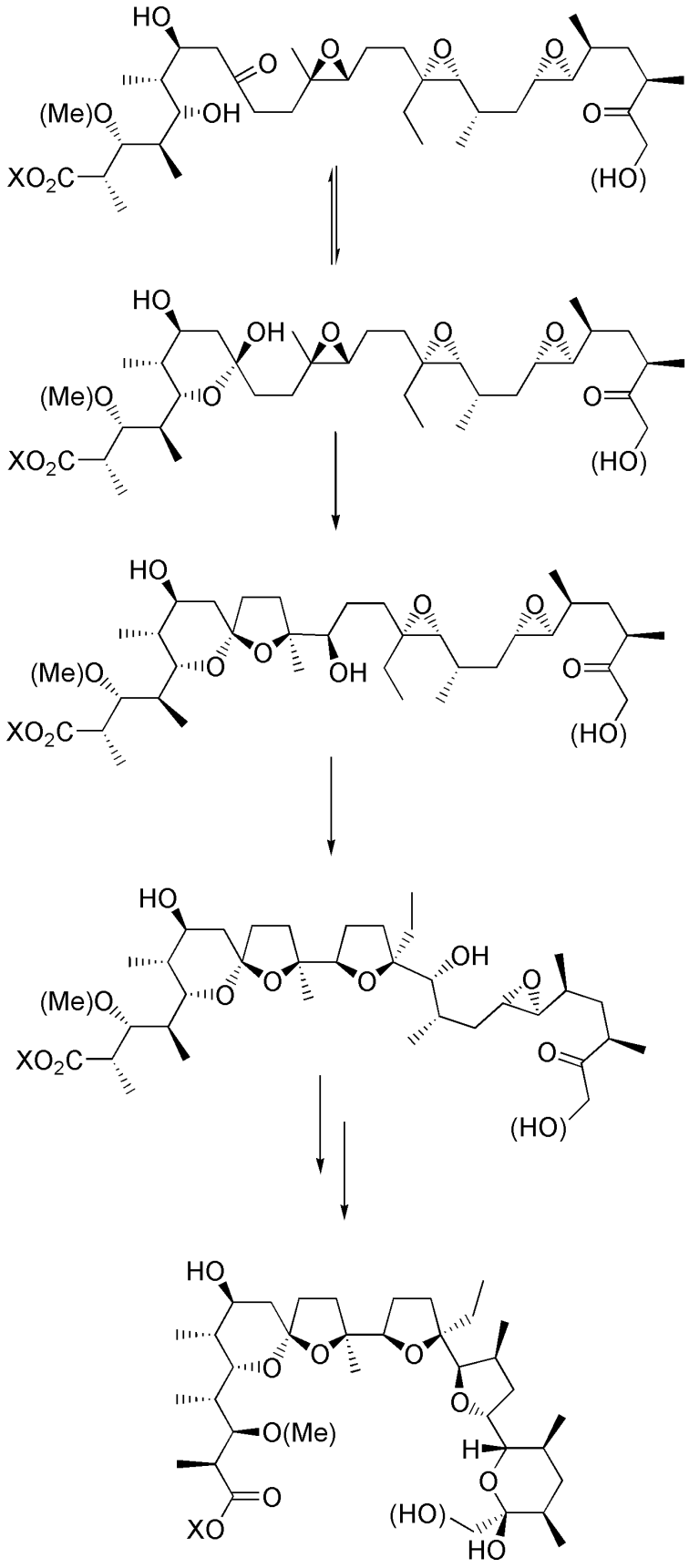

Figure 4.4 Proposed cyclisation intermediates in culture broth of *S. cinnamonensis monB*-null mutants.

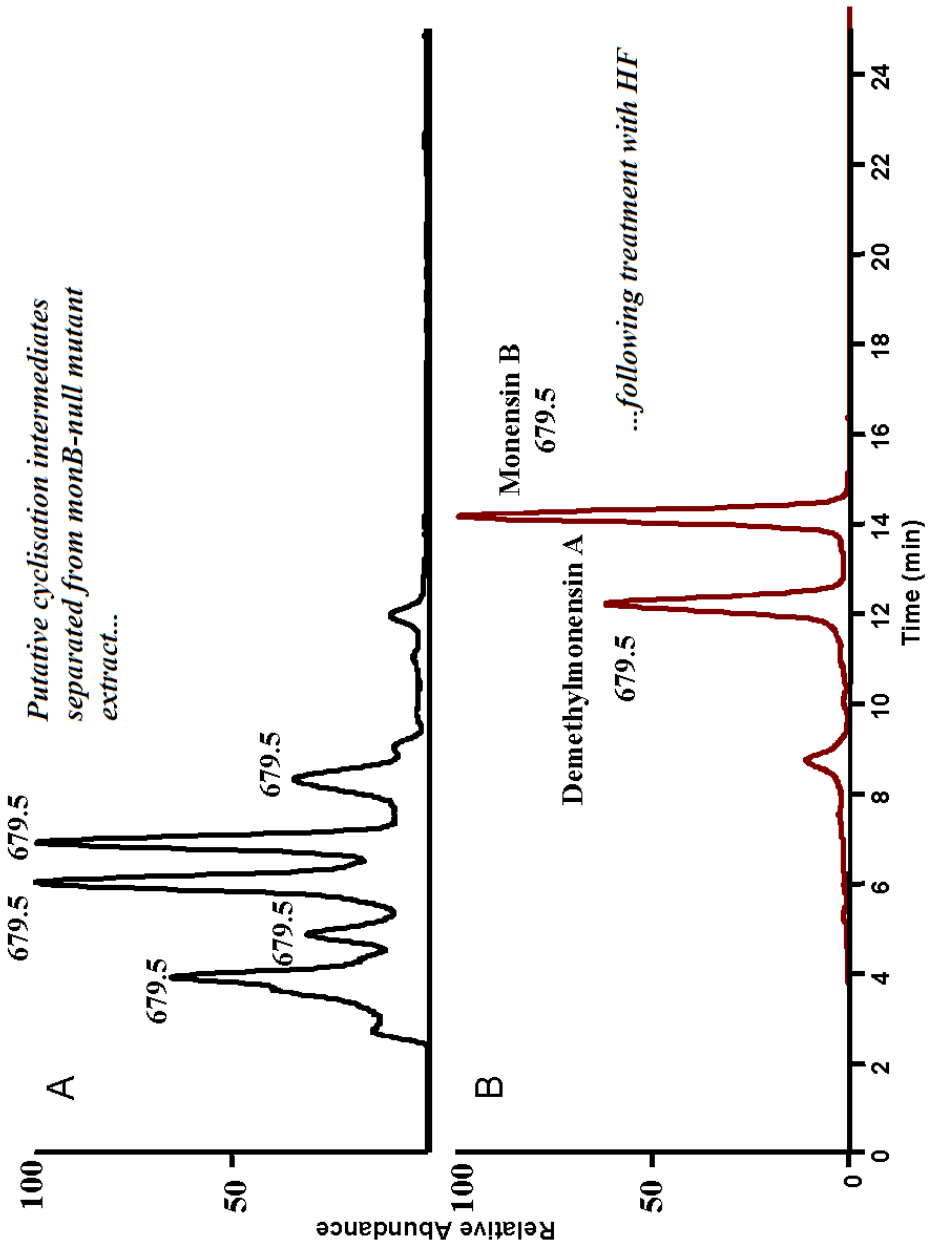

Figure 4.5 Acid-catalysed cyclisation of putative cyclisation intermediates with mass coincident with that of monensin B and demethylmonensin A.

MonB-type Enzymes as Epoxide Hydrolases Involved in Polyether Ring Formation

The product of the gene *monCII* shows significant sequence and structural similarity, over about 260 amino acids, to the epoxide hydrolases of the α,β hydrolase family, and was previously proposed as governing epoxide ring opening in monensin biosynthesis. Recently, however, MonCII has been re-assigned as a thioesterase[48] required for release of protein-bound intermediates in monensin biosynthesis (i.e. it is *not* involved in cyclisation, as originally surmised).

Nanchangmycin is a polyether antibiotic isolated from *Streptomyces nanchangensis*. Its analogous gene cluster is the only one to have been sequenced besides that of monensin[49]. The putative final intermediate of nanchangmycin is a diepoxide, akin to the monensin triepoxide. Importantly, the gene cluster for nanchangmycin also contains a gene analogous to the *monB* genes in monensin. The counterpart in nanchangmycin biosynthesis, however, is the internally duplicated *nanI* gene that appears to comprise *monBI* and *monBII* homologues fused head-to-tail.

The *monB* and *nanI* genes belong to the adaptable α + β barrel fold family, the members of which share common structural characteristics, but have diverse catalytic activities. The α + β barrel fold comprises a curved six stranded mixed β-sheet, with four α-helices packed onto it to create a barrel-like structure housing a conical pocket open at its larger end, with most residues lining this pocket being hydrophobic. The active site residues lie deep inside this pocket. Members of this family include Nuclear Transport Factor 2[50], scytalone dehydratase[51], Δ^5-3-ketosteroid isomerase (refer to the Leadlay-Staunton cyclisation model) and, notably, limonene epoxide hydrolase from *Rhodococcus erythropolis*[52].

The *monBI* gene has been cloned and expressed and small-angle X-ray scattering studies (carried out by Dr. V. Bolanos Garcia, Dept. of Biochemistry, University of Cambridge) have provided a preliminary structural model (Figure 4.6). The closest structural template for MonBI and MonBII is the aforementioned limonene epoxide hydrolase from *R. erythropolis*. The active site of limonene epoxide hydrolase contains two aspartate residues, one (D101) acting as a general acid to promote opening of the epoxide ring and the other (D132) as a general base to assist the nucleophilic attack of a water molecule. A tyrosine residue (Y53) is also proposed to participate as a general base (Figure 4.7). The MonB and NanI proteins do not

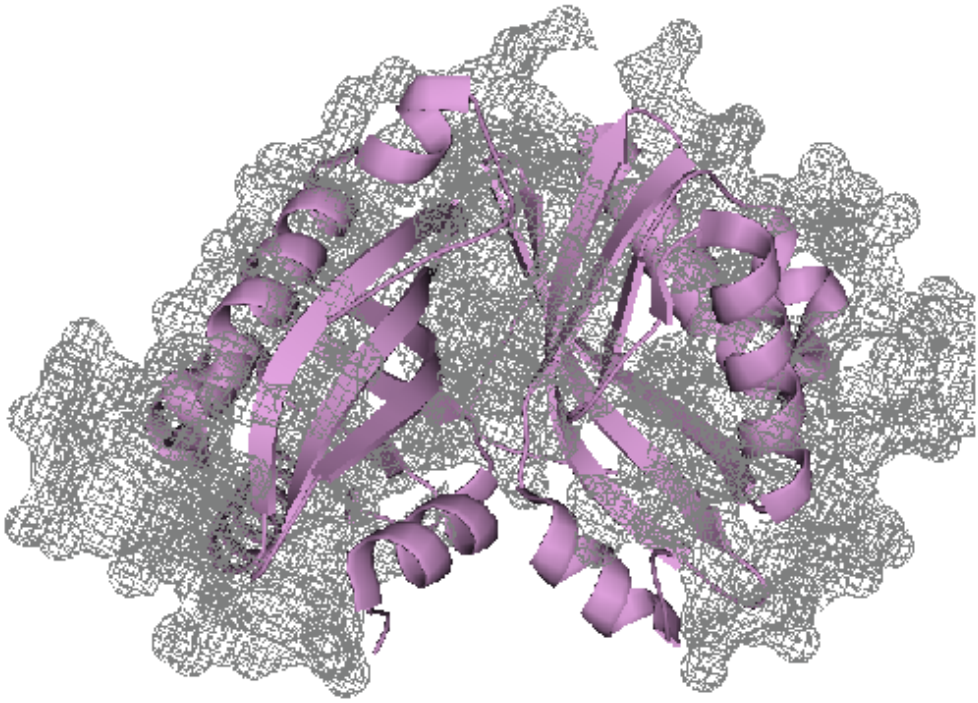

Figure 4.6 Model of purified MonBI from small-angle X-ray scattering in solution (V. Bolanos-Garcia)

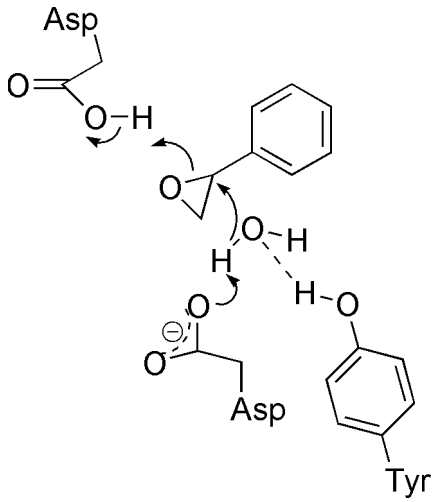

Figure 4.7 Proposed mechanism of limonene epoxide hydrolase from *Rhodococcus erythropolis*

share conserved active site residues with any of the previously studied proteins of this superfamily. However, between MonBI, MonBII, and the domains NanIa and NanIb, there are a number of wholly conserved polar residues, including ones (for example E36 and E64) that are predicted to lie deep within the hydrophobic pocket, and which are plausible candidates as active site residues involved in acid-base catalysis. Although such ideas are somewhat speculative, this analysis served to confirm that the inferred structure of the MonB and NanI proteins is compatible with the proposal that they function as epoxide hydrolases akin to limonene epoxide hydrolase. This is *not* the crux of this proposal, however; the crucial point is that the MonB enzymes have the key role in the cyclisation process.

The newly proposed role for the MonB proteins makes excellent sense. The α/β-hydrolase fold epoxide hydrolases, the family *monCII* was originally thought to be a representative of, are rather large, elaborate enzymes designed to exhibit broad substrate specificity, often involved in xenobiotic detoxification of potentially harmful epoxides[53]. The mechanism of hydrolysis involves the formation of an enzyme-substrate ester intermediate[54] and the molecular oxygen-derived epoxides would not be retained with this mechanism. This is crucial, as the labelling with $^{18}O_2$ is well established[18]. Limonene epoxide hydrolase, in contrast, is an excellent example of a simple and efficient enzyme - a small, compact protein designed to exhibit tight substrate specificity[55]. Further to this, limonene epoxide hydrolase is one of the few enzymes known that are able to process trisubstituted epoxides [56].

It is perhaps very significant that two MonB enzymes catalyse the cyclisation of the putative monensin triepoxide. If one considers the stereochemistry of the epoxides, both of the trisubstituted epoxides result from epoxidation from the *Re* face of each double bond, whereas the disubstituted results from *Si* face epoxidation. It is thus clear why two enzymes might be required to process these stereochemically distinct epoxides. Also, whilst not actively catalysing formation of the A-ring hemiacetal, it is likely that the relevant MonB enzyme only accepts the natural stereoisomer. Thus control of the spiroketal is achieved without a separate enzyme.

So, it is possible to reasonably conclude that the role of the MonB enzymes is to catalyse the cyclisation of the final triepoxide intermediate in the monensin biosynthetic pathway, most likely acting as epoxide hydrolases. In the absence of the

MonB enzymes, the cyclisation of the triepoxide is a stereo- and regiochemically favoured process, with the C9 spiroketal being the only ambiguous centre.

Chapter Five

Approaches to Trapping a Triepoxide

The task of elucidation of the biosynthetic pathway to monensin has now reached a point close to its conclusion – beginning with the hypothetical triepoxide model of Cane, Celmer and Westley through to the classical labelling experiments to sequencing of monensin's biosynthetic gene cluster and, most recently, to the isolation of the monensin triene shunt-metabolite, as described earlier. This was truly a landmark experiment in that it served to help validate the over thirty-year-old triepoxide cyclisation model for monensin biosynthesis and for polyether antibiotic biosynthesis in general. Further, assignment of the geometry of the three double-bonds lent strong support to the original Cane-Celmer-Westley model, in particular. The experiments described in the preceding chapters have now carried this forward to some understanding of how the final intermediate, the triepoxide, is cyclised and the enzymes involved in this process. Thus, it seems, that isolation and characterisation of this final intermediate would represent the apex of this academic undertaking to grasp the entire biosynthetic process from primary metabolites to the complete monensin structure.

In attempting the realisation of this goal, however, one is met with an inherent problem that should be clear from the preceding chapter. It is now evident that the MonB enzymes are likely responsible for conversion of this final intermediate to the polycyclic structure of monensin. Thus, had this been understood before the *monB* deletion experiments had been carried out, it might have been predicted that this would, indeed, lead to the isolation of the triepoxide, just as disruption of *monCI* lead to the isolation of the triene. However, as has been described, this was not the result of this experiment. Instead of the triepoxide, isolation of several other metabolites was the outcome. Detailed consideration of, and interpretation of the implications of these metabolites endorsed the conclusions made as to the role of the monB genes. The problem clearly lies in the observation that, even in the absence of the cyclisation-catalysing enzymes, the triepoxide will tend to cyclise spontaneously, whether entirely "correctly" or not. Apparent partially cyclised triepoxide intermediates were observed in very small quantities, but their identification was only made possible by their behaviour (i.e. conversion to authentic monensins) in the presence of acid. Thus,

it is reasonable to suggest that isolation of the actual open intermediate might be an unrealistic aim.

A Strategy to Prevent Epoxide Opening and Ring Closure

In light of this spontaneous cyclisation problem, it was necessary to develop an alternative strategy to attempting direct isolation of the true final triepoxide intermediate. The tactic was to prevent cyclisation at its origin – closure of the A-ring by attack of the C5 hydroxyl at the C9 carbonyl. The formation of the hemiacetal generates the hydroxyl nucleophile that subsequently opens the first epoxide and closes the B-ring. Complete cyclisation then follows, owing to the facility of this process, as explained in the previous chapter. Thus, it is the presence of the C5 hydroxyl that permits spontaneous cyclisation; without this, cyclisation could not begin. If the C5 hydroxyl could either be removed or altered to destroy its nucleophilicity, the triepoxide system would be trapped, barring other side reactions.

In order to understand the strategy adopted, it is necessary to refer to the process of construction of the polyether backbone on the polyketide synthase. The C5 hydroxyl is created by reduction of the default carbonyl by the ketoreductase on module eleven (*monKR11*). By deleting or inactivating this ketoreductase, in theory, the β-carbonyl would remain unaltered and the chain passed to module twelve for the final round of chain extension. The result would be the polyketide chain with a carbonyl at the C5 position, rather than a hydroxyl. Assuming that the subsequent epoxidation steps occurred as normal, the shunt-metabolite produced would be a triepoxide that could not cyclise in the normal manner (Figure 5.1).

Ketoreductase Inactivation as an Approach to Producing Novel Polyketides

The idea of inactivating a ketoreductase, in order to generate a novel polyketide analogue, is not a new one. The first example of such appeared in 1991, and involved the first modular polyketide gene cluster to be fully sequenced – the deoxyerythronolide B synthase (DEBS), which produces the macrolide precursor to erythromycin. Donaldio and co-workers deleted the ketoreductase (KR4) responsible for production of the C5 hydroxyl in deoxyerythronolide B and were able to isolate 5,6-dideoxy-5-oxoerythronolide B, as predicted (Figure 5.2)[57].

More recently, the delineation of the precise mechanism of reduction by polyketide ketoreductases and the active-site catalytic residues involved[58], has enabled us to understand the how certain ketoreductases that are physically present in a polyketide synthase appear to be inactive. In the monensin cluster, itself, modules one and nine both contain an inactive ketoreductase. If these *were* active, then the polyketide chain would, obviously, have hydroxyl groups positioned in place of the carbonyls. In fact, the effect, in this example, would not be an oxo-analogue of monensin, but an entirely different structure, as the crucial C9 carbonyl would be reduced. So, it appears in this case, that Nature has employed a ketoreductase-inactivation strategy to dramatically alter the product of the biosynthetic pathway. Modern approaches to the purposeful disruption of ketoreductase have mimicked this; site-directed mutagenesis of key catalytic residues has afforded the same outcome as the earlier, more brutal, in-frame deletion approaches. A possible advantage of this newer methodology is a reduced risk of seriously affecting the architecture of the ketoreductase and thus, potentially, compromising the activity of the surrounding enzymes as a consequence of disturbances in protein folding or stability, which may result in lower yields of the desired oxo-analogue or complete abolition of its biosythesis owing to a more thorough disruption of the polyketide synthase. The adjacent acyltransferase domain is aberrantly affected by in-frame deletion of KR6 of the DEBS cluster, with the corresponding site-directed mutant shown to have better catalytic activity. This methodology, utilising the Tyr→Phe mutation (see below), has been successful in generating novel analogues of the cytotoxic epothilones, for example – lead compounds as potential anticancer agents[59].

Despite this clearly superior methodology, the in-frame deletion strategy has recently been successfully employed in producing an oxo-analogue of nanchangmycin, the polyether antibiotic relative of monensin[49].

Catalytic Mechanism of Polyketide Ketoreductases

Although the mechanism of reduction by ketoreductases is not a straightforward matter if the stereochemistry of the hydroxyl product is considered[60], for our purposes, it is sufficient to discuss the general mechanism of catalysis. The basic catalytic triad of the ketoreductase consists of tyrosine, serine and lysine. Tyrosine acts as the proton-donor to the carbonyl oxygen in the reduction, whilst the serine is thought to stabilise substrate binding, by means of hydrogen-bonding interactions.

The positively charged ammonium group of lysine acts to lower the pKa of the tyrosine hydrogen through ionic interactions, whilst also providing hydrogen-bonding interactions with the nicotinamide ribosyl moiety of the NADPH co-factor (Figure 5.3). Site-directed mutagenesis studies have shown that point mutations, at any one of these positions, have a highly detrimental effect on the activity of the enzyme. Most notably, mutation of the catalytic tyrosine in DEBS KR6 completely abolishes activity.

Approaches to Inactivation of Monensin Ketoreductase 11

Rather than rely upon a single approach to devastating KR11, it was decided that both the classical, in-frame deletion approach and the modern site-directed mutagenesis methodology would be attempted in parallel. For reasons discussed earlier, whilst ensuring abolition of KR activity, the in-frame deletion approach might also have additional detrimental effects on the PKS and thus this method could not be relied upon. Also, as point mutations in the monensin PKS KRs, or those of polyether antibiotics in general, are unprecedented, one could not be sure that mutations, analogous to those created in other polyketide KRs, would completely abolish activity.

Sun *et al*, recently performed the aforementioned mutation of KR6 of the nanchangmycin PKS by removing 62 internal amino acids in-frame. It was decided that a similar approach would be utilised for KR11 in the monensin PKS. However, somewhat arbitrarily, only 33 amino acids were deleted. It was reasoned that this would be more than sufficient to abolish activity of the enzyme. Although, in theory, the mutation in wild-type *S. cinnamonensis* should have the same effect, the mutation was created in the ΔBII mutant; this decision will be discussed shortly. Conventional in-frame deletion methodology was employed to yield the KR11 mutant with 33 amino acids excised; the E. Coli/Streptomyces shuttle vector, pKC1139[61], containing the temperature-sensitive psG5 replicon, was used to introduce the deletion via homologous recombination with a double crossover[62] (Figure 5.4; see experimental section, Ch.9, for details).

Owing to its catastrophic effect on KR6 of the DEBS cluster, the catalytic tyrosine (Tyr-150) was mutated to phenylalanine, using the same methodology as for the in-frame deletion, and was also created in the Δ*monBII* mutant.

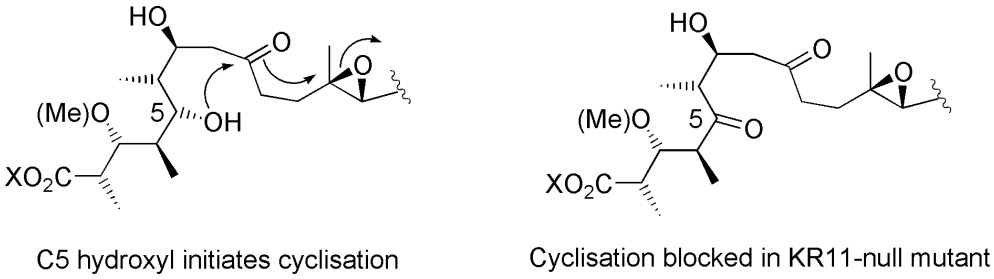

Figure 5.1 Preventing cyclisation of triepoxide by removing nucleophilic C5-hydroxyl

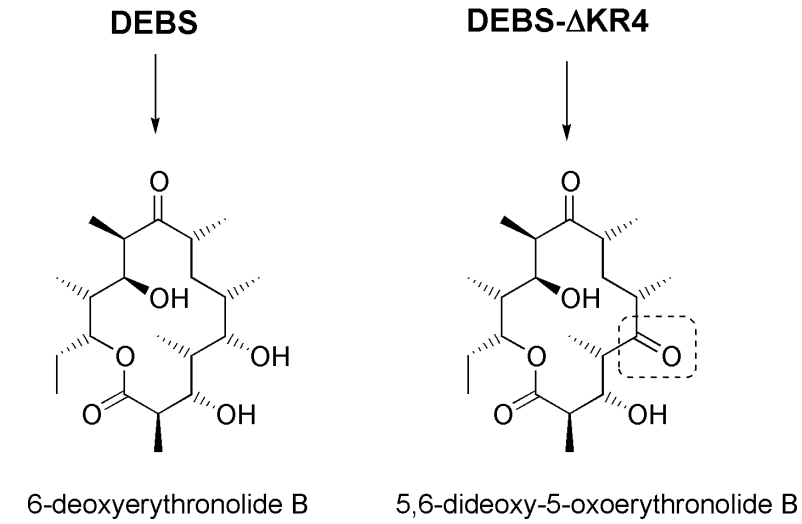

Figure 5.2 Production of a novel oxo-analogue of deoxyerythronolide B by inactivation of DEBS-KR4.

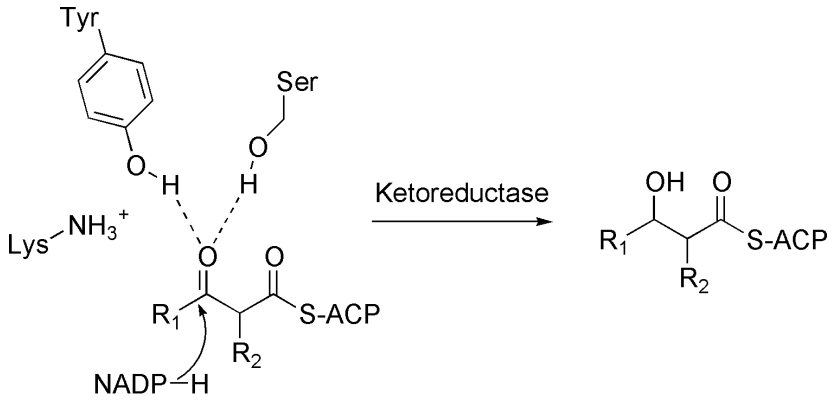

Figure 5.3 Basic mechanism of carbonyl reduction by a ketoreductase

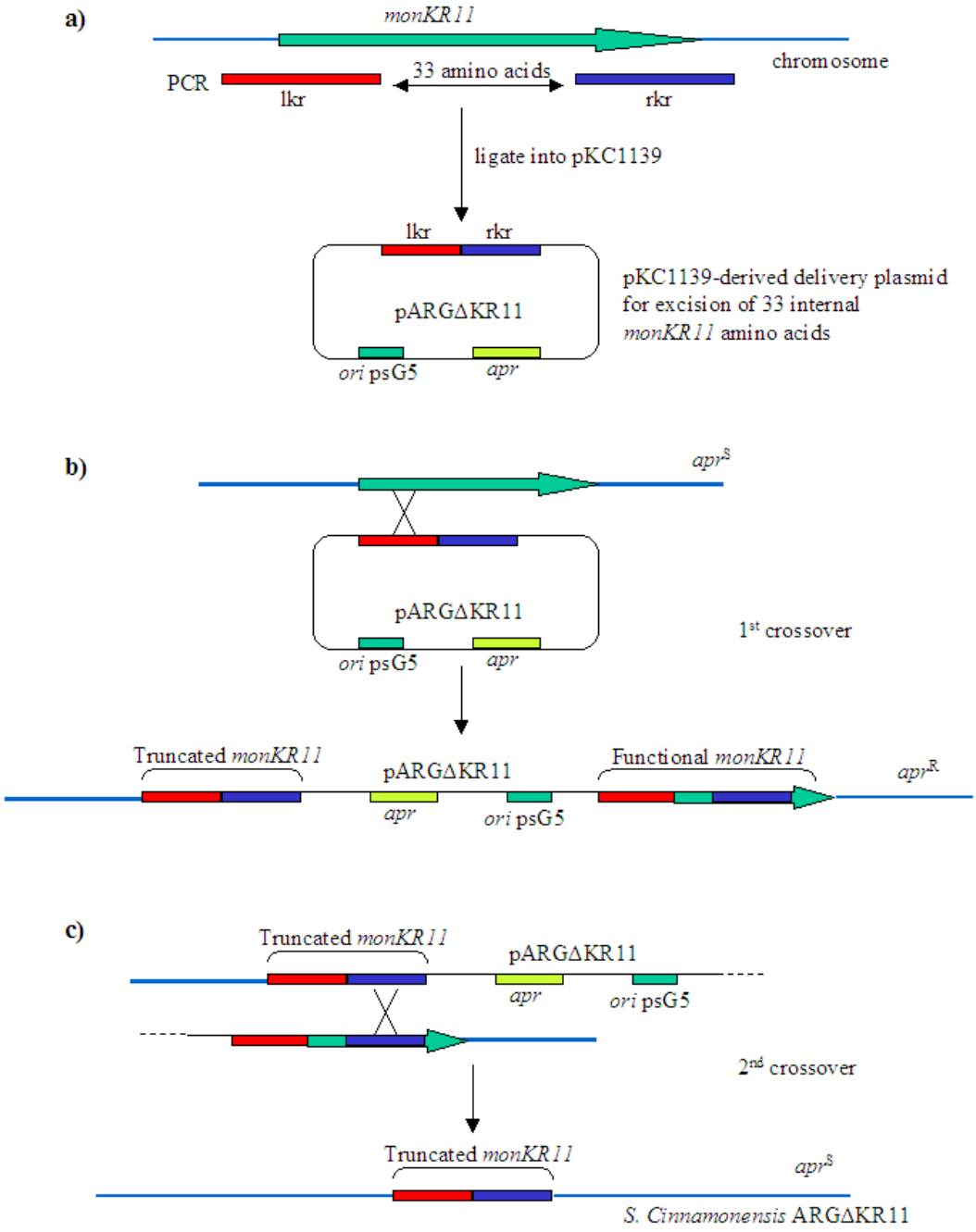

Figure 5.4 General approach to inactivation of *monKR11* by successive homologous recombination (*double crossover*). a) Construction of pARGΔKR11; b) 1st crossover resulting in plasmid insertion and apramycin resistance; 2nd crossover resulting in excision of plasmid and complete mutation with loss of apramycin resistance.

Expectations of the KR11 Mutations

Before describing the results of the mutations, it is helpful to explain how, ideally, the mutations would affect the metabolite profile of the ΔBII mutants and, in doing so, should clarify why the ΔBII mutant was chosen over the wild-type for this experiment.

One of the most striking, and, initially, most puzzling, features of the metabolite profile of the ΔBII mutant, is the appearance of the very polar (early eluting in the LCMS trace) species, that have now been identified as being the partially cyclised triepoxides. Now, the aim of this experiment was to prevent this cyclisation by removal of the C5 hydroxyl that initiates this cyclisation. Thus, according to this model, the successful inactivation of KR11 would satisfy this aim. So, one should expect, for each of the monensin analogue masses, this range of polar partially cyclised species to be replaced with a single species with a mass loss of 2Da for each of the masses seen in the ΔBII mutant (i.e. a single 691 species instead of a range of 693 species, etc). Each of these species would represent a deoxy-5-oxo-triepoxide in a neatly revealing manner (Figure 5.5).

The Effects of the KR11 Mutations

Considering, firstly, the in-frame deletion experiment, as expected, removal of 33 amino acid residues from the middle of monKR11 did indeed completely abolish its activity. The metabolite profile also changed dramatically; the polar partially cyclised range of metabolites were no longer produced. Further to this, as hoped, a single peak was observed with mass 691 (corresponding to the C5-deoxy-oxo derivative of the premonensin A triepoxide), likewise with mass 677 (C5-deoxy-oxo premonensin B triepoxde, or the corresponding C3-demethyl derivative of premonensin A triepoxide). A species with mass 663 was not clearly observed, suggesting that its production was diminutive, or that the C3-demethylated species were not produced and, thus, 677 corresponded to the premonensin B triepoxide, although the production level of species 677 was much higher than that of species 691. Subsequent MSMS fragmentation confirmed this, as loss of methanol was observed in both species, which could only arise from the C3-methoxy position. The peaks were not separated in the LCMS, but co-eluted with a degree of smearing. Their elution times were as expected, occurring around 7-9 minutes, suggesting a polarity similar to the partially

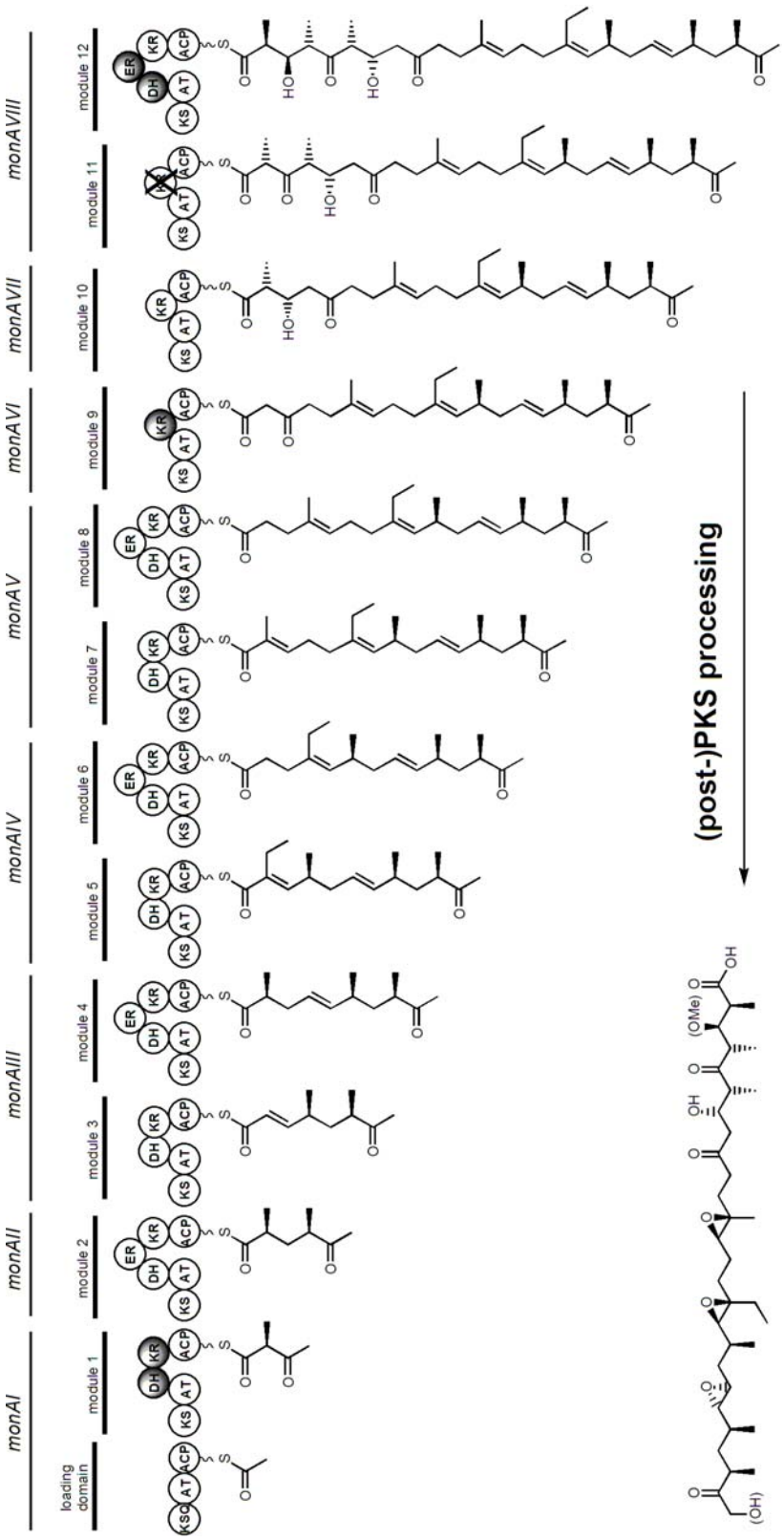

Figure 5.5 Formation of an oxo-analogue of the triepoxide precursor to monensin A by inactivation of *monKR11*

cyclised species observed in the *monB* mutants (Figure 5.6). Additional masses were observed, 695 and 709, which suggest the addition of water, possibly as a result of hydrolysis of one of the epoxides, or ketone hydration. A mass of 723 was also observed as a very small peak in the mass spectrum, suggesting further hydration reactions. Owing to the likely inherent reactivity of the epoxides, this was in no way surprising. Importantly, none of these species were observed in the putative mutants that had, in fact, reverted to the ΔBII mutant at the second crossover.

So far, limited high-resolution mass spectral studies have been performed on these species, but masses of all the species (barring 695, which was present in too small a quantity to be observed) have been obtained to an accuracy of within 1ppm. Also, some high-resolution MSMS fragmentation studies have confirmed the expected methanol and water losses, but further work is needed to elucidate the complete fragmentation pathways (Figure 5.7-5.9).

The tyrosine→phenylalanine mutation did not have the expected effect on *monKR11*. Although the point mutation *did* produce the species as observed in the in-frame deletion mutant, these appeared as part of a mixture; a quantity of the partially cyclised species characteristic of the monB mutants, as well as much more demethylmonensin A, were also present, as was C9-*epi*-26-deoxy-monensin A eluting ~20min (Figure 5.10). This suggests that mutation of the active site tyrosine is, in itself, insufficient to completely abolish the activity of the enzyme. It is possible that a nearby proton donor was able to substitute for the tyrosine in the active site, though somewhat less efficiently.

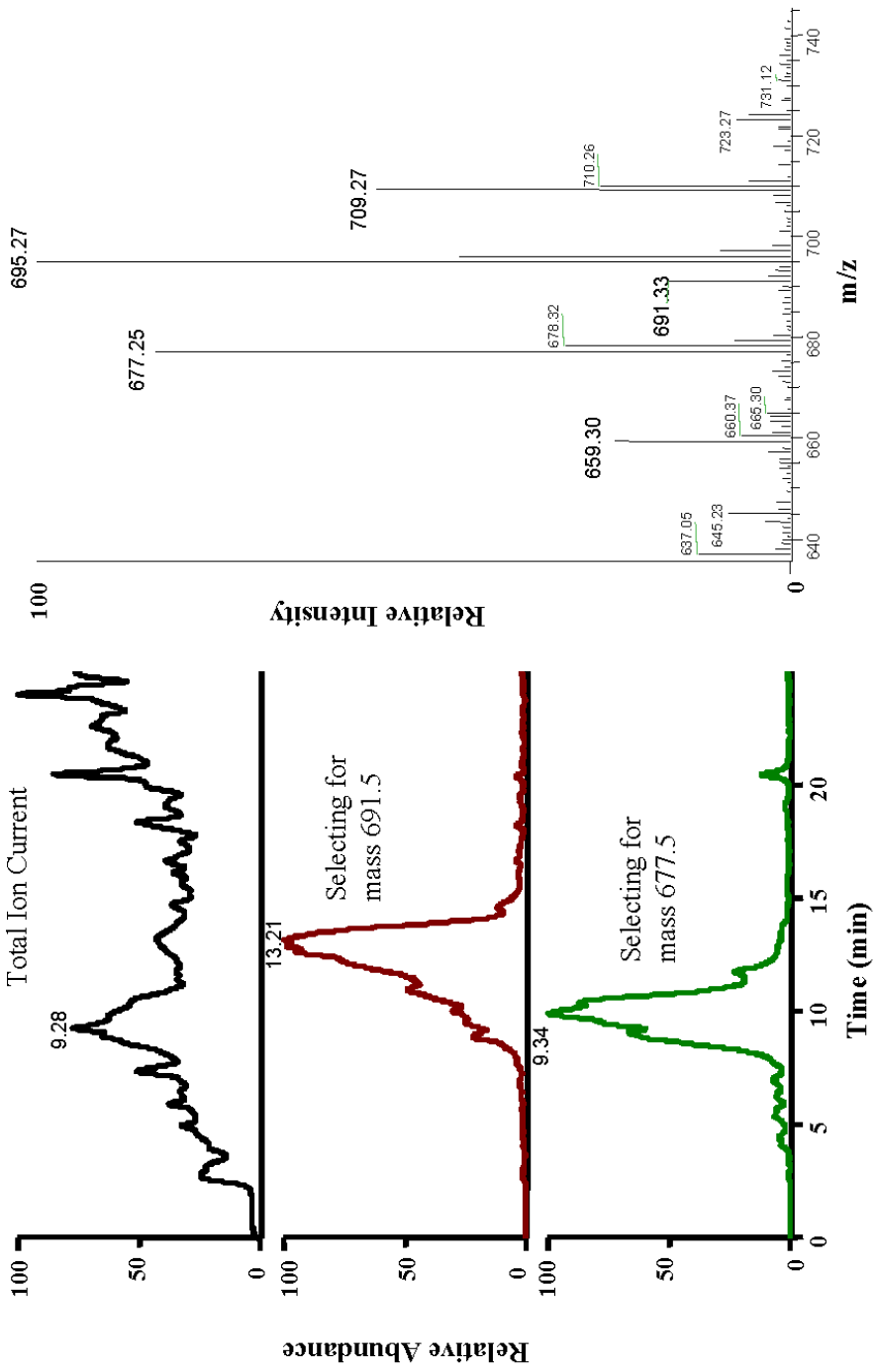

Figure 5.6 LCMS trace of *S. cinnamonensis* Δ*monBII,* Δ*monKR11*

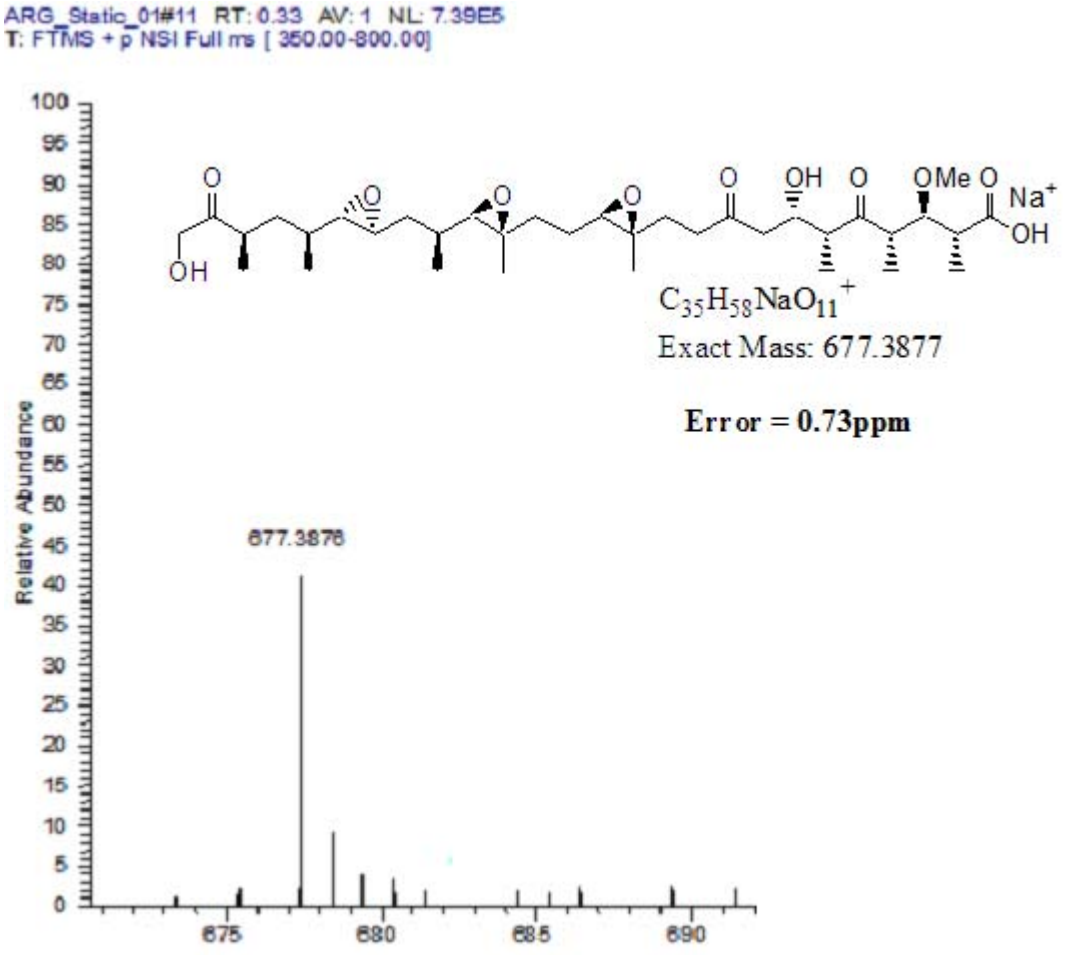

Figure 5.7 High resolution mass of putative oxo-analogue of monensin B triepoxide precursor.

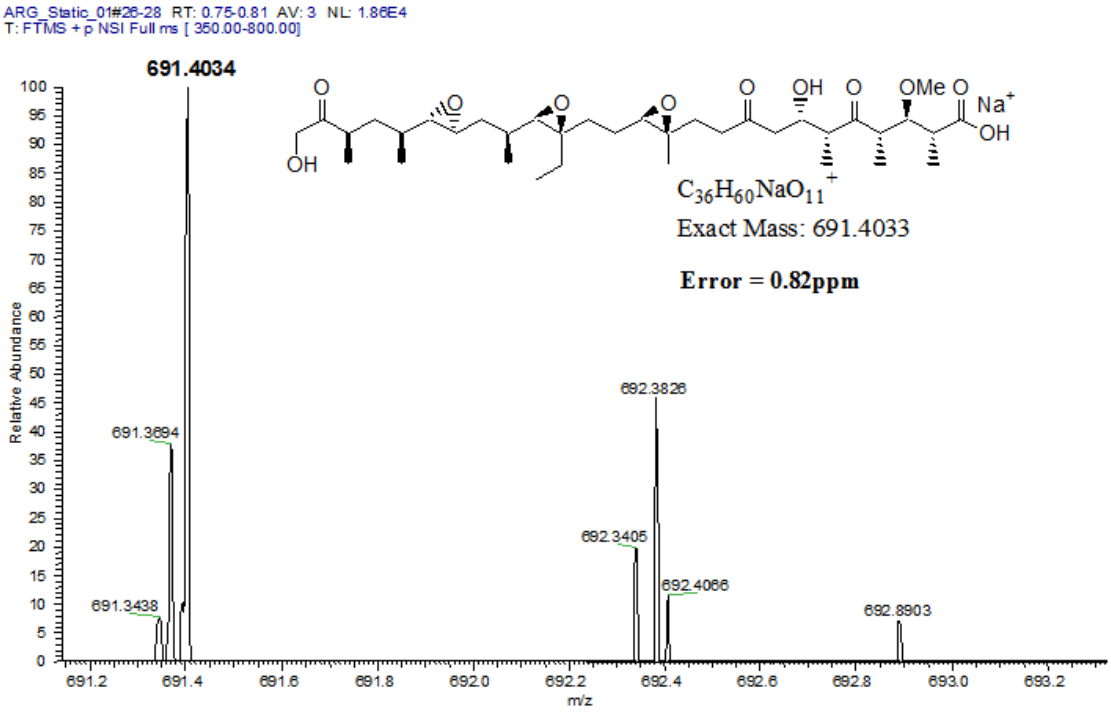

Figure 5.8 High resolution mass of putative oxo-analogue of monensin A triepoxide precursor.

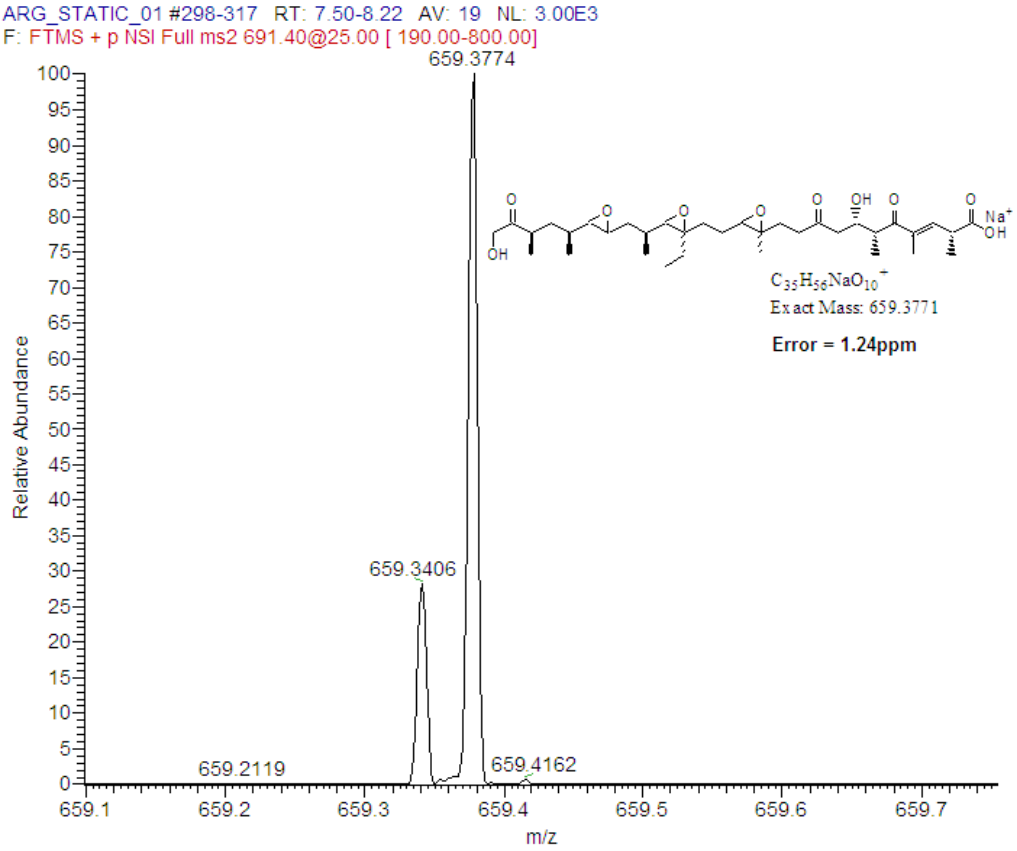

Figure 5.9 High resolution mass of MS/MS methanol-loss peak from species (m/z = 691.4034) in figure 5.8.

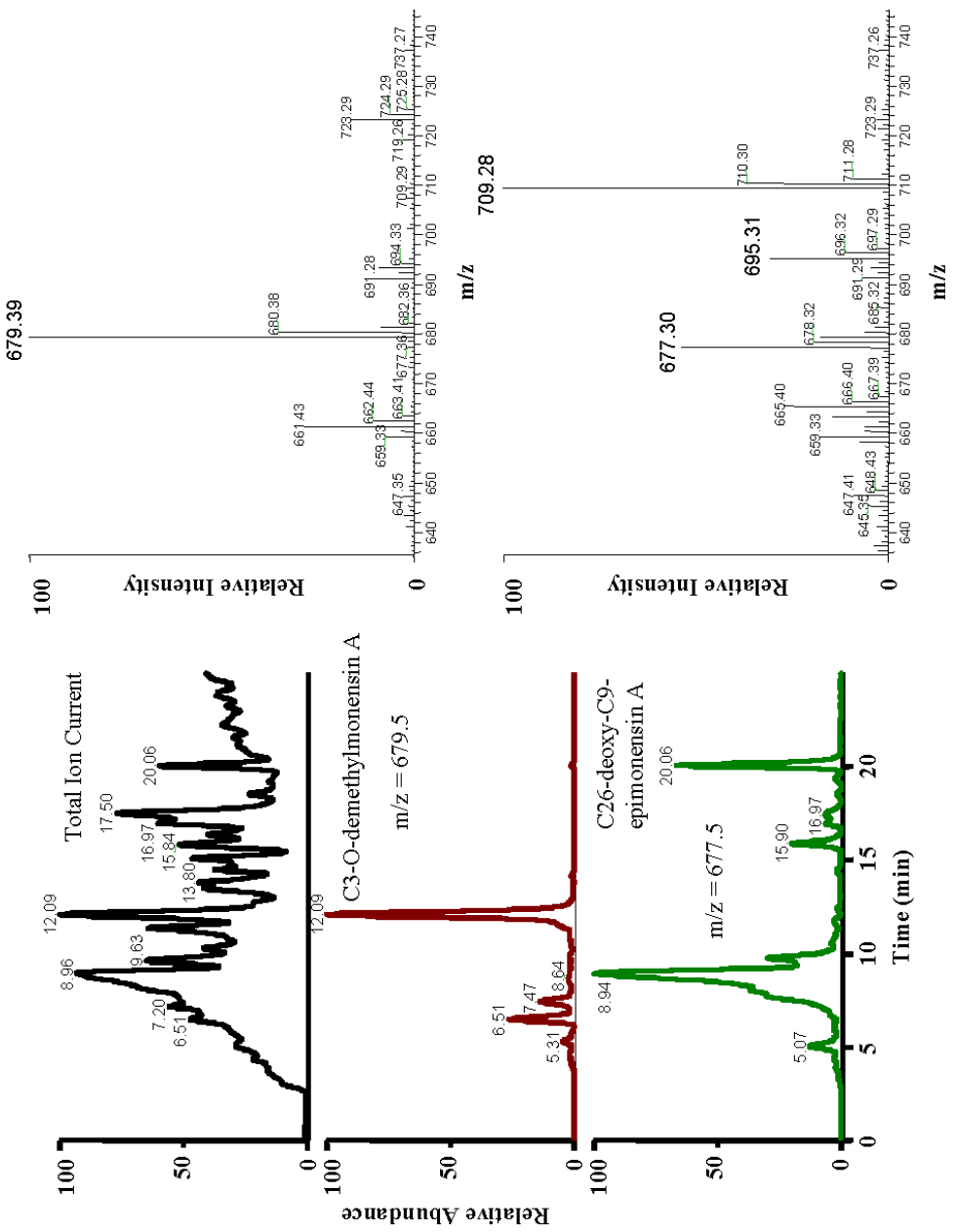

Figure 5.10 LCMS trace of *S. cinnamonensis* Δ*monBII*, *monKR11*[Y150F].

Chapter Six

Introduction to Marine Polyethers and their Structural Characteristics

Polyketide-derived marine polyethers are dichotomously distinct from the terrestrial, *Streptomyces*-derived polyethers. All polyketide-derived marine polyethers, thus far isolated, have a contiguous, fused ring system, with each oxygen constituting a single-atom bridge between adjacent rings (terpene-derived marine polyethers, in contrast, often contain both fused and non-fused ring systems)[63]. This gives them a characteristic ladder-like appearance, hence they are generally referred to as ladder polyethers. There are, up to this point in time, fourteen distinct ladder structures, distributed into various classes.

The Brevetoxins

The first of the ladder polyethers to be isolated were the brevetoxins A[64] and B[65], isolated from the dinoflagellate, *Karenia brevis* (formerly *Gymnodinium breve*). Since then, a total of 10 analogues of both brevetoxin A and B have been isolated; these are notated from PbTx-1 to PbTx-10, according to the numbering system of Shimizu[66] (Figure 6.1). These can be subdivided into two subclasses, according to the structure of their ring systems. Brevetoxin A (PbTx-1), PbTx-7 and PbTx-10 are known as Type 1 (or Type A), and PbTx-2, PbTx-3, PbTx-5, PbTx-6, PbTx-8 and PbTx-9 are the Type 2 (or Type B) brevetoxins. Within each subclass, the brevetoxins differ only in the structure of the chain at the 'tail' end of the molecule (except PbTx5 and PbTx6, which can be considered PbTx-2 derivatives, with an epoxidised H-ring and acetylated C37-hydroxyl, respectively). There is, as yet, no structural information published on PbTx-4. Four additional brevetoxins, based on the Type B backbone, have also been reported; BTX-B1, BTX-B2 and BTX-B4 have very unusual tail structures, whereas BTX-B3 appears to have undergone an unusual oxidative D-ring opening and esterification with either a C14 or C16 fatty acid[67].

The brevetoxins have long been associated with the 'Red Tide' phenomenon, caused by the dense aggregation of a variety of toxin-producing unicellular

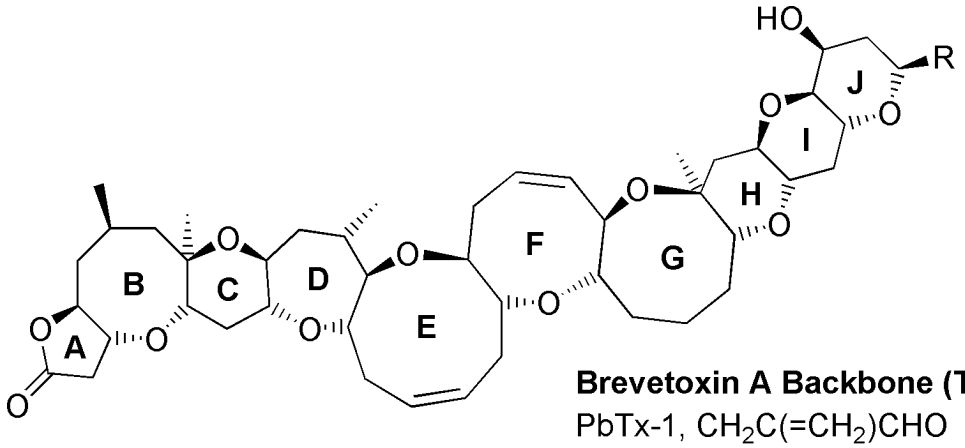

Brevetoxin A Backbone (Type 1), R=
PbTx-1, $CH_2C(=CH_2)CHO$
PbTx-7, $CH_2C(=CH_2)CH_2OH$
PbTx-10, $CH_2CH(CH_3)CH_2OH$

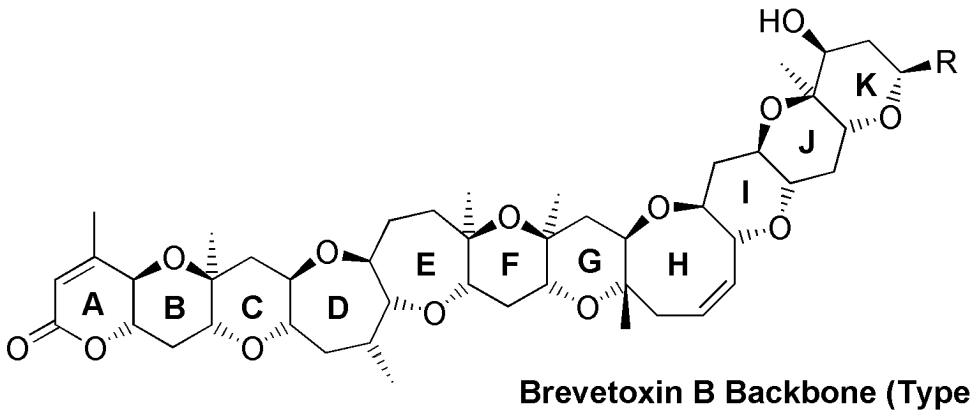

Brevetoxin B Backbone (Type 2), R=
PbTx-2, $CH_2C(=CH_2)CHO$
PbTx-3, $CH_2C(=CH_2)CH_2OH$
PbTx-5, [PbTx-2, C37 OAc]
PbTx-6, [PbTx-2, H-ring epoxide]
PbTx-8, CH_2COCH_2Cl
PbTx-9, $CH_2CH(CH_3)CH_2OH$

Figure 6.1 Structures of the brevetoxins.

phytoplankton, including *K. brevis*. This is characterised by a deep discolouration of the sea-water as a result of the dense algal blooms and accumulation of dead and dying fish. These Red Tides pose a serious threat to aquatic ecosystems by killing a range of flora and fauna[68].

Biological Activity of the Brevetoxins

The toxicity of the brevetoxins results from their interaction with voltage-sensitive sodium channels (VSSCs), located in the membranes of various excitable cells. The α-subunit (the channel itself) comprises 24 transmembrane helices, grouped into four domains (I-IV), each of which is subdivided into six subdomains (S1-S6). The channel has three functionally distinct conformations – open, closed (or resting) and inactivated. Only the open state is conducting (allows Na^+ influx). Depolarisation of the neuronal (or other excitable) cell membrane triggers the closed→open transition. The channel will then go into an inactivated, non-conducting state before returning to its closed (resting) state[69]. The brevetoxins bind 'head-down' between domains III and IV, at a unique site (Site 5), located on domain IV (Figure 6.2). The major effect of this is a shift of the threshold activation potential of the channel to a more negative membrane potential, causing the channel to be open even at resting potentials[70], and is likely caused by a conformational change in the channel protein induced by brevetoxin binding. Another effect of this is a prolonged opening of the channel caused by a destabilisation of the inactivated state or by it being made kinetically inaccessible (slowing the open→inactivated transition) (Figure 6.3). Overall, the result is an increase in conductance across the membrane, caused by excess Na^+ influx, owing to the prolonged 'mean open times'. It is this excitatory effect on neuronal membranes that is responsible for most of the toxic effects (e.g. convulsions and cardio-ventricular fibrillations)[71].

The Ciguatoxins

The ciguatoxins were originally named as being associated with a type of food poisoning known as 'ciguatera', which is caused by the ingestion of many species of fish in subtropical and tropical regions of the worlds, with 20,000-60,000 cases being reported annually. One of the major culprits is a small surgeon-fish, *Ctenochaetus striatus*, which accounts for ~65% of ciguatera outbreaks in Tahiti. This fish was

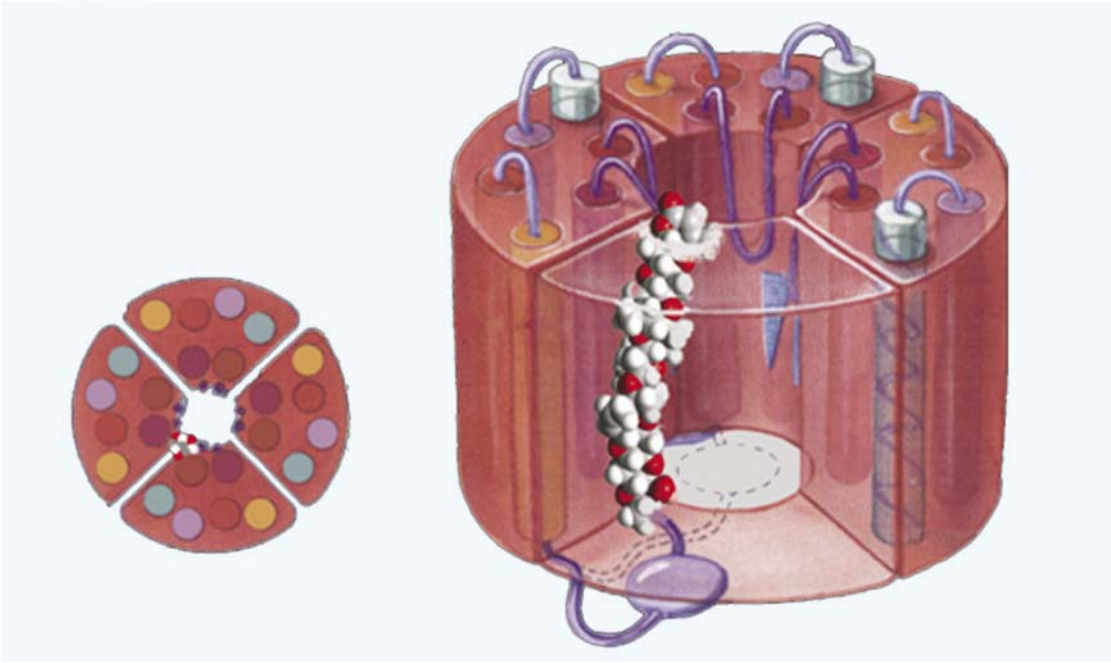

Figure 6.2 Binding of brevetoxin to voltage-sensitive sodium channel (VSSC) (adapted from Baden *et al* 2005)

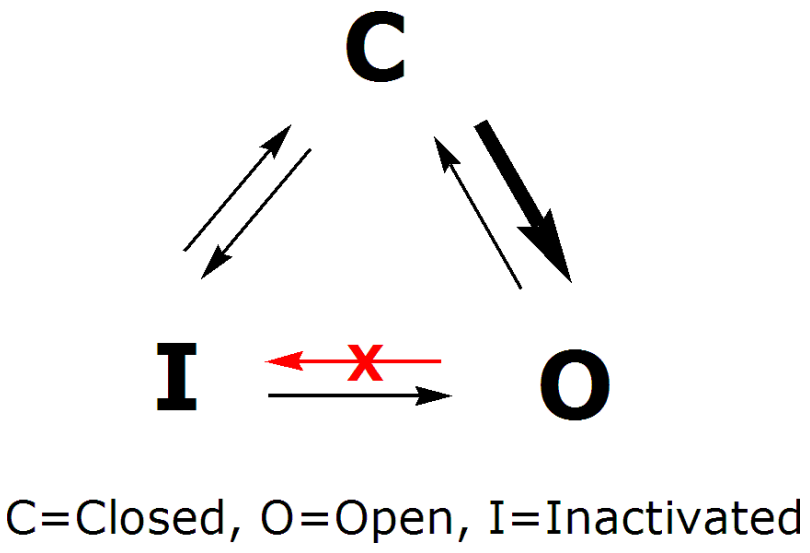

Figure 6.3 Representation of brevetoxin's effects of VSSCs (adapted from Baden *et al* 2005)

frequently found in the stomach of larger, carnivorous fish, implying that it may represent an important link to the larger fish often responsible for poisoning. The digestive contents of this fish were found to contain an abundance of the disk-shaped dinoflagellate, *Gambierdiscus toxicus*, which grows densely on the surface of certain calcareous algae[72]. Cells of *G. toxicus* were collected and found to contain a lipophilic toxin, which was named ciguatoxin (CTX). They also contained a more polar toxin, which was later identified as maitotoxin (MTX). Cultured cells of *G. toxicus* confirmed that the dinoflagellate itself, rather than any other contaminant organism, was the producer of the toxins[73].

Structures of the Ciguatoxins

The structure of CTX was not determined for over ten years, and required the collection of 4 tons of moray eels from ciguatera-endemic areas of French Polynesia. 124kg of the eel viscera was extracted to yield 0.35mg of pure CTX[74]. Additionally, five other CTX analogues were isolated (each with the same ring structure as CTX, but with differing side chains, as will be seen), as well as an analogue (CTX-3C) with a slightly different ring structure, in which an eight-membered ring was present in place of the seven-membered ring of the other analogues[75]. Since this time, a total of six ciguatoxin analogues have been characterised (CTX-1, CTX-2, CTX-3, CTX-4A, CTX-4B and CTX-3C), with each having one of the two ring backbone structures initially exemplified by CTX (Type 1 backbone) and CTX-3C (Type 2 backbone – notably, CTX-3C is, thus far, the only member of this family). In addition to this, are the more recently isolated Caribbean ciguatoxins (C-CTX-1 and C-CTX-2, differing only in the configuration of the terminal hemiacetal), which have the Type 2 backbone structure, but contain an additional ether ring[76] (Figure 6.4). A variety of congeners (hydroxy-, deoxy-, oxo-, methoxy-, seco-, etc.) have also been identified, in minute quantities, by FAB mass spectrometry. These are simply thought to be metabolic products of the parent ciguatoxins[77].

Biological Activity of the Ciguatoxins

The pharmacological effect of the ciguatoxins is identical to that of the brevetoxins, as discussed, and is mediated mainly through binding at a specific site (Site 5) on the

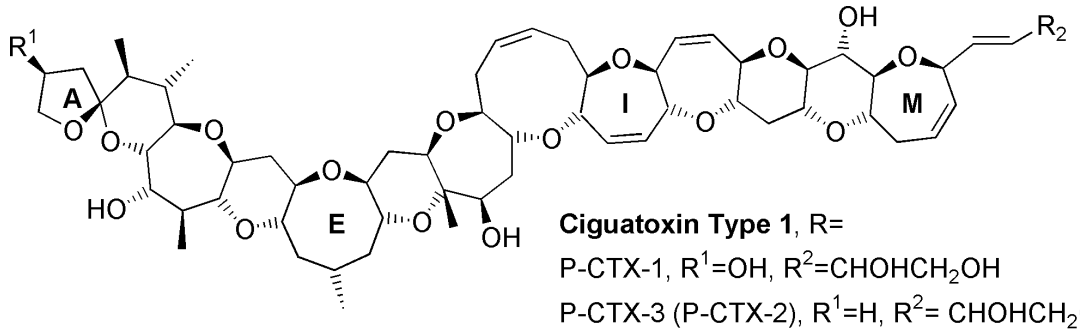

Ciguatoxin Type 1, R=
P-CTX-1, R^1=OH, R^2=$CHOHCH_2OH$
P-CTX-3 (P-CTX-2), R^1=H, R^2= $CHOHCH_2OH$
P-CTX-4B (P-CTX-4A), R^1=H, R^2=$CHCH_2$

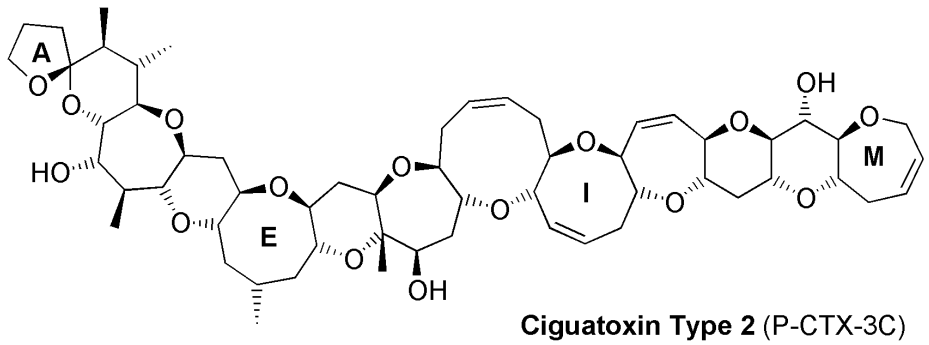

Ciguatoxin Type 2 (P-CTX-3C)

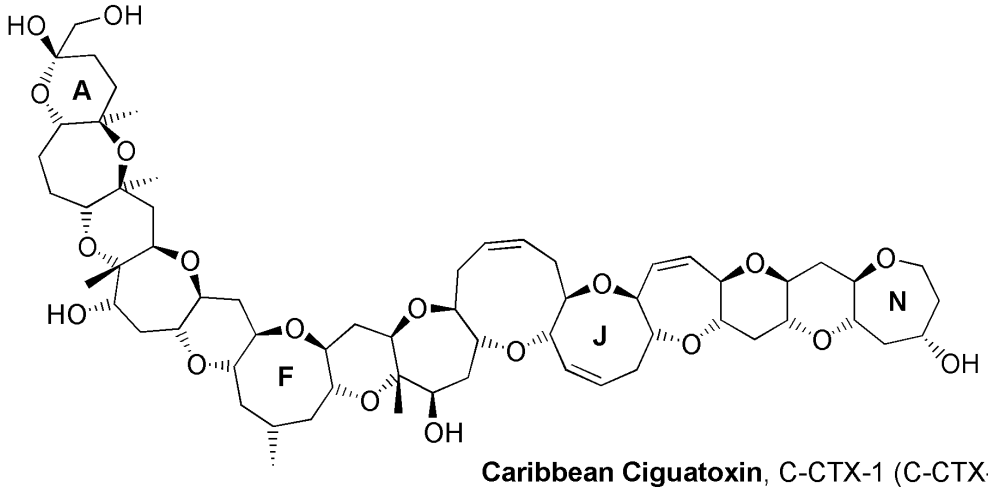

Caribbean Ciguatoxin, C-CTX-1 (C-CTX-2)

Figure 6.4 Structures of the ciguatoxins.

voltage-sensitive sodium channel (VSSC). Indeed, ciguatoxin competitively inhibits the binding of brevetoxin at this site[78]. As with the brevetoxins, this binding causes the threshold firing potential of the neuron to be shifted to more negative membrane potentials. Thus, the neuron requires a lesser degree of depolarising stimulation before initiating an action potential and, hence, neuronal excitability is increased[79]. Like the brevetoxins, this is probably a result of a CTX-induced conformational change in the channel protein. However, the affinity of the ciguatoxins to VSSCs in fish is four-fold lower than brevetoxin B. Thus, the ciguatoxins, whilst exhibiting significant ichthyotocixity, are far less toxic to fish than the brevetoxins. It is this feature that allows them to accumulate in a huge variety of relatively large edible fish, through the food chain, from dinoflagellate upwards. Conversely, the ciguatoxins are more than ten times more potent at mammalian VSSCs than brevetoxin B, thus explaining their high toxicity in humans[80].

Structure-Activity Relationships of the Brevetoxins and Ciguatoxins

All natural brevetoxins have certain structural characteristics in common. The 'head' of the molecule consists of a lactone ring (A-ring) and the 'tail' is a rigid system of four rings. Various modifications occur at this end of the molecule, giving rise to the various brevetoxins, as discussed. The 'head' and 'tail' are separated by a more flexible, 'spacer', region; all active natural and synthetic derivatives of the brevetoxins possess these three features (Figure 6.5). Alterations in the lactone 'head', the rigid 'tail', or shortening of the flexible 'spacer', have all been shown to have dire effects on activity[81].

Although brevetoxin B was initially described as a "rigid ladder-like structure"[65], the medium-sized rings of both types of brevetoxin ring system, and the ciguatoxins, suggest more flexibility. Indeed, no rigid conformations exist of monocyclic saturated ether rings above six-membered, although conformational restraints *are* imposed when the ring is internal to fused flanking rings, as with these structures[82]. The potential conformational complexity of the toxins increases from brevetoxin B (with 16 rotatable bonds), to brevetoxin A (31 rotatable bonds), to ciguatoxin (38 rotatable bonds). For the brevetoxin B backbone, there are only two areas where the molecule might flex: the two 7-membered D and E-rings, and the 8-membered H-ring. Computational studies have shown that brevetoxin B is relatively

rigid, and possesses two major low-energy conformations – essentially straight and bent[83].

The brevetoxin A backbone is inherently more complex. Firstly, the B-ring, adjacent to the A-ring lactone, is 8-membered, and can occupy two essentially isoenergetic conformations: a crown and a boat-chair. However, when these conformations are superimposed, the position of the lactone is unaffected, suggesting that the flexibility of the B-ring may not be significant with respect to binding.

The second important feature concerns the 'tail' regions of both brevetoxins. The four terminal rings of each (G-J in BTX-A and H-K in BTX-B) are virtually identical, differing only in a double-bond (in the H-ring of brevetoxin B) and the position of two methyl groups. The important point here, however, is that both the G-ring of brevetoxin A and the H-ring of brevetoxin B have the same preference for the boat-chair conformation, which is essential for binding[84]. It is likely, therefore, that these structurally, and conformationally, analogous tails occupy the same region in the binding site.

This is not the end of the story, however, as the 'spacer' regions of brevetoxins A and B are markedly different, although both molecules maintain a low energy 'straight' conformation and the same 30Å length necessary for binding. The 'spacer' of brevetoxin A, with its 8- and 9-membered E and F-rings, is more flexible and has a larger variety of available conformations. Brevetoxin A also has a higher binding affinity than brevetoxin B, possibly suggesting the more flexible brevetoxin A may wrap around, or fold into or against, its binding site, thus allowing a tighter fit. It has been suggested that the flexibility of the polyether backbones is directly related to their relative toxicities[83]. Indeed, in mice, the binding affinity to VSSCs is proportional to toxicity. It is possible that the flexibility of the molecule allows it, once bound (by 'head' and 'tail'), to induce the conformational change in the channel protein that results in the observed effects on its activation, or, that the process of binding itself induces this change. Notably, ciguatoxin is both the most flexible and toxic of the three classes of VSSC toxins discussed so far. It is interesting to note that ciguatoxin is known to undergo a slow, spontaneous, conformational change around the 8-membered F-ring and the 7-membered G-ring, which can be observed by broadening of peaks in the ^{1}H-NMR. It has been suggested that this sort of conformational movement may account for ciguatoxin's activation of VSSCs once bound[85].

Although conformational studies on other polyether ladders are lacking, an interesting and characteristic feature of the fused polyether structure begins to emerge, which may explain Nature's utilisation of these structures. The brevetoxins and ciguatoxins are examples of flexible molecules with a defined shape, essentially populating one or two conformations whilst maintaining full conformational flexibility. In general, the design of a fused polyether can be tailored to exhibit very specific characteristics; small, 5 and 6-membered rings can be utilised to create strictly rigid sections of polyether with a well-defined shape, whilst medium-sized, 7 to 9-membered rings, can be used to create sections with controlled degrees of conformational mobility with well-defined energy barriers between conformers[86]. Varying degrees of saturation and functionalisation may also be employed. This strategy appears to have been exploited in the construction of the brevetoxins; both types exhibiting the necessary lactone 'head' and 'tail' section structures, both necessary for binding, whilst brevetoxin A employs larger rings in the 'spacer' region (without affecting the overall length of the molecule); this gives it additional flexibility, resulting in tighter binding and higher toxicity. Ciguatoxin, analogously, has a flexible F-G ring system that appears to undergo slow conformational changes with no distinct energy minima; this feature may well be related to its biological activity. At this point, however, more detailed conformational studies on ciguatoxin are absent. Figure 6.6 shows two analogous synthetic heptacyclic polyethers, and illustrates the effect of rearranging a six and seven-membered ring on the conformation and flexibility of the molecule.

Gambierol and the Gambieric Acids

The initial analyses of *Gambierdiscus toxicus*, by the Yasumoto group, afforded not only pure samples of the two types of ciguatoxins, but also two other novel polyether ladders, gambierol and gambieric acid[87] (Figure 6.7). Although displaying no toxicity towards mice, gambieric acid was found to have unprecedented antifungal activity against *Aspergillus niger*, inhibiting its growth with a potency exceeding that of amphotericin B by a factor of 2×10^3[88]. Four analogues of gambieric acid, denoted A-D have now been fully characterised[89]. Gambierol[90], however, was found to be a potent toxin in mice, with effects resembling those of ciguatoxin, suggesting it might play a role in ciguatera poisoning[91].

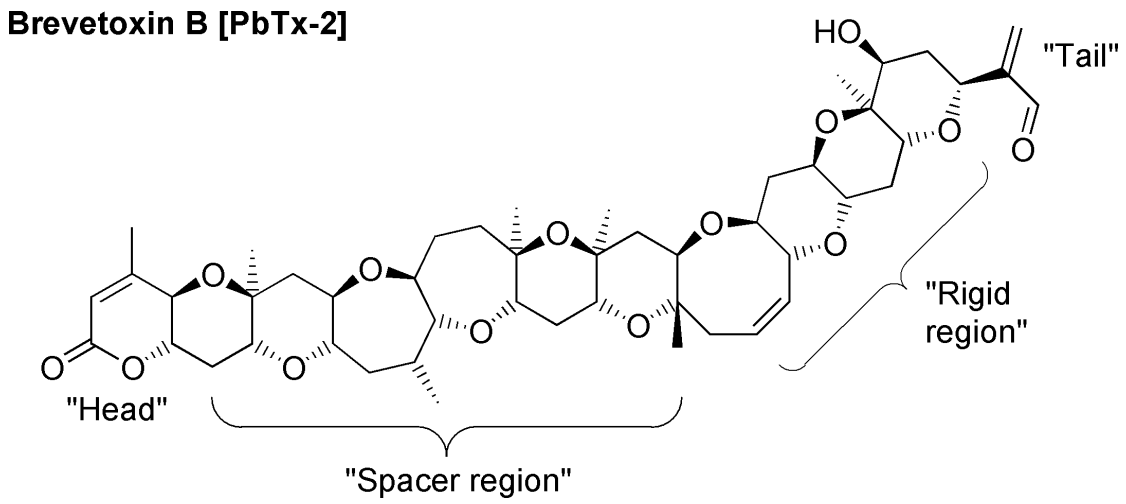

Figure 6.5 Structural features of brevetoxins (Type A and B) necessary for activity (redrawn from Baden *et al* 2005)

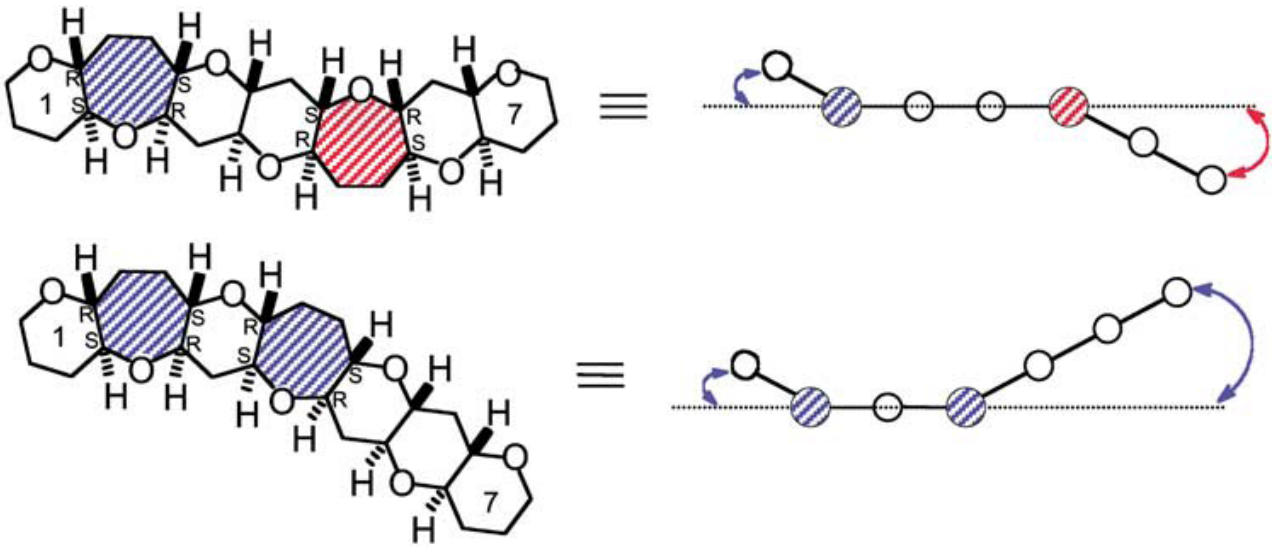

Figure 6.6 Effects of ring rearrangements on fused polyether conformation and flexibility (adapted from Candenas *et al* 2002)

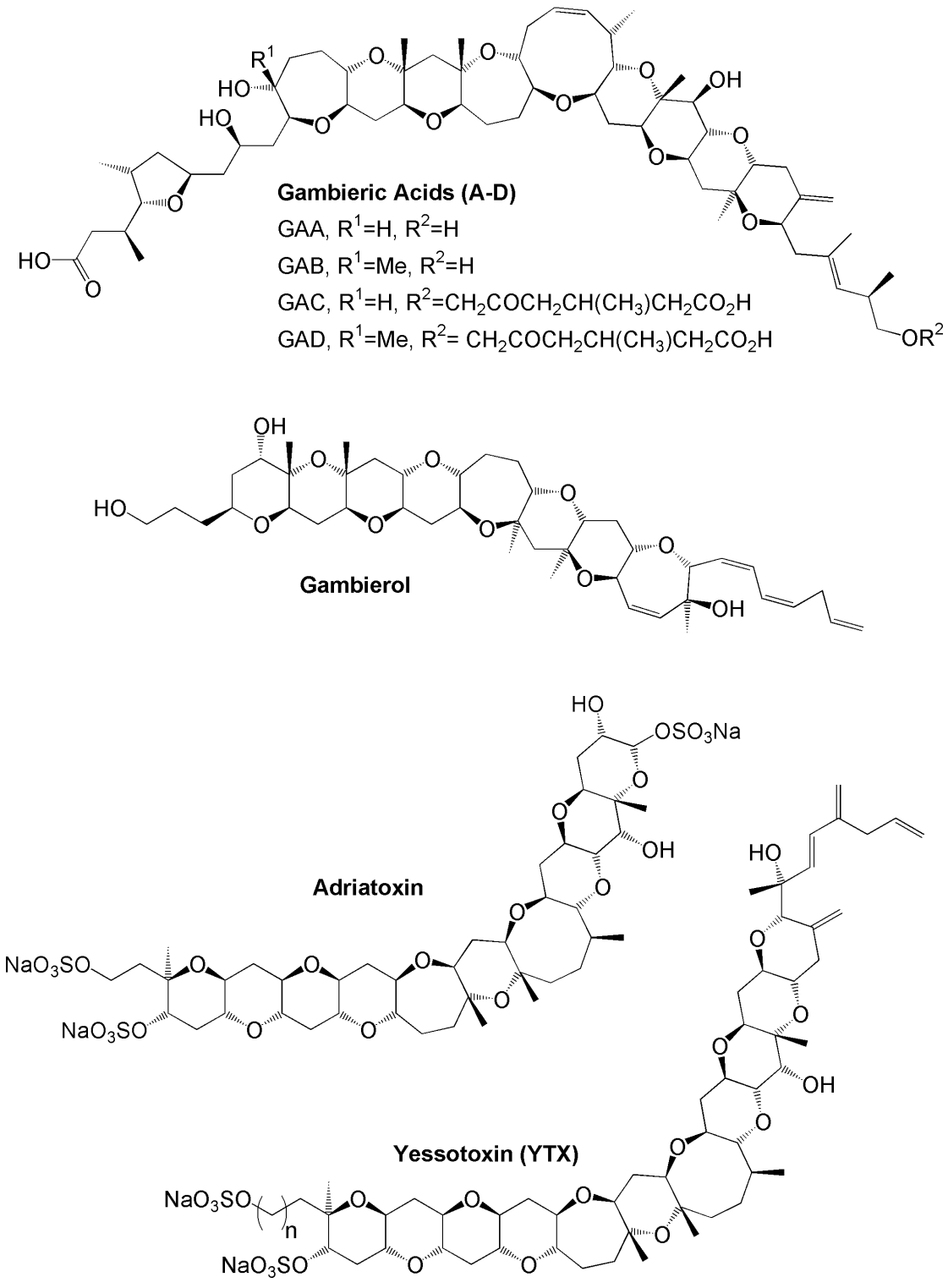

Figure 6.7 Structures of the gambieric acids, gambierol, adriatoxin and yessotoxin.

The Yessotoxins

Yessotoxin is a disulphated polyether ladder consisting of eleven fused rings, first isolated from the digestive glands of the scallop, *Patinopecten yessoensis*[92], and later found to be produced by the dinoflagellate, *Protoceratium reticulatum*[93]. Since its first isolation, a number of analogues of the original structure have been characterised, differing only by the structure of the terminal side-chain[94], although a glycosylated derivative has recently been isolated[95], which is the first example of such a derivative amongst all known polyether ladders. A truncated version of yessotoxin has also been isolated from the Adriatic mussel, *Mytilus galloprovincialis*, and has been named adriatoxin (Figure 6.7). Its backbone structure is identical to that of yessotoxin, except it is missing a terminal ether ring. Three side-chain analogues of adriatoxin have been identified[96].

Yessotoxin displays lethal toxicity in mice when injected intraperitoneally, but its mode of action remains unclear[97]. However, it has been shown to elevate calcium levels in cells, possibly in a manner similar to that of maitotoxin[98]. Indeed, yessotoxin has been shown to stimulate maitotoxin-induced calcium influx[99]. One of the effects of this is a dramatic lowering of cytosolic cAMP levels, owing to Ca^{2+}-mediated activation of phosphodiesterase[100]. A more striking feature of yessotoxin, however, is its potent neurotoxic effects on cultured cerebellur neurons, causing extensive fragmentation of neuronal networks and complete neuronal disintegration and death[101]. It is still unknown whether yessotoxin is a contributing factor in shellfish poisoning, but such studies suggest that it could well be a cause for concern.

The Gymnocins

The gymnocins are relatively new members of the polyether ladder family, with gymnocin A being first characterised in 2002, from the red tide dinoflagellate *Karenia* (formerly *Gymnodinium*) *mikimotoi*[102]. Gymnocin A is distinctive in being a relatively simple and, yet, very long example of a polyether ladder, consisting of an unprecedented fourteen fused rings – a mixture of a single five-membered ring, nine six-membered and four seven-membered. More recently, the slightly longer, gymnocin B has also been isolated from *K. mikimotoi*, and very closely resembles gymnocin A[103]. Gymnocin B, however, has a total of *fifteen* fused rings, making it the polyether ladder with the largest number of contiguous rings thus far isolated (Figure 6.8). Both structures possess an identical α,β-unsaturated aldehyde 'head',

which is tailed by a snake-like ring system. Although appearing, at first sight, almost identical, closer examination reveals an interesting feature of these tails. Both ladders are composed of only 5, 6 and 7-membered rings, but the linear arrangement of these is somewhat different between them. The structures and ring sequences have been overlaid in figure 6.8 to illustrate. This is an important point to note, as it shows that gymnocin A is not simply a truncated version of gymnocin B (as adriatoxin is of yessotoxin); they are, in fact, very much individual molecules, and their shapes and flexibility, discussed earlier with regard to the brevetoxins, will likely reflect this. This becomes of particular interest when one considers the biosynthesis of these structures, which will be the focus of the following chapter, as well as their biological activity. Gymnocin A is highly cytotoxic, but limited studies have shown only weak toxicity to fish. Owing to the fish kills attributed to *K. mikimotoi*, this was initially surprising. However, there have been concerns over the reliability of these preliminary experiments, owing to gymnocin A's poor water solubility. There have been, so far, no published toxicological research on gymnocin B, but such studies may be very revealing, owing to the significant structural differences between the two toxins.

Hemibrevetoxin B and Brevenal

Like the brevetoxins, hemibrevetoxin B was isolated from *Karenia* (*Gymnodinium*) *brevis*[104], and was originally noted as essentially being the right half of brevetoxin B (BTx-2). This is valid, to some extent, as the terminus constitutes an α,β-unsaturated aldehyde moiety. However, the ring system, consisting of only four rings, is different from both brevetoxins A and B. Hemibrevetoxin B, unlike its larger cousins, is non-toxic. However, it is a natural inhibitor of the brevetoxins, likely by acting as a competitive antagonist at the VSSC binding site, and has been found to protect fish from the neurotoxic effects of brevetoxin exposure[105]. This observation may serve useful in the development of therapeutics to prevent, or reverse, the effects of brevetoxin exposure in humans.

Brevenal is the newest member of the 'brevetoxin family', isolated from *K. brevis*, and is a five-ring polyether ladder. It is not yet known whether it has any biological activity.

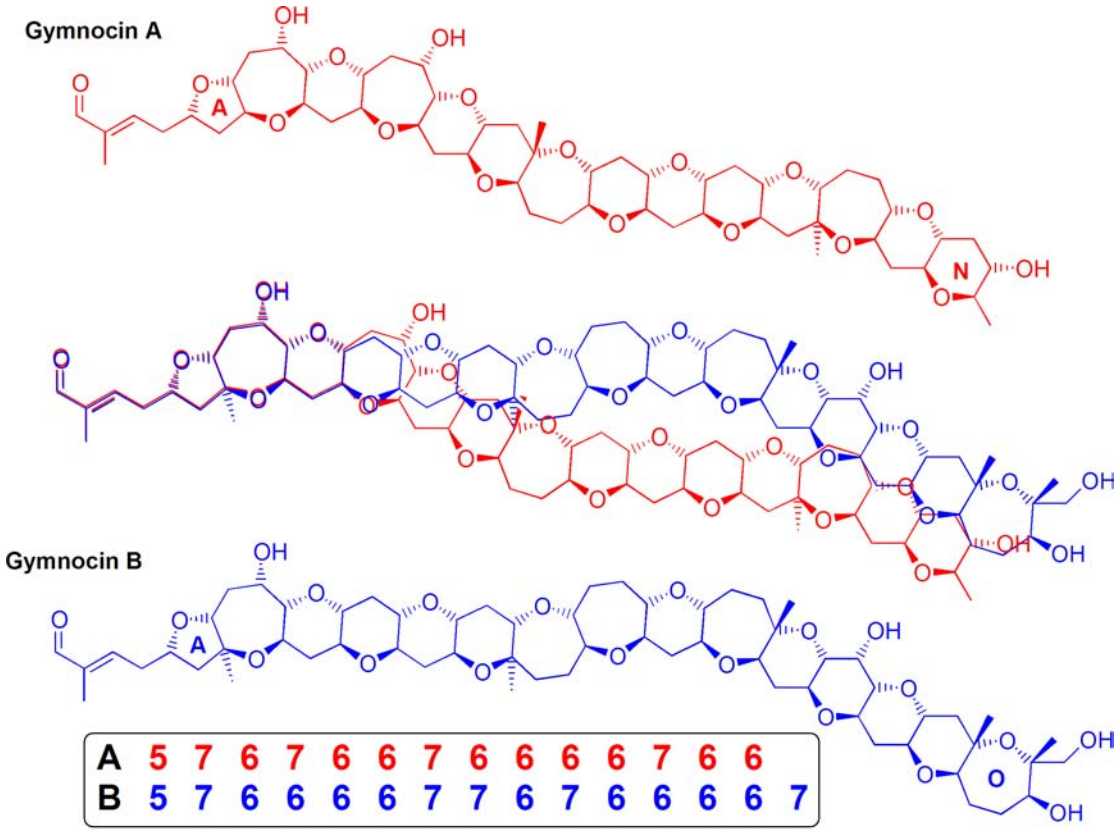

.**Figure 6.8** Structures of gymnocins A and B, with structural overlay and comparison of ring sequences

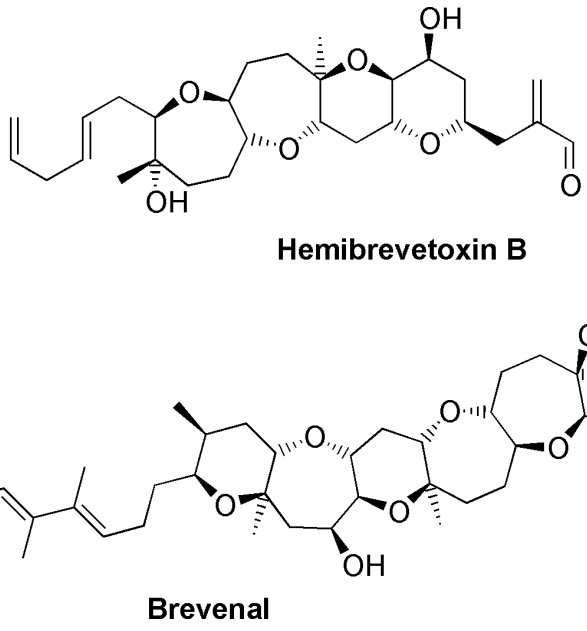

Figure 6.9 Structures of hemibrevetoxin B and brevenal.

Chapter Seven

Extrapolation of the Terrestrial Biosynthetic Model to Marine Polyether Ladders and Development of the "Stereochemical Uniformity Rule"[106]

"Nature operates in the shortest way possible." Aristotle

The biosynthesis of the polyether ladders, whilst attracting speculation, has actually advanced little further than the identification of their polyketide origin. Although labelling studies have shed some light on the construction of the obligatory polyketide chain precursor[107], anything further than this remains speculative. However, the model that has been proposed, and now validated, for monensin, was likely the inspiration for the most prominent model for the biosynthesis of the most well-known of the polyether ladders, brevetoxin. Both Shimizu and Nakanishi independently proposed this model - an octaepoxide precursor cyclises in a cascade of S_N2 epoxide openings, mechanistically similar to that initially proposed for monensin[108] (Figure 7.1). Although, up to this point, nobody has *specifically* pointed this out, the structure of all the marine polyether ladders suggests that cyclisation of a polyepoxide precursor might be a general biosynthetic strategy for their construction. Indirect evidence for such a mechanism is provided by the $^{18}O_2$-labelling pattern of okadaic acid, a related marine polyether, suggesting an epoxide intermediate[109]. Also, the isolation of 27,28-epoxy-brevetoxin-B (double-bond in 8-membered H-ring epoxidised) may suggest the extraneous over-epoxidation of a polyene precursor[110].

Although a polyepoxide intermediate may be feasible *en route* to the brevetoxin skeleton, a straightforward extrapolation of the Cane-Celmer-Westley cyclisation mechanism cannot be considered wholly satisfactory. The most notable concern is the manner in which the polyepoxide must cyclise in order to generate the contiguous fused ether rings characteristic of these toxins. Unlike the monensin triepoxide intermediate, which must cyclise in a series of favoured *exo*-tet S_N2 closures, a *pre*-brevetoxin polyepoxide would entail nine disfavoured *endo*-tet closures, each violating Baldwin's rules[44] (Figure 7.2). As yet, no satisfying and unifying hypothesis has been proposed for all polyether ladders beyond the idea of a *pre*-brevetoxin polyepoxide intermediate.

A characteristic feature of the toxins is the *syn/trans* stereochemistry of the ring junctions (Figure 7.3). Examination of all known polyether ladders demonstrates

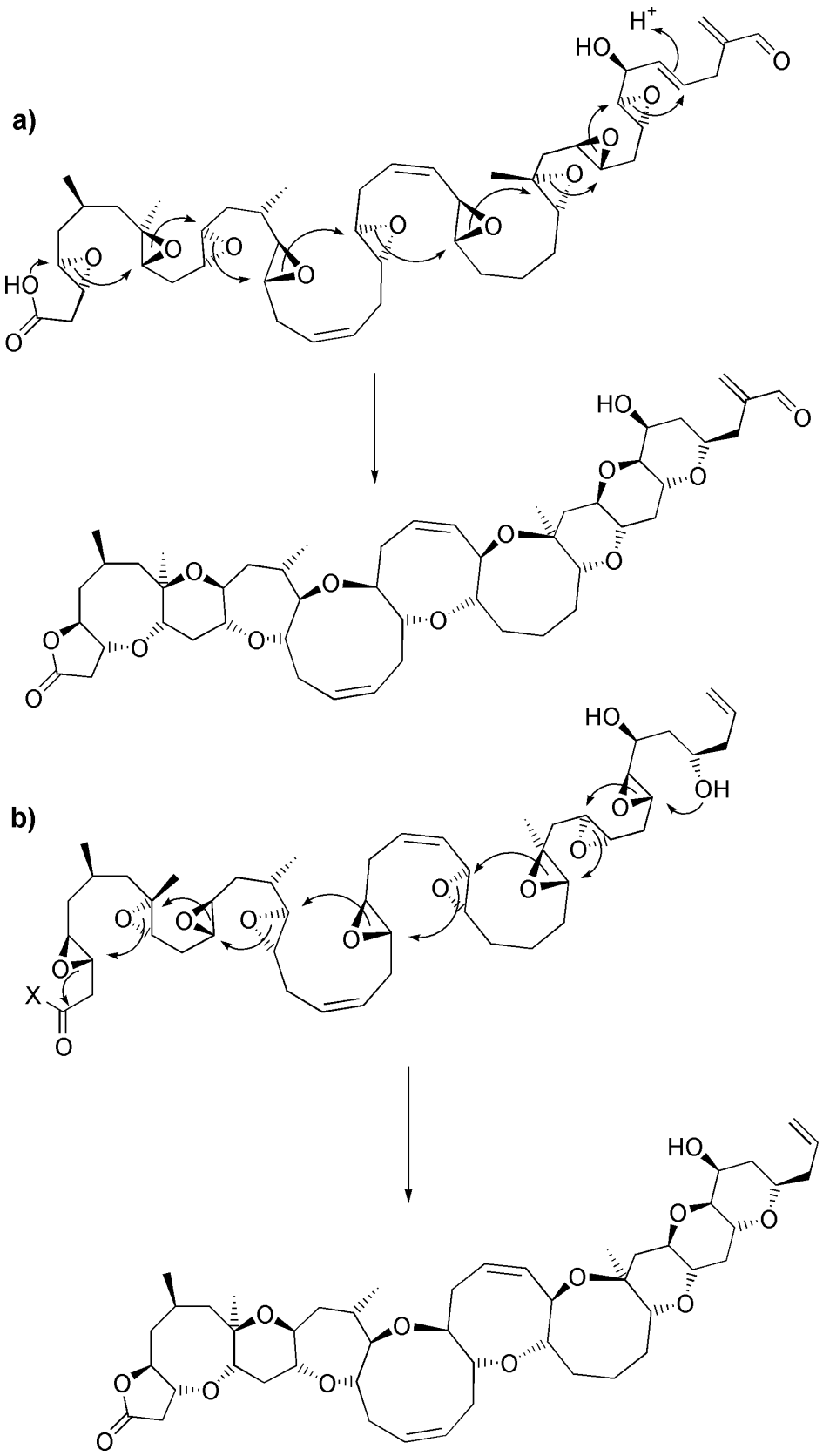

Figure 7.1 a) Shimizu/Nakanishi hypothetical mechanism of brevetoxin cyclisation; b) Alternative mechanism of cyclisation.

that this feature is conserved across the family. Using retrobiosynthetic analysis, it was possible to take these structures back to their hypothetical polyepoxide precursors. This revealed, for the first time, that all of the contiguous rings, in any single polyether, can be derived from stereochemically identical, either all (R,R)- or (S,S)-, *trans*-epoxides. Since the mechanism of terminal ring formation is unclear in some cases, this rule can only be generally applied to ring junctions. However, when terminal ring closure *does* appear to involve a *trans* epoxide, then this rule is not deviated from. Further, the direction of cyclisation is always, to some degree, ambiguous. To illustrate this, Shimizu and Nakanishi show the cyclisation of the *pre*-brevetoxin A polyepoxide from a series of (R,R)-*trans* epoxides, terminating in protonation of a double-bond. However, by simply invoking a series of (S,S)-*trans* epoxides, the cyclisation may proceed from the opposite direction, terminating by closure of the lactone ring and yielding the same structure (see Figure 7.1b). This is clearly the more plausible of the two mechanisms and yet doesn't appear to have been considered before. What is important is the *relative* stereochemistry of the epoxides and, thus, likewise of the final cyclised structure.

It follows, from these retrobiosynthetic analyses, that all of the *trans* double-bonds in any polyene precursor would be epoxidised *from the same face* and, thus, a single monooxygenase could be responsible for all of the *trans* epoxides (Figure 7.4). The polyene intermediate may contain over twenty double-bonds, as would be the case with maitotoxin. Differential epoxidation of these would, obviously, require them to be distinguished by their individual monooxygenase enzymes. Intuitively, this seems unlikely and, indeed, examination of the ladder structures supports this view. A broadly specific monooxygenase could effect all of the asymmetric epoxidations without difficulty, from one face of the polyene. This rule is shown to apply to all the polyether ladders thus far characterised – namely, the brevetoxins, hemibrevetoxin B, the yessotoxins, the Pacific and Caribbean ciguatoxins, gambieric acids, gambierol, gymnocin A and B and brevenal (Figures 7.5 to 7.10). Interestingly, maitotoxin *appears* exceptional, but this will be discussed in the next chapter.

Assuming a polyepoxide precursor to the polyether ladders, the mechanism of cyclisation is of fundamental concern. The cyclisation of polyepoxide precursors, in the construction of fused polycyclic ethers, has been explored as an approach to total synthesis, as well as facilitating mechanistic proposals for their biosynthesis.

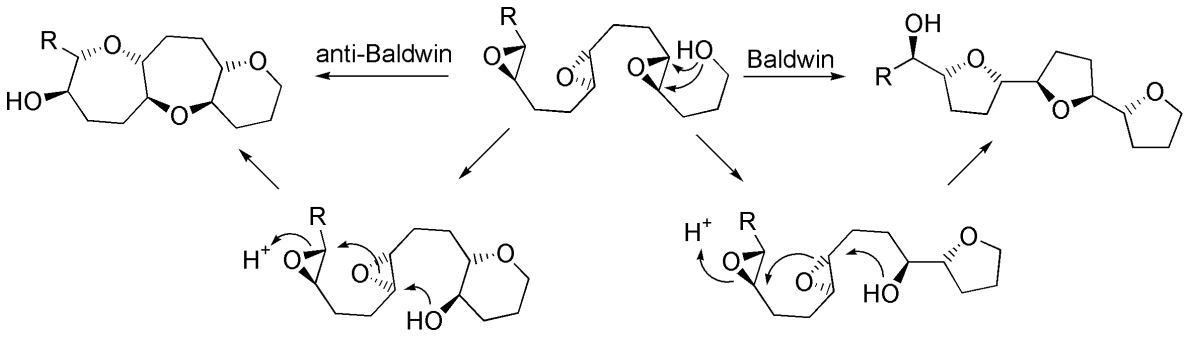

Figure 7.2 Baldwin vs. anti-Baldwin epoxide opening in polyether ring formation

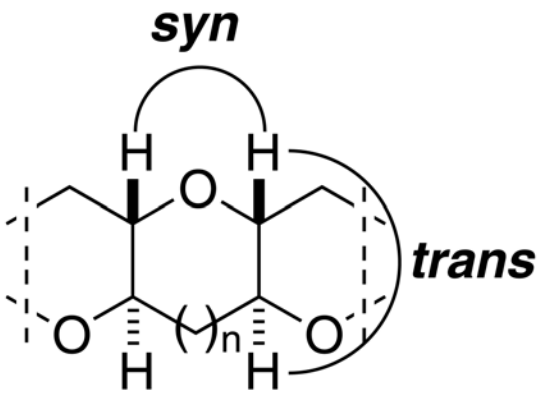

Figure 7.3 Conserved feature of marine ladder polyethers.

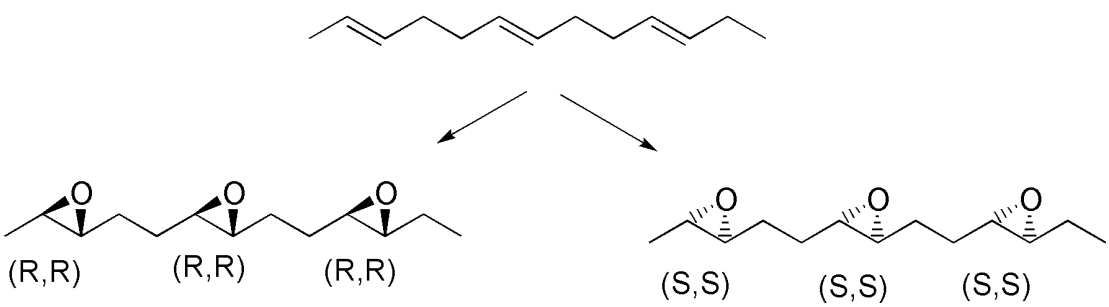

Figure 7.4 Uniform epoxidation patterns of hypothetical polyene precursors.

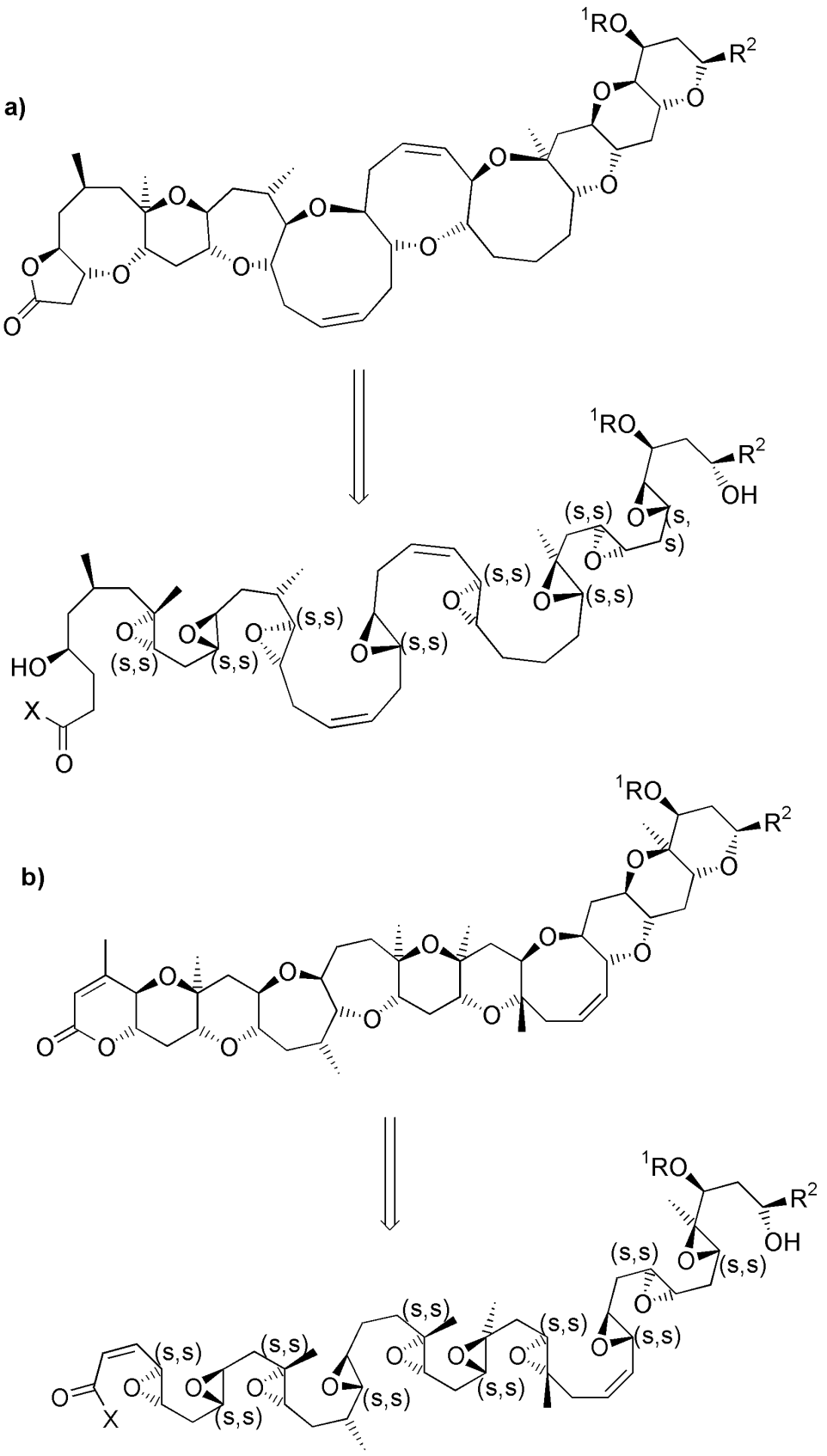

Figure 7.5 Retrobiosynthetic analysis of a) Type A brevetoxin; b) Type B brevetoxin backbones.

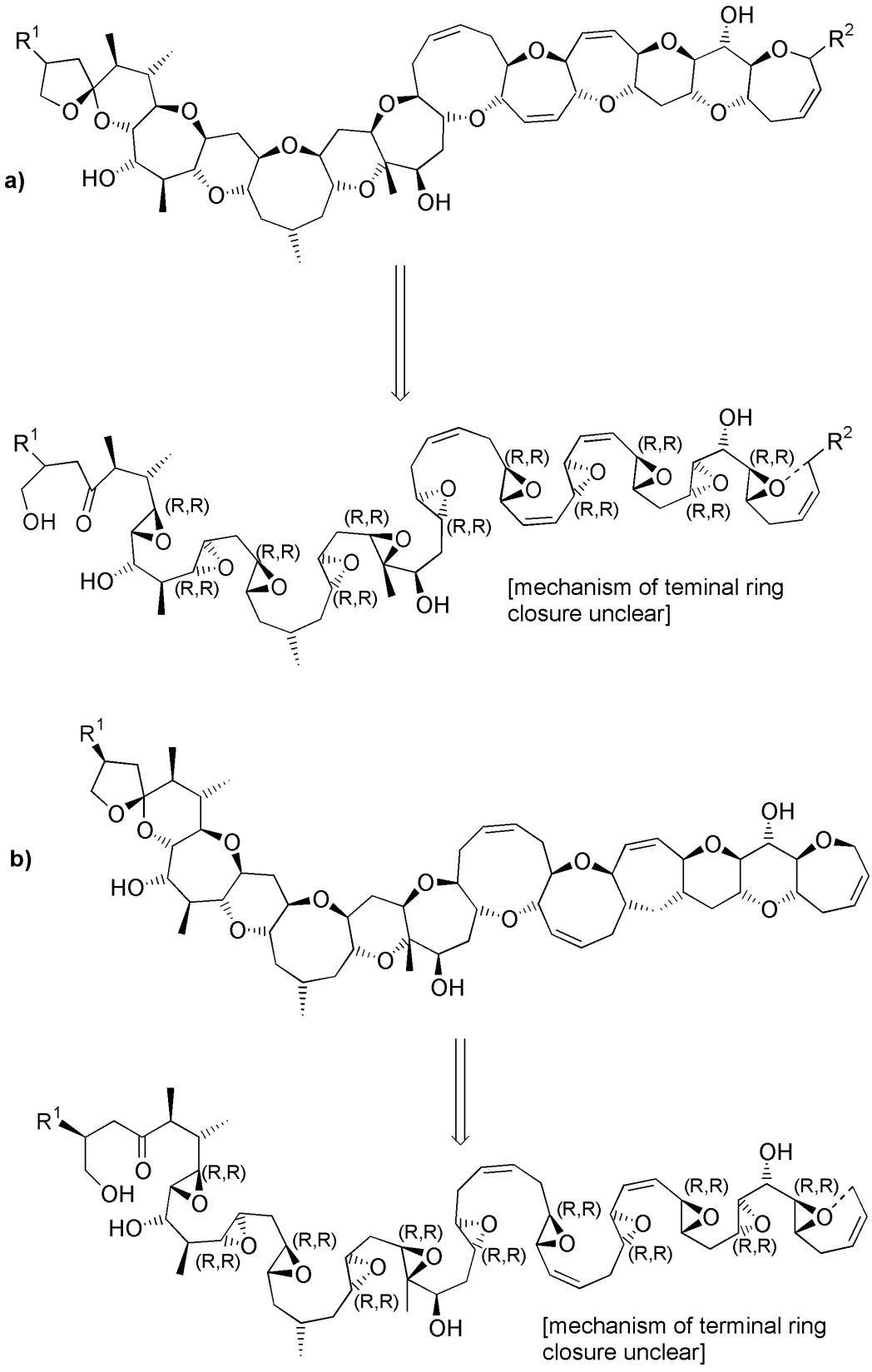

Figure 7.6 Retrobiosynthetic analysis of a) Ciguatoxin Type 1; b) Ciguatoxin Type 2 backbones.

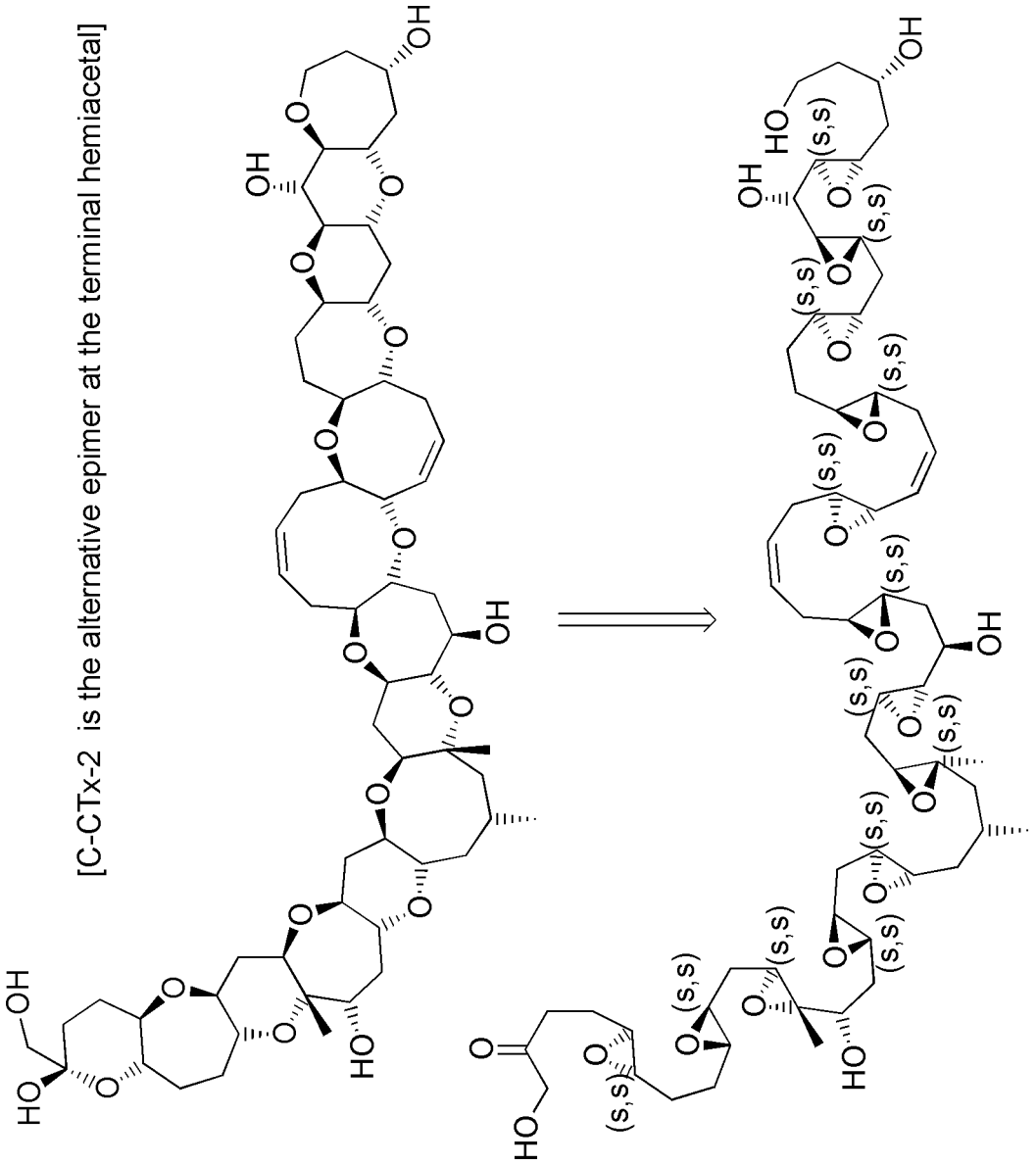

Figure 7.7 Retrobiosynthetic analysis of Caribbean ciguatoxin backbone.

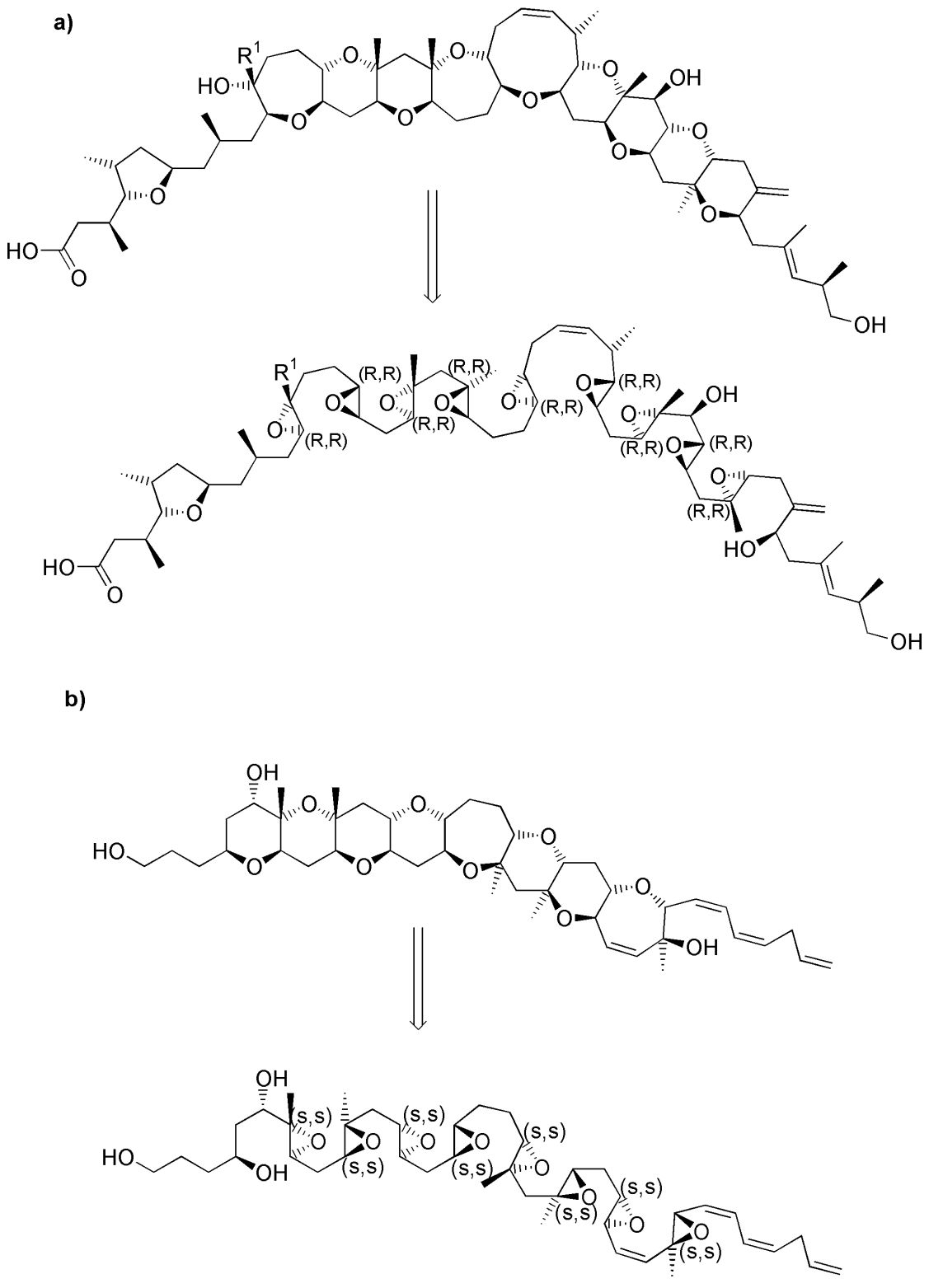

Figure 7.8 Retrobiosynthetic analysis of a) Gambieric acid; b) Gambierol backbones.

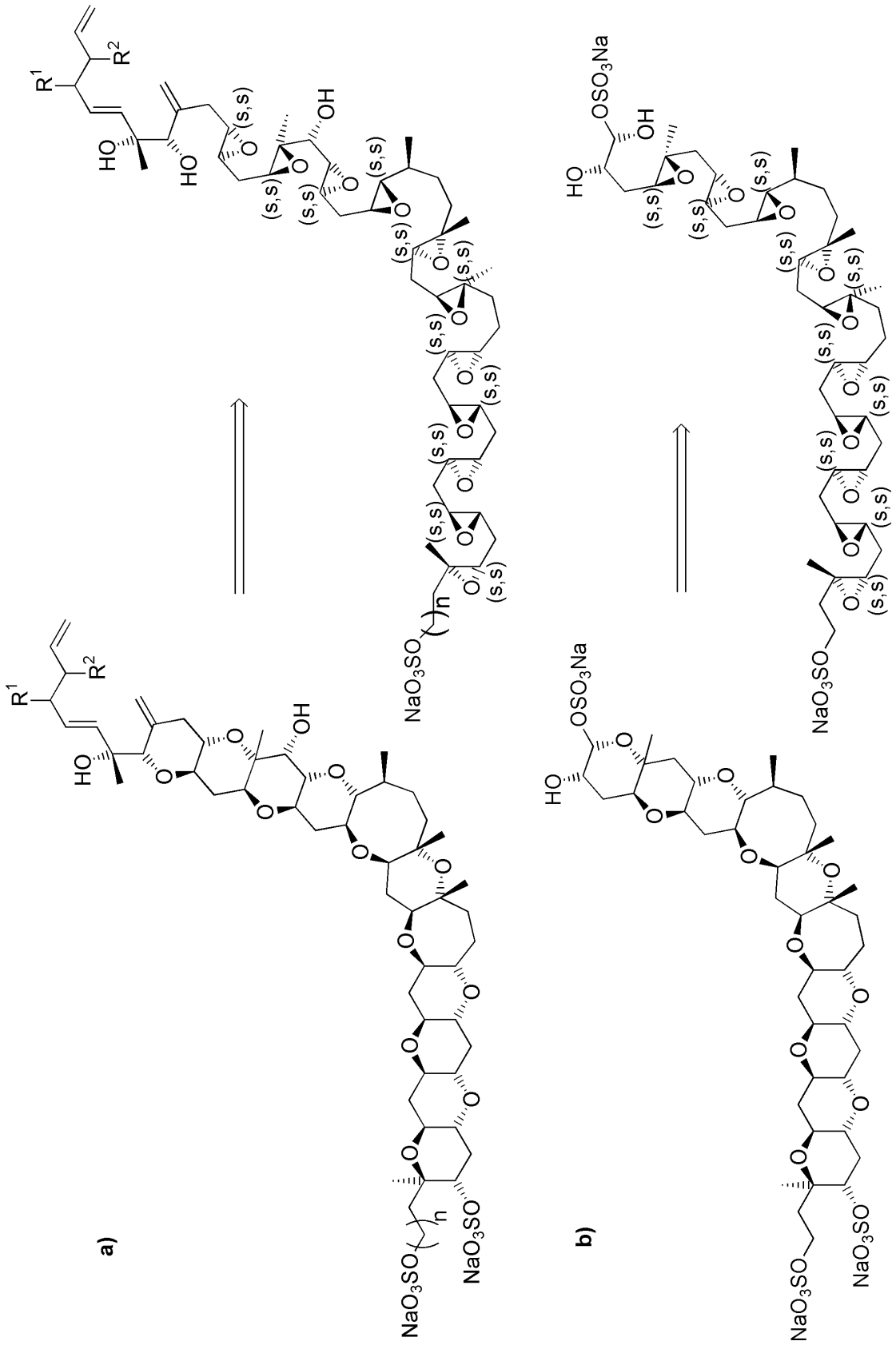

Figure 7.9 Retrobiosynthetic analysis of a) Yessotoxin; b) Adriatoxin backbones.

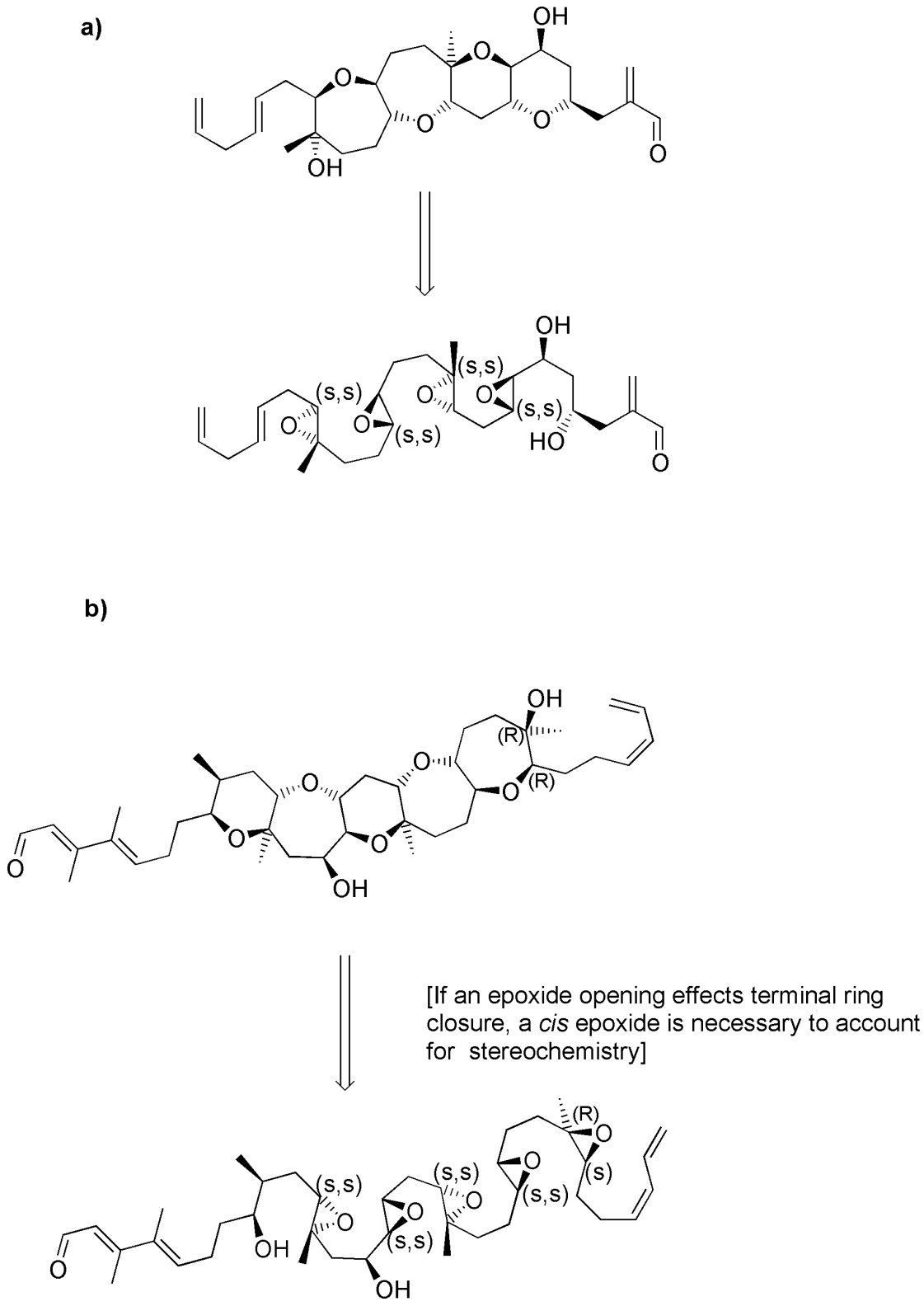

Figure 7.10 Retrobiosynthetic analysis of a) Hemibrevetoxin B; b) Brevenal backbones.

Although synthetic models have shown that formation of polycyclic ethers from polyepoxides is facile, Baldwin's rules are adhered to in simple, acid-catalysed reactions[111]. However, there have been three distinct biomimetic approaches taken to effect *endo*-selective epoxide opening in ring closure[112]. The first method uses successive ring closure of a hydroxy polyepoxide, which is analogous to the CCW mechanism. However, the attack is guided electronically by substituents on the *endo* position of the epoxide. In the early work of Nicolaou, for example, an electron-rich double-bond is placed adjacent to the *endo* position and stabilises the *endo* transition state by electron donation from the π-orbital. This has been effective in achieving both 6-*endo* over 5-*exo* selectivity, as well as 7-*endo* over 6-*exo*, in such epoxide openings[113]. The putative biosynthetic polyepoxides do not have such convenient directing groups, however, so the selectivity could not occur in this manner.

The second method that has been used to obtain *endo*-selectivity is a successive ring expansion of a polyepoxide, in which the epoxide acts as a nucleophile (Figure 7.11). This methodology typically employs a suitable Lewis acid to activate the terminal epoxide[114]. The first step in such a reaction is the intramolecular attack by an adjacent epoxide on the activated terminal epoxide to generate a bridged oxonium ion intermediate – the initiation step. The next step is the nucleophilic attack of the second epoxide, either *exo* or *endo*, to open the oxonium ion. Thus, the first ether ring is completed and a second oxonium ion is formed. This forms the electrophilic site for the next epoxide, and so on. The *endo*-regioselectivity has been explained by minimisation of ring strain in the formation of each oxonium ion. *Endo* attack, although disfavoured in terms of Baldwin's rules, generates a less strained oxonium ion, an effect that appears to dominate[115]. In theory, the Lewis acid-mediated initiation step, *or its enzymatic equivalent*, could generate the complete polycyclic structure. This could be an elegant biosynthetic strategy and might be considered as a feasible alternative to the Cane-Celmer-Westley extrapolation. However, the synthetic methodology has serious limitation in terms of the number of rings that may be assembled, as well as the substituents and ring sizes, perhaps making it less appealing as a general biosynthetic proposal for the polyether ladders[116].

The third approach, developed by Giner, involves the rearrangement of an epoxy ester and is a very different mode of cyclisation from the other two biomimetic

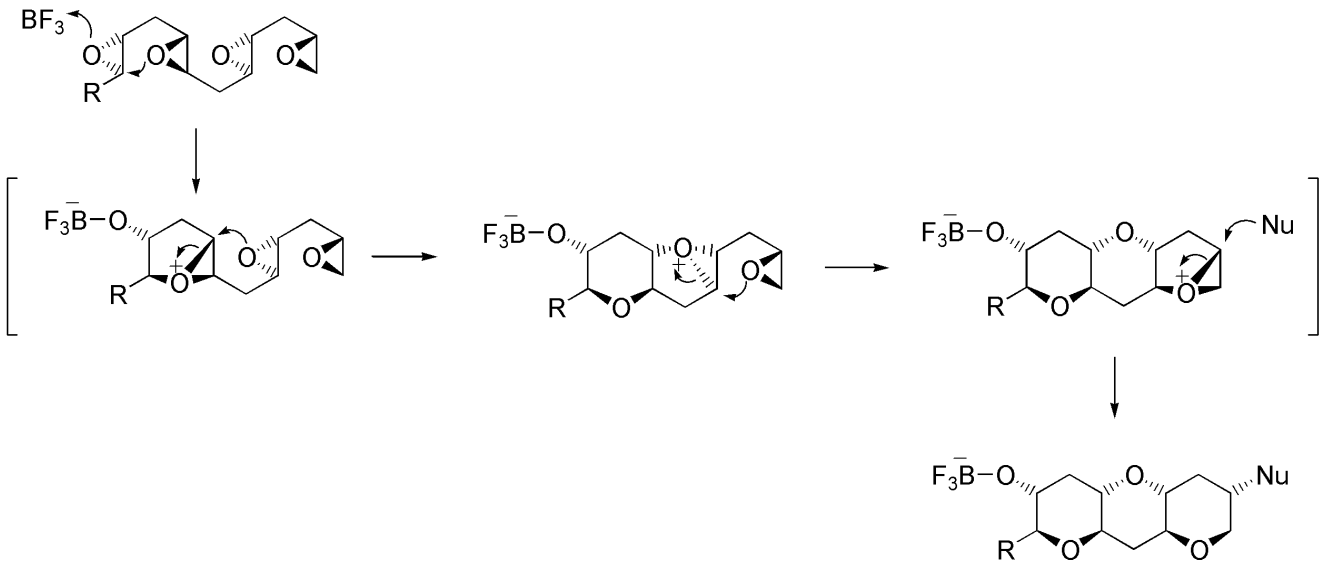

Figure 7.11 Lewis-acid initiated approach to achieving endo-selectivity.

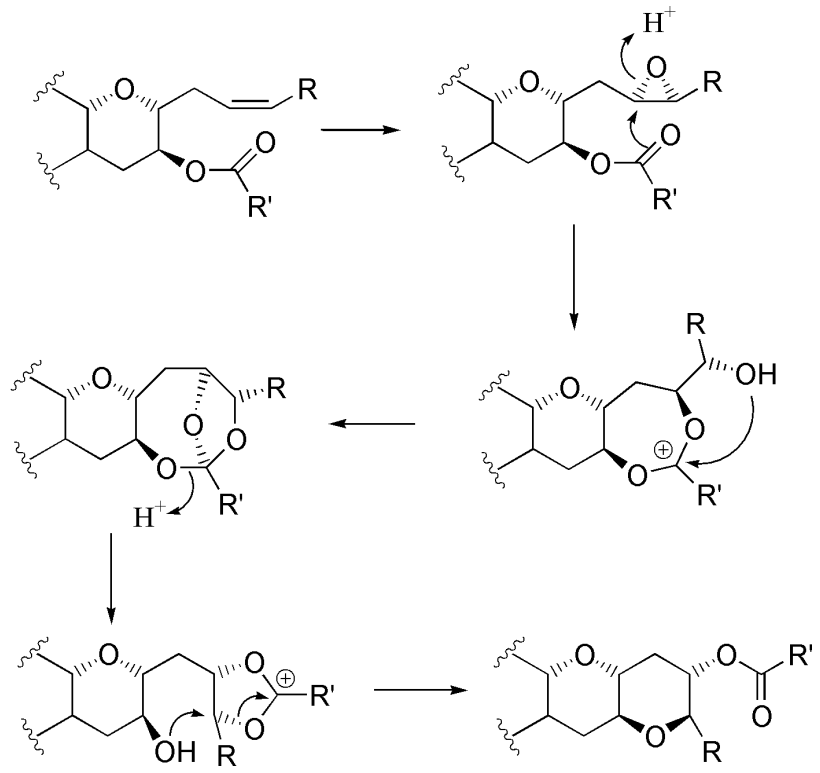

Figure 7.12 Formation of a fused polycyclic ether via an epoxy-ester rearrangement.

models (Figure 7.12)[117]. Extrapolating this synthetic strategy to the biosynthesis of polyethers would require an all-*cis* polyene precursor, noted as advantageous in explaining the *cis*-bonds in the brevetoxins and ciguatoxins. This is unpersuasive, however, as the formation of selectively positioned *cis*-bonds in polyketide chains is precedented[118]. Although an inventive synthetic approach to obtaining *endo*-selectivity, it seems a somewhat uneconomical biosynthetic strategy.

Perhaps the most straightforward biosynthetic methodology would involve the stepwise closure of each ring by an epoxide hydrolase, analogous to what has been proposed for monensin in the previous chapters (Figure 7.13)[119]. The role of the enzyme would simply be to protonate the epoxide and direct the hydroxyl nucleophile so as to close the ring in an *endo*-selective manner. Further to this, the uniform stereochemistry of the proposed marine polyepoxides suggests a single epoxide hydrolase could well be responsible for all of the ring closures. Notably, this does contrast with monensin, in that the triepoxide has mixed stereochemistry and, thus, requires two separate epoxide hydrolases. It is not unreasonable to argue, therefore, that the epoxidation and cyclisation of monensin is, from an enzymatic standpoint, a more challenging task than that of any marine polyether.

Although a stepwise cyclisation accomplished by an epoxide hydrolase is a rational model, the inherent reactivity of the hypothetical polyepoxide intermediate may itself be a cause for concern. All of the double-bonds of the prerequisite polyene must each be epoxidised and, *only when this is complete*, may the process of cyclisation begin, so as to effect the smooth conversion of the polyepoxide to polycyclic ether. An *in trans* epoxidation process, in which each double-bond is epoxidised as it is formed on the polyketide synthase, would provide a more closely controlled sequential model. However, potentially, there is also the problem of avoiding non-enzymatic side-reactions during the construction of a series of somewhat reactive epoxides. The instability to hydrolysis of at least one of the epoxides, of only three, in the monensin intermediate, described in the previous chapter, is testament to this. So far, gymnocin B contains the largest number of contiguous rings (15) of any polyether ladder. However, there is no reason to suggest that gymnocin B represents the ceiling level in this respect. Any sequential biosynthetic model would, ideally, be applicable to any hypothetical polyether ladder of any length.

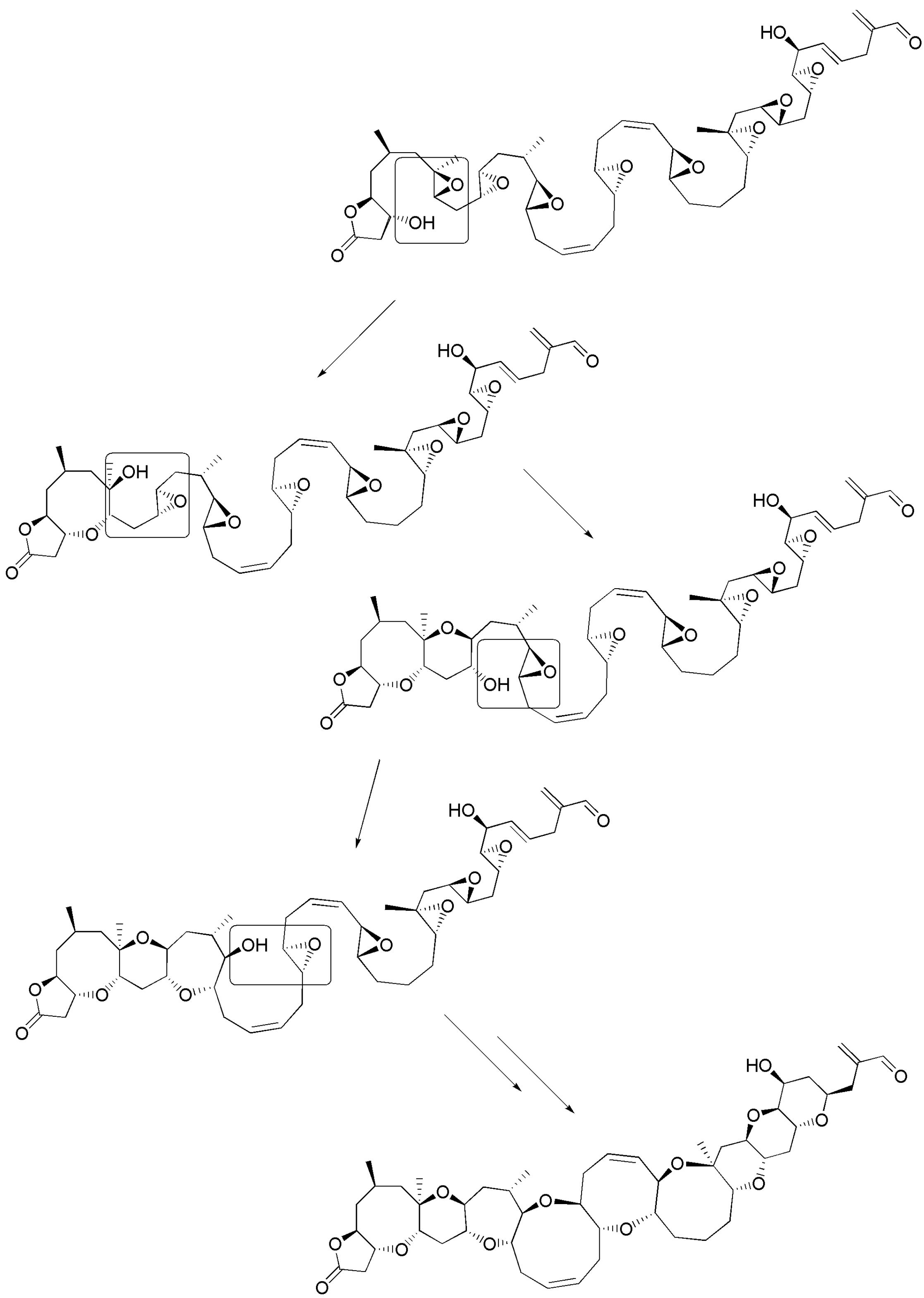

Figure 7.13 Proposed stepwise cyclization in the biosynthesis of brevetoxin A, catalysed by a MonB-like epoxide hydrolase. The boxed regions indicate the loci for the successive action of an epoxide hydrolase.

By coupling the epoxidation and cyclisation steps more closely, this concern could be circumvented – the epoxidation of the first double-bond creates the substrate for the epoxide hydrolase and the first ring is closed. Epoxidation of the second double bond then presents the epoxide hydrolase with its next substrate. This iterative process continues until the final polycyclic structure is realised. The epoxidase and hydrolase enzymes would thus work in close cooperation, perhaps as a multienzyme complex (Figure 7.14). This bis-enzymatic model avoids constructing a polyepoxide prior to cyclisation and may, in fact, be simplified further.

Janda *et al* have utilised a 'catalytic antibody' to direct the *endo* cyclisation of hydroxy-epoxides[120]. These antibodies are generated by means of a hapten that mimics the *endo* transition state. The suitably programmed antibody merely intercedes at, or near, the transition state to alter the energy balance in favour of the otherwise disfavoured reaction pathway (Figure 7.15). It is hypothesized that, through suitably placed charged residues, the antibody simply stabilises the *endo* transition state relative to the *exo* as the tethered hydroxyl attacks. Applying this to polyether construction, it is feasible that, as the monooxygenase epoxidises each double bond of the polyene, the bound enzyme acts in such a manner and facilitates *endo* attack of the hydroxyl nucleophile. The size of the ring being closed would be largely irrelevant (the nine-membered ring of brevetoxin A *may* represent a realistic limit in this regard). The role of the enzyme at this stage would be no more than to bind and activate the newly formed epoxide, ensuring that the energy of the *endo* transition state is lowered relative to the *exo*. Once the ring is closed, the enzyme naturally dissociates and moves on to the next double-bond (Figure 7.16 illustrates both mono and bis-enzymatic [Re: Figure 7.14] mechanisms). A distinct hydrolase enzyme catalysing ring-closure may be superfluous. The oxidation-cyclisation may be considered a single step and, overall, a single enzyme converts a simple polyene chain to a more sophisticated polyether ladder.

It is highly significant that neither of these models inherently place any limitation on the number of contiguous rings that may be constructed. Once the polyene precursor is assembled, conversion to the polycyclic structure is relatively straightforward. This could provide an explanation as to how polyether biosynthesis can be effected on such a grand scale, as exemplified by maitotoxin. Considering the remarkable biological activity of this structure, such scaling has clearly been a successful strategy.

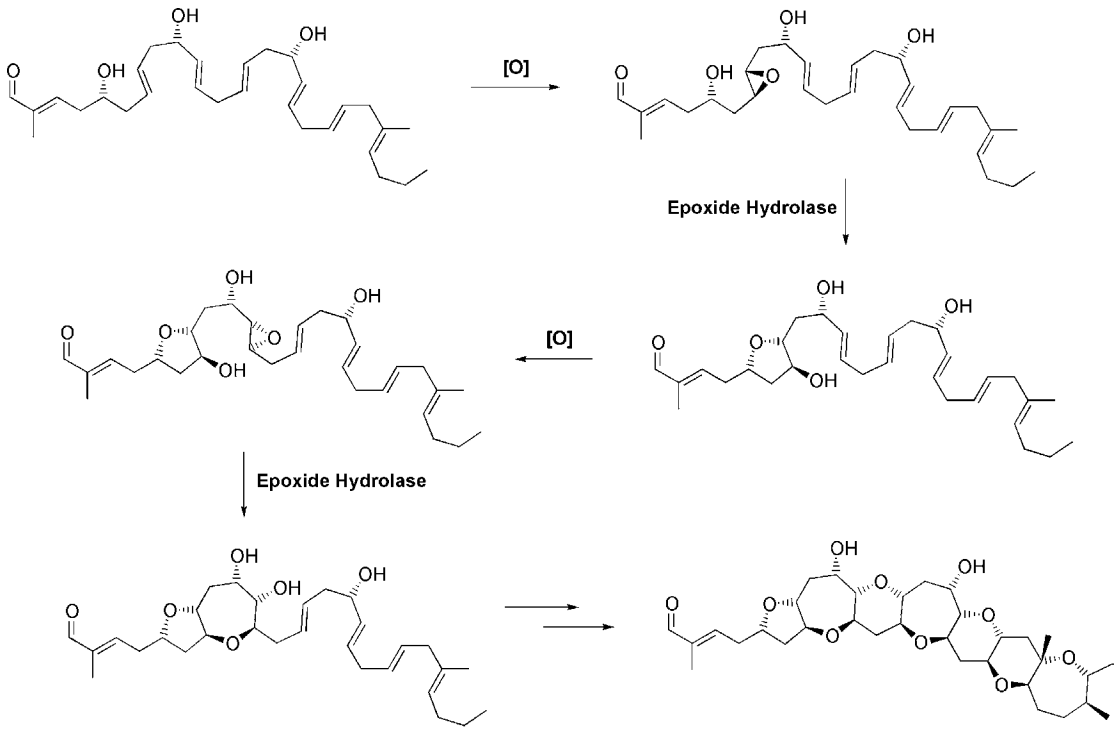

Figure 7.14 Alternating epoxidation-cyclisation mechanism for polyether construction

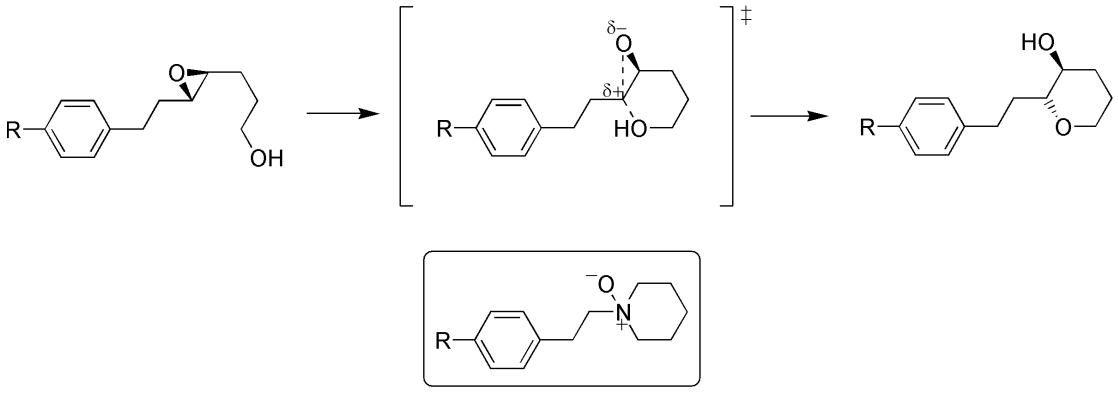

Figure 7.15 Antibody-mediated endo-cyclisation. Antibody generated from hapten (boxed) that mimics endo transition state.

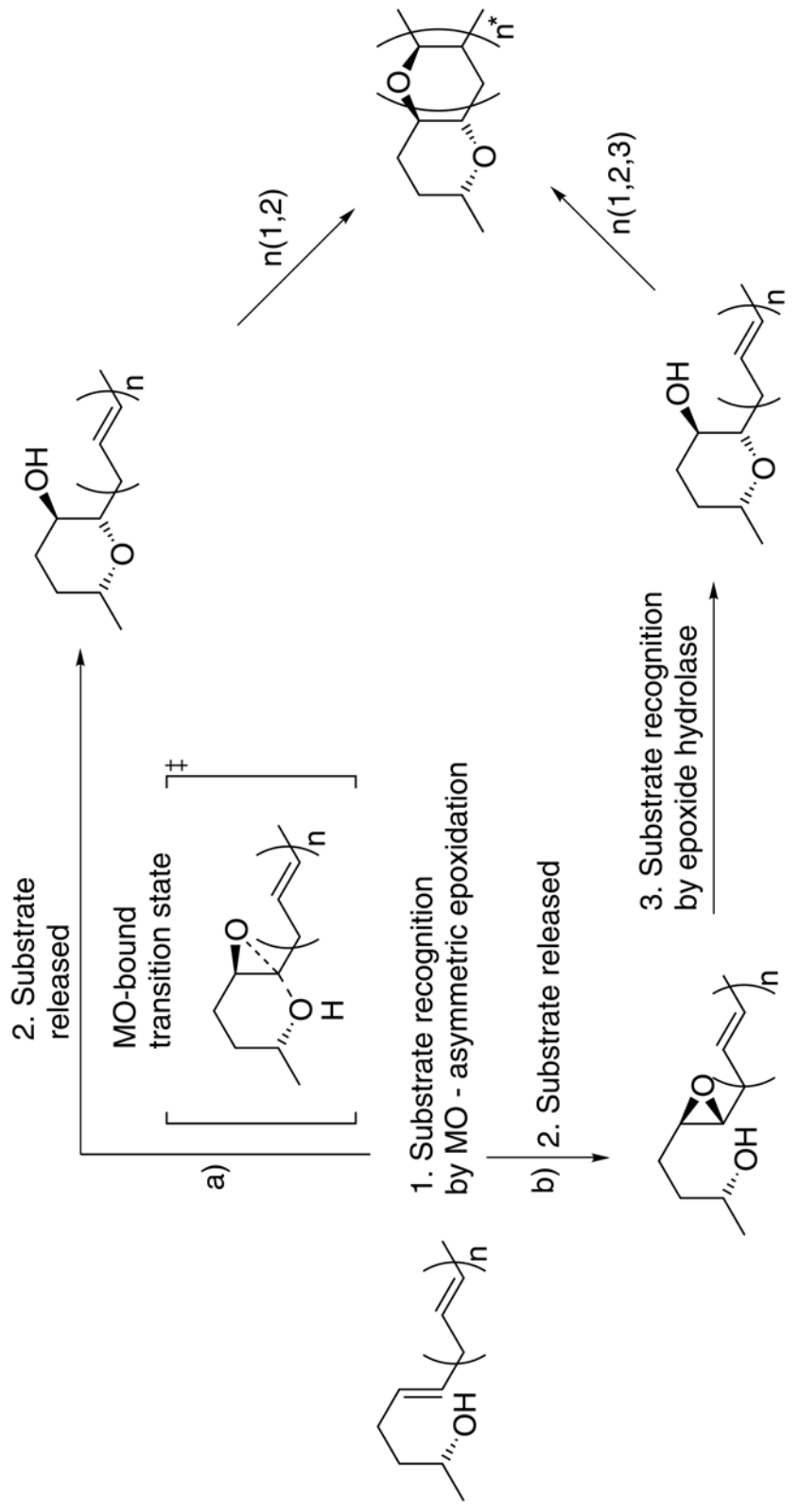

Figure 7.16 a) Mono-enzymatic route to a fused polyether; b) Bis-enzymatic route (MO = monooxygenase, * = alternating orientation of oxane ring).

Although the genes responsible for the formation of marine polyethers are difficult to obtain, it is noteworthy that the terminal ring of the ionophore, lasalocid A, produced by *Streptomyces lasaliensis,* also appears to be formed from a disfavoured, *endo*-tet, epoxide opening (Figure 7.16)[121]. Interestingly, a very small quantity of the *exo*-tet product (<1%) has also been isolated, presumably resulting from the kinetically favoured, non-enzymatic cyclisation. Alborixin, salinomycin and narasin also have such terminal rings[7]. The gene clusters for lasalocid A and the other three polyethers should be obtainable, as the organisms can be cultured and the microbiology of *Streptomyces* is well established. Such studies could confirm a role of *endo*-directing epoxide hydrolases in polyether biosynthesis.

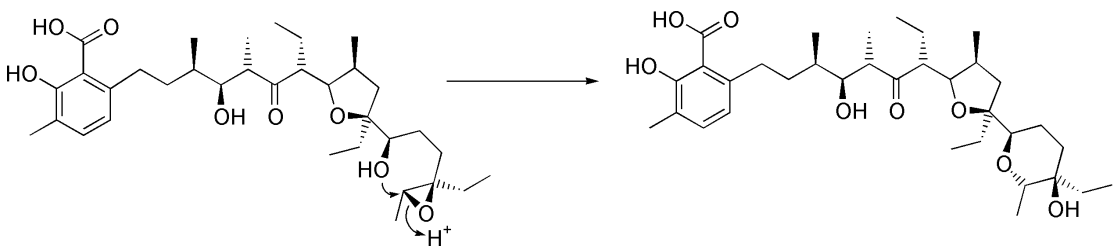

Figure 7.16 Proposed formation of lasalocid via *endo-tet* epoxide opening

In conclusion, until now, mechanistic hypotheses for marine polyether ladder biosynthesis have not been considered in detail. Little has been discussed beyond the original Cane-Westley extrapolation, as initially proposed by Shimizu and Nakanishi, which was restricted to the brevetoxins. Synthetic approaches to fused polyether systems have facilitated some additional deliberation, but this has been very limited and not based on any real consideration of the possible enzymology. However, the retrobiosynthetic analyses of all the polyether ladders has enable a simple model, and "Stereochemical Uniformity Rule", to be proposed that can explain the biosynthesis of the ring structure of all the marine polyether ladders thus far characterised. However, as mentioned earlier, there does appear to be one exception to this model – maitotoxin. Being the largest of the ladder polyethers, and of all known non-polymeric molecules, this exception cannot be dismissed.

Chapter Eight

Maitotoxin – A Structural and Biosynthetic Analysis

Maitotoxin (Figure 8.1) holds a unique position in the world of natural products, in being, not only, the largest non-polymeric natural product characterised[1], but also the most toxic. Like the ciguatoxins, it is produced by the dinoflagellate, *Gambierdiscus toxicus*, and is thought to be a contributing toxin in ciguatera poisoning. The mechanism of its toxic action is not fully understood, as it displays a number of distinct pharmacological effects. However, its most well-studied effect is that upon voltage-sensitive calcium channels; its interaction with these results in a massive influx of Ca^{2+} ions into cells[122], activating numerous signalling pathways as well as causing a Ca^{2+}-mediated depolarisation of excitable cells[123].

The first structural study of this giant molecule was carried out by the Yasumoto group at Tohoku University[124]. The toxin was obtained directly from cultured *Gambierdiscus toxicus*, and the diol moieties cleaved with periodate to yield three fragments (A, B and C); these were analysed separately (Figure 8.2). With data from extensive 2D-NMR and FAB-MSMS experiments, the structure of the C142 chain with composition, $C_{164}H_{256}O_{68}S_2Na_2$ (as the disodium salt) was disclosed, having an unprecedented molecular mass of 3422. The structure comprises 32 ether rings, 28 hydroxyls and 2 sulphate esters, and consists of four separate fused polyether ladder sections (A-D), as well as a central 'hinge' consisting of two bicyclic ethers. An acyclic chain is also located at both termini (C1-14 and C135-142).

The relative stereochemistry of the bulk of the molecule was established soon after[125], and, like other polyether ladders, showed the main ladders sections as being *trans*-fused. The central bicyclic ethers were, however, *cis*-fused. As for the original structural elucidation, the majority of data was obtained from the periodate cleavage fragments, and the relative stereochemistry deduced chiefly from ^{1}H-NOE data. However, rings K, L and N, with each having a vicinal diol, were opened by periodate treatment. This resulted in the direct loss of six stereogenic centres, as well as potentially informative NOE correlations. The stereochemical assignments in this region of the molecule had, thus, to be carried out using intact maitotoxin; this, naturally, made the assignments less straightforward, owing to the increased complexity of the NMR spectra. In fact, such was the problem with overlapping NOE

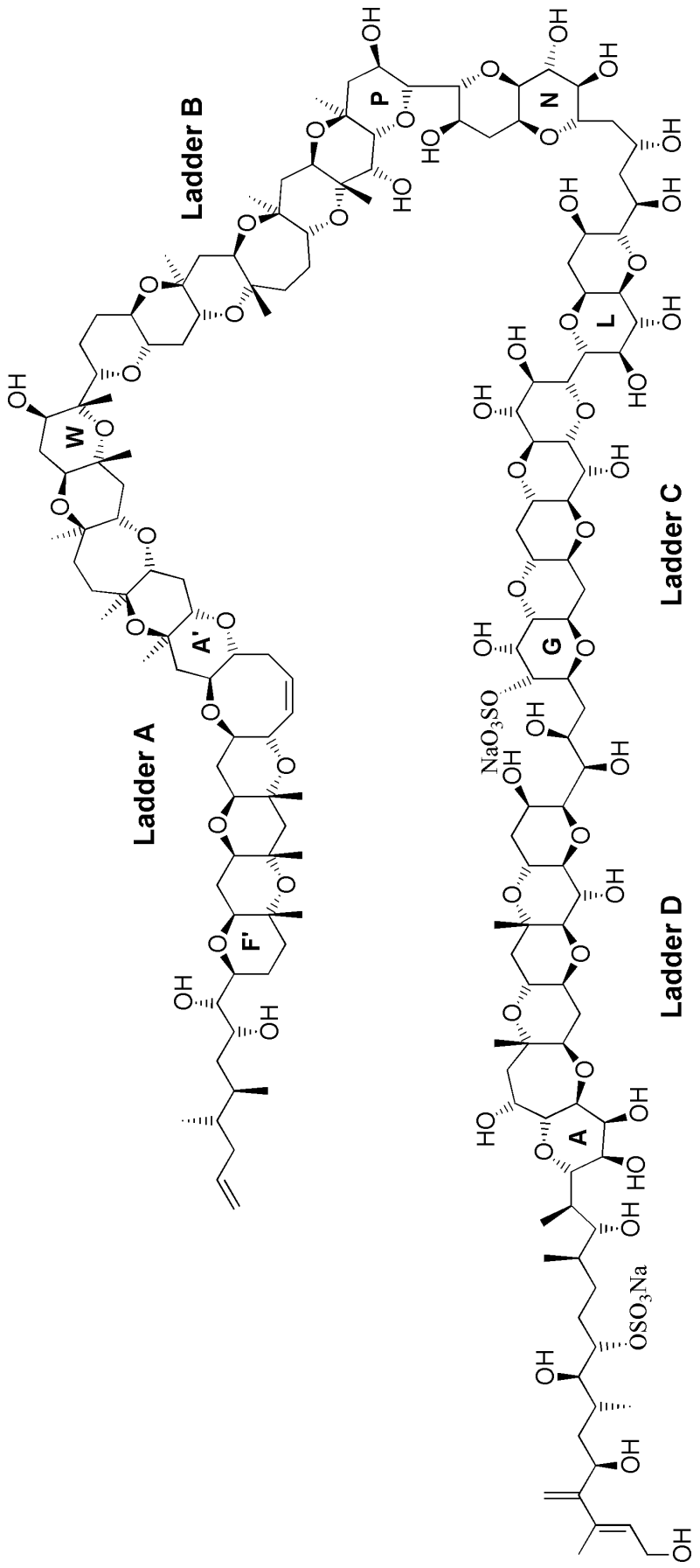

Figure 8.1 Maitotoxin with rings and ladder sections labelled.

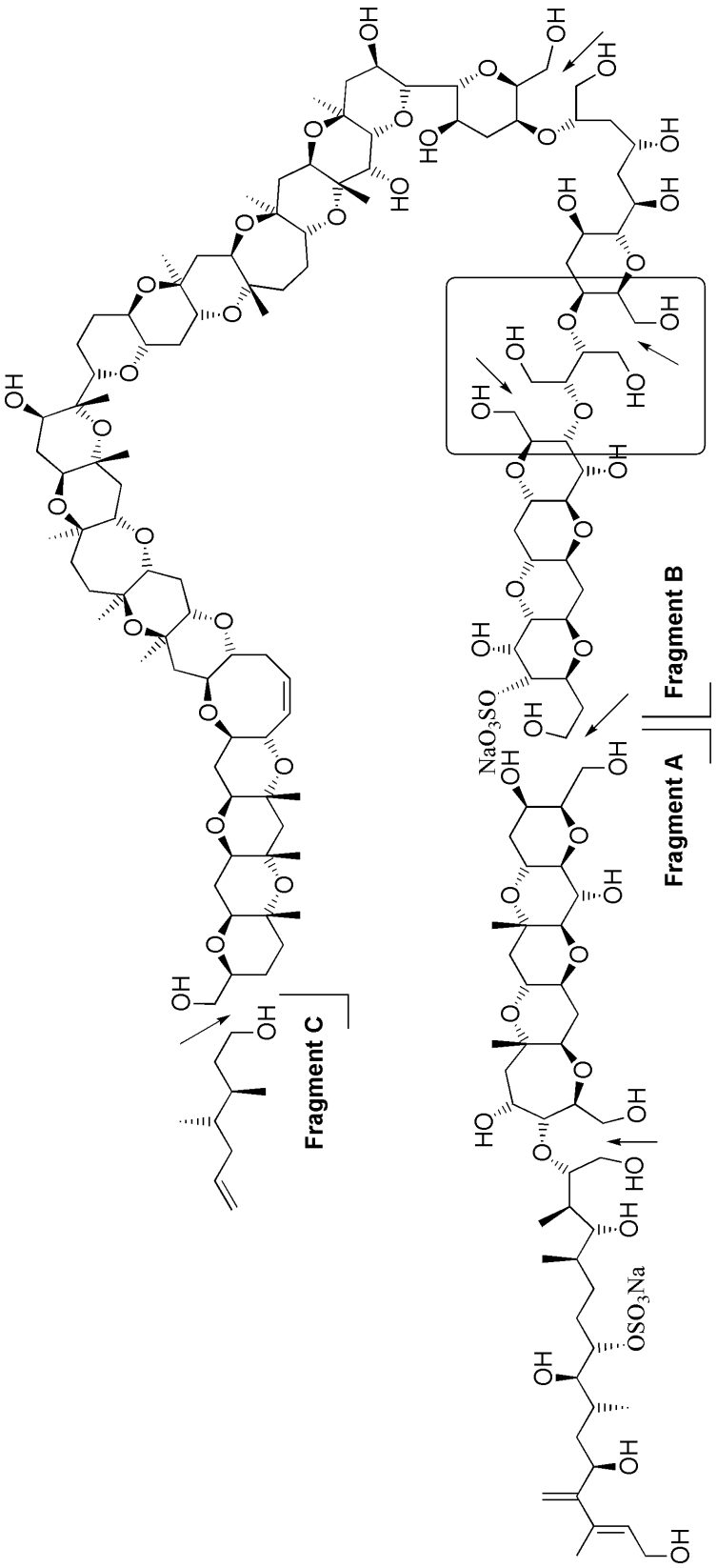

Figure 8.2 Treatment of maitotoxin with periodate and borohydride to yield fragments A, B and C for NMR analysis. The boxed region indicates the area of the (intact) molecule that was difficult to assign owing to signal overlap.

signals, that more advanced 3D NOESY-HMQC experiments were necessary to confirm the assignments[126].

The Kishi group carried out thorough synthetic studies on the acyclic portions of the molecule to complete the assignment of the relative stereochemistry of the entire molecule[127]. The absolute stereochemistry has now been established[128], and is that shown in Figure 8.1.

Application and Implications of the "Stereochemical Uniformity Rule" to the Structure of Maitotoxin

As noted in chapter seven, maitotoxin appears to be exceptional. As discussed, the main body of the molecule consists of four separate ladder sections (A-D), as well as a central 'hinge' consisting of two identical bicyclic structures. This identicality suggests a common mechanism of construction, distinct from the ladder sections. Although each of these ladder sections was treated as a separate entity in performing the retrobiosynthetic analyses, it was thought that, in order to satisfactorily conform to the stereochemical uniformity rule, the direction of cyclisation of the four ladder sections should proceed in one direction along the polyketide chain. Thus, *all* of the epoxides, not just those within a single ladder section, should have the same relative stereochemistry. Whilst conforming to the stereochemical rule in three of the ladder sections (Figures 8.3, 8.4 and 8.6), retrobiosynthetic analysis of ladder C revealed an epoxide with the opposite stereochemistry to all the others (Figure 8.5). This is striking, as this leads to the only example of an exceptional ring junction (the "J-K ring junction") (Figure 8.7) in any of the known polyether ladders.

From the twenty-eight *trans* double-bonds that must be epoxidised to construct the maitotoxin ladders, the selective discrimination of one double bond appears unrealistic. Without exception, none of the other polyether ladders, deriving from considerably fewer double bonds, display any such stereochemical variation. As discussed, a single monooxygenase is likely to be responsible for epoxidation of all the *trans*-double bonds in any single polyether. In order to arrive at maitotoxin, this enzyme would be required to skip the double-bond in question, despite having broad enough specificity to recognise all of the others. Differential epoxidation of this double bond would certainly require a separate enzyme.

It is more than a little striking that the stereochemical assignment in this particular region of the molecule was noted as being highly challenging, owing to ^{1}H-

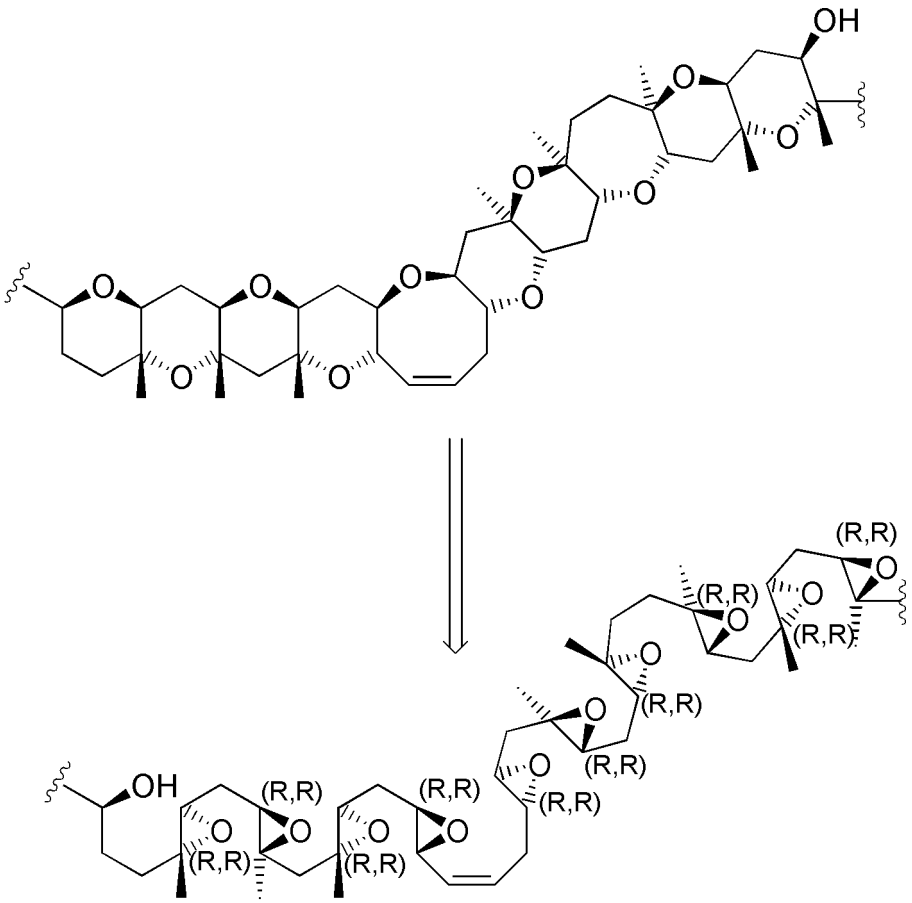

Figure 8.3 Retrobiosynthetic analysis of maitotoxin A ladder.

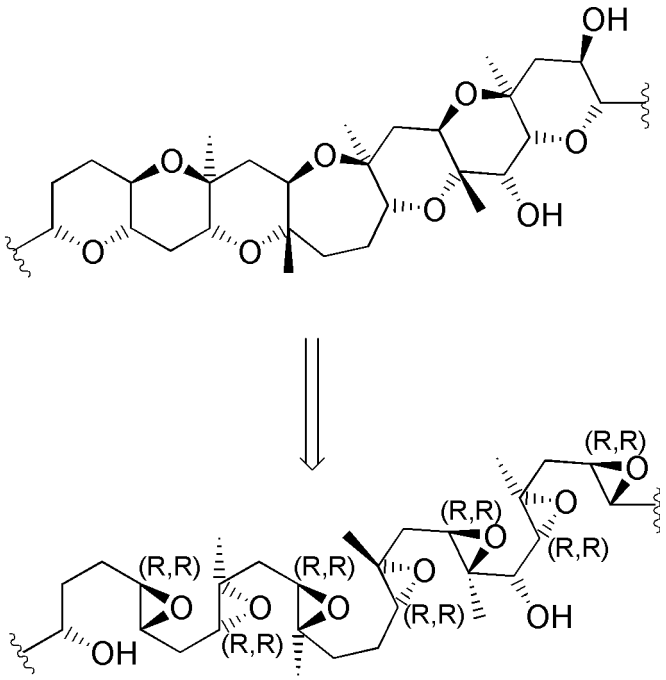

Figure 8.4 Retrobiosynthetic analysis of maitotoxin B ladder.

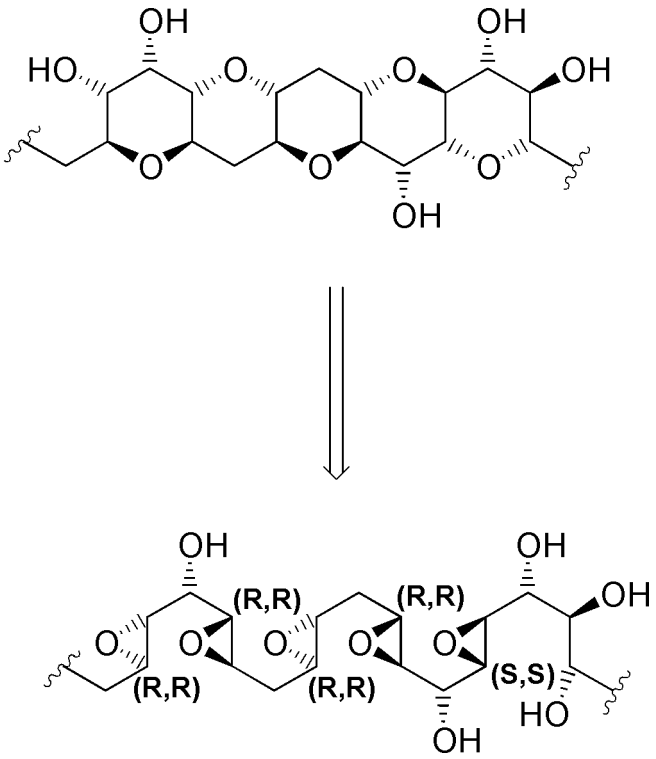

Figure 8.5 Retrobiosynthetic analysis of maitotoxin C ladder, showing exceptional (S,S)-trans epoxide.

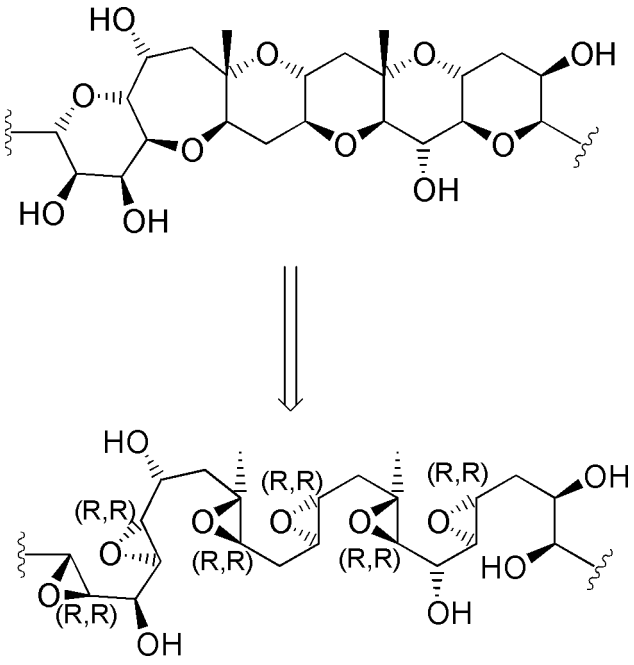

Figure 8.6 Retrobiosynthetic analysis of maitotoxin D ladder.

NOE signal overlap; this difficulty being a consequence of, or, at least, exacerbated by, the necessary use of intact maitotoxin, rather than the periodate cleavage fragments, in assigning the K, L and N rings. The most relevant proton in this discussion is that at C55, at δ^1H 4.03ppm, which overlaps those at C50 and C62. Thus, it was not possible to definitively assign the NOEs from this proton. However, by the use of the 3D PFG NOESY-HMQC experiment, the ^{13}C-shifts were separate enough to allow these protons to be distinguished. This allowed an NOE between the C51 and C55 proton to be observed, noted as valuable in confirming the original assignment at the J-K ring junction (Figures 8.7). Figure 8.8a shows the structure of the C ladder as it is assigned, in which the geometry of the ring junction forces the J-ring into a boat conformation, with the crucial C51-C55 NOE pointed out. By inverting the stereochemistry at the junction carbons (i.e. to conform to the *stereochemical uniformity rule*), it is clear why the C51-C55 NOE wouldn't be expected. However, if the C55 stereochemistry is also inverted, then this NOE *would* be expected. Overall, despite the utility of these advanced NMR experiments, the fact that the *stereochemical uniformity rule* appears to have been violated at this position, considered together with the difficulty in assigning this region of the molecule, it is thought prudent to initiate a thorough re-examination of this assignment. Structural misassignments of natural products are not uncommon[129] and, as maitotoxin is currently the most ambitious target for synthetic organic chemists, it might be very unwise to ignore this discrepancy.

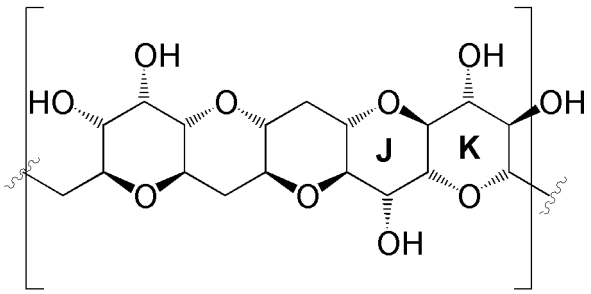

Figure 8.7 The exceptional J-K ring junction of maitotoxin

In conclusion, the *stereochemical uniformity rule*, that has been developed and justified in the preceding chapter and applied to maitotoxin in this, could prove valuable in the future assignment of new polyether ladders, and may have uncovered a very important structural misassignment in the largest known non-polymeric natural product.

a)

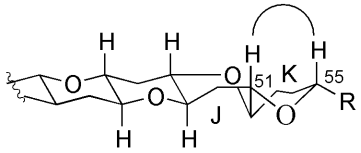

NOE between C51 and C55 protons

b)

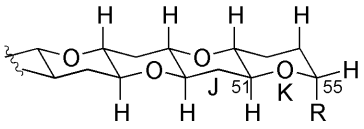

No NOE expected with alternative structure
(assuming stereochemistry at C55 assigned correctly)

c)

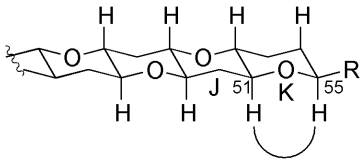

NOE expected with alternative assignment at C55

Figure 8.8 a) Assigned structure at J/K ring junction; b) Structure obtained by simply flipping J/K ring junction; c) Speculative alternative structure by additionally flipping configuration at C55 (additional functionality omitted for clarity).

*It appears that maitotoxin's size record (but not toxicity) has now been beaten, by a new polyketide isolated from a newly recognised species of dinoflagellate, *Gambierdiscus yasumotoi*. "GYC" has a molecular weight of 4,820Da, which is more than 1,400Da larger than maitotoxin. So far, only preliminary structural studies have been carried out[130], but it is thought to have a palytoxin-like polyhydroxy structure, whilst also containing a number of fused polyether rings and a sulphate group, reminiscent of maitotoxin[131].

Chapter Nine

Materials and Methods

All NMR studies were carried out on a Bruker Biospin Avance 700MHz.

1. Culture Media for *S. cinnamonensis* ATCC15413 and A516 (Bulgarian over-producer)

TSB

Tryptic soy broth powder was dissolved in MilliQ water at a rate of 30g per litre and gently warmed to aid dissolution. The solution was autoclaved prior to use.

SM16-1

Dissolved in MilliQ water in order:

MOPS free acid	20.9g
L-proline	10g
Glucose	20g
NaCl	0.5g
K_2HPO_4	2.1g
EDTA	0.25g
$MgSO_4.7H_2O$	0.49g
$CaCl_2.2H_2O$	0.029g
10x Trace elements No.1	1ml
MilliQ Water	to 1 litre

- pH adjusted to 7.0 with NaOH

autoclave prior to use

10x Trace elements No.1

Dissolved in MilliQ water in order:

1M H_2SO_4	10ml
$ZnSO_4.H_2O$	8.6g
$MnSO_4.4H_2O$	2.23g

H_3BO_3	0.62g
$CuSO_4.5H_2O$	1.25g
$Na_2MoO_4.2H_2O$	0.48g
$CoCl_2.6H_2O$	0.48g
$FeSO_4.7H_2O$	18.0g
Potassium Iodide	0.83g
MilliQ Water	to 1 litre

- autoclave prior to use.

Bulgarian Proprietary Germinative Medium for *S. cinnamonensis* A519

Soya Flour	7.5g
Dry yeast	0.75g
Glucose	2.5g
Calcium carbonate ($CaCO_3$)	0.5g
Dextrin	10g
MilliQ water	to 500ml

Soya flour and yeast heated in solution at 70°c for 30min and then remaining ingredients added. pH adjusted to 6.4 with NaOH before autoclaving.

Bulgarian Proprietary Production Medium for *S. cinnamonensis* A519

Glucose	20g
Soya flour	33g
Methyloleate	9.25g (10.7ml)
Calcium carbonate	2g
Sodium sulphate anhydrous	2.15g
Sodium nitrate	2.2g
Manganese II chloride	0.33g
Iron II sulphate	0.11g
1-Ascorbic acid	0.019g
Aluminium sulphate	0.705g
Potassium phosphate dibasic	0.075g

Silicon A (Antifoam)	0.2g
MilliQ water	to 1 litre

pH adjusted to 6.6-6.9 with NaOH before autoclaving.

2. General Methods.

2.1 Growth of *Streptomyces cinnamonensis* ATCC15413, A516 and their mutants.

In SM16-1.

A stock mycelium suspension (10µl) [stored at -80°c, 20% glycerol] was used as an inoculum for a 10ml TSB seed culture and grown at 30°c, 200rpm for 2 days. 2.5ml of this culture was then used as a 5% (by volume) inoculum for a 50ml SM16-1 production culture in a 250ml flask with springs. This was grown under the same conditions for 5 days and the cell harvested by centrifugation at 7,500g for 40mins.

Larger, 500ml cultures were grown under identical conditions in 2 litre flasks.

According to Bulgarian Proprietary Method.

Seed cultures of wild type or mutant *Streptomyces cinnamonensis*, were grown in tryptic soy broth medium in flasks fitted with springs at 30°C, 200 rpm for 24 hr. These cultures (2.5 ml) were then used to inoculate 25 ml of the Bulgarian germinative medium (Professor I. Agayn, personal communication) or in a 250 ml Erlenmeyer flask and grown at 32°C and 200 rpm for 24-48 hr. From these seed cultures, each 2.5 ml portion was used to inoculate 40 ml of the Bulgarian production medium in a 250 ml Erlenmeyer flask. The cultures were grown at 32°C, 200 rpm for 12 days. The relative humidity was maintained at 90%. Flasks were weighed before the start of fermentation and any loss by evaporation was compensated with sterile water.

2.2 General Extraction Procedures.

From cultures grown in SM16-1 medium.

Culture broths were centrifuged at 7,500rpm for 45mins and the supernatant separated and extracted twice with an equal volume of ethyl acetate. The organic phase was dried over magnesium sulphate, and the solvent removed *in vacuo*. The residue was then redissolved in minimal ethyl acetate and flushed through a short silica column, packed with ethyl acetate, to remove polar metabolites, and the solvent removed *in vacuo*. A sample of the crude extract thus obtained was dissolved in HPLC-grade methanol and analysed by LCMS before commencing further purification.

From cultures grown according to Bulgarian proprietary method.

Culture broths were centrifuged at 7,500rpm for 45mins and the supernatant separated and extracted twice with an equal volume of ethyl acetate. The organic phase was dried over magnesium sulphate, and the solvent removed *in vacuo*. The residue was then re-dissolved in excess hexane and shaken vigorously with an equal volume of methanol:water (75:25). This mixture was then centrifuged at 7,500rpm for 30mins and the methanolic layer removed. This was repeated twice with fresh methanol:water. The combined methanolic fractions were evaporated, as far as possible *in vacuo*, and then lyophilised to dryness. A sample of the crude extract thus obtained was dissolved in HPLC-grade methanol and analysed by LCMS before commencing further purification.

2.3 HPLC-MS Analysis of Extracts

Analysis of all extracts was carried out principally by HPLC-MS. All extracts were analysed on a Phenomenex Prodigy 5µm ODS3 100Å column (250 x 4.6mm). The solvent gradient program is detailed below:

Solvent A = 20mM Ammonium acetate in water
Solvent B = HPLC-grade methanol

Time	Composition
0	A=20%, B=80%
25mins	A=0%, B=100%
30mins	A=20%, B=80%

- flow rate was set at 1ml/min.

2.4 Preparatory HPLC Purification of Metabolites

Extracts purified as far as possible by silica column chromatography (up to ~20mg) were dissolved in HPLC grade methanol (1.5ml) and loaded onto a Phenomenex Luna 10µm C18(2) column (2120 x 250mm) and eluted utilising the same solvent system and gradient as detailed above. However, the flow rate was set at 15ml/min. Fractions were collected at 30 second intervals using an automatic fraction collector. Fractions were analysed, initially, by direct injection into mass spectrometer to identify required masses and the relevant fractions analysed via the HPLC column, as above, to observe purity. The relevant fractions were then evaporated *in vacuo* and resuspended in water. The product was then desalted (to remove ammonium acetate) using an 'Isolute C18(EC) 500mg' cartridge (obtained from Jones Chromatography Ltd, UK).

3. Specific Methodology

3.1 Creation of monB-null Mutants in Bulgarian Over-producing Strain

The method employed here was identical to that used by Dr. A. Bhatt, and is detailed in PF Leadlay *et al* 2001[24]. Samples of Dr. Bhatt's own plasmid constructs were used.

3.2 Purification of C3-O-demethylmonensin A

S. cinnamonensis ΔBII cultures (3x50ml), grown according to the Bulgarian protocol, were directly extracted (without centrifugation) with ethyl acetate (3x150ml), and the organic phase dried over magnesium sulphate and the solvent removed in vacuo. The oily black residue (~4.5g) was resuspended in hexane (100ml). This was shaken vigorously with MeOH:H2O (3:1) (200ml) and the mixture centrifuged at 10,000rpm for 10mins. The methanolic lower phase was removed and the organic phase re-extracted. The combined methanolic fractions were evaporated as far as possible in vacuo and the aqueous residue lyophilised to dryness, to yield to brown powder (150mg). A

silica column (35x100mm) was packed with ethylacetate (5% MeOH):dichloromethane (2:1), and the crude extract dissolved in minimal volume of this solvent system and loaded. Fifteen fractions (25ml) were taken and 100μL aliquots analysed by LCMS. Fractions 9-12 contained the desired metabolite with mass 679.5. These fractions were combined and the solvent removed *in vacuo*. The semi-pure extract was dissolved in 1.5ml MeOH and purified by preparatory HPLC as described in 2.4. After the relevant fractions were desalted, a pure sample of demethylmonensin A (~100μg) was obtained as a white powder, and analysed by NMR (1D-^{1}H, COSY, HSQC, NOESY).

3.3 Purification of C9-*epi*-monensin A

Cultures of *S. cinnamonensis* ΔBII [Bulgarian Strain A519] (30x40ml), were directly extracted with ethyl acetate (3x800 ml) and the combined organic fractions evaporated *in vacuo*. The residue was re-dissolved in hexane (250ml) and shaken vigorously with an equal volume of methanol:water (75:25 v/v). This mixture was then centrifuged at 7,500 x *g* for 30 min and the methanolic layer was removed. This was repeated twice with fresh methanol:water. The combined methanolic fractions were evaporated *in vacuo* and then lyophilised. The black oily residue (~10g) was dissolved in minimal ethyl acetate and passed twice through a silica column (35 x 100 mm) eluted with ethyl acetate:methanol (95:5). The solvent was removed *in vacuo* and the residue was re-dissolved in minimal ethyl acetate and loaded onto a silica column (35 x110 mm) packed in ethyl acetate (containing 5% methanol (v/v):dichloromethane (2:1 v/v) and eluted with the same solvent mixture. Eight small fractions were taken (25ml), followed by five larger fractions (50ml) and, finally, two large (150ml) fractions. 100uL aliquots were directly injected in the mass spectrometer and those containing the product with mass 693.5 (fractions 5-9) were combined and evaporated *in vacuo* to yield a light brown oily residue (2.5g). This sample was then further purified through silica using the same method as in the previous step, but with 25 fractions (18ml) being taken. The relevant fractions, 13-17, from MS analysis, were pooled and the solvent removed. The sample was then redissolved in methanol (1.5 ml) and purified by preparative HPLC as described in 2.4. Isomonensin A12 was obtained cleanly in fractions 11 and 12 from the preparatory HPLC, and

isomonensin A16 in fraction 16. After desalting, isomonensin A12 was obtained as a white powder (250μg) and isomonensin A16 also as a white powder (100μg). 1H-NMR was obtained on both species: 1D, COSY, HSQC, NOESY. Isomonensin A12 converted to A16 and thus NMR data was unclear. Isomonensin A16 NMR data was clean, and all of the above experiments could be performed at 700MHz before signs of degradation were observed, precluding further experiments.

3.4 Epimerisation of C9-*epi*-monensin A.

A sample of *epi*-monensin A (~5-10 μg) was dissolved in acetonitrile (1 ml). One drop of 48% aqueous hydrofluoric acid was added and the reaction mixture was stirred at room temperature for 2 hr. The reaction mixture was adjusted to ~pH 9 with aqueous sodium hydroxide (1 M) and the acetonitrile was removed *in vacuo*. The aqueous residue was extracted twice with ethyl acetate (1.5 ml), the organic extracts were combined and dried over anhydrous $MgSO_4$, and the solvent removed. The sample was dissolved in HPLC grade methanol (200 μl) and analysed by LC-MS.

3.5 Cyclisation of intermediates obtained from cultures of *S. cinnamonensis monB* mutants.

An SM16-1 *S. cinnamonensis* ΔBII (50ml) culture was extracted twice with ethyl acetate (50 ml) and the combined fractions were dried and then evaporated *in vacuo.* The crude product was adsorbed to a plug of silica, eluted with ethyl acetate and the dried product was re-dissolved in methanol (100μL). The extract was analysed by LC-MS and the early-eluting (3-8mins) polar metabolites were collected separately. These were dried, re-dissolved in acetonitrile and treated with hydrofluoric acid, as described for the epimerisation of *epi*-monensin A.

3.6 High-resolution mass spectrometric analysis of *epi*-monensin A.

Accurate mass analyses were performed on a BioApex II (4.7 Tesla) Fourier-transform cyclotron resonance instrument (Bruker Daltonics, Billerica, USA). Solutions were infused from the Analytica ESI source at 100 μl min^{-1}. CID

fragmentation was performed on the isolated ions with CO_2 as the collision gas.

3.7 In-Frame Deletion of 33 Amino Acid Residues from *monKR11.*

3.7.1 Construction of delivery plasmid pARGΔKR11.

Primers lkr1 [5'-GCCATGACCATCTAGATCACACCGGCGACACCGG-3'] and lkr2 [5'-GTTGCCCATATGGGCGTTCGTGATGTTCTCGTCGGGCGCA-3'] were used to amplify a 1.85 kbp *Xba*I-*Nde*I fragment flanking the chromosomal region to the left of *monKR11.* Primers rkr3 [5'-CGAGACATATGTAGTTCGGCACGCCGGCCGCGTGGATG-3'] and rkr4 [5'-ACGCGCTTCGTAAGCTTCAAGGGCACGGCGACATGGCCTC-3'] were used to amplify a 1.85 kbp *Nde*I-*Hind*III fragment flanking the chromosomal region to the right of *monKR11*. Both fragments were PCR-amplified using *Pfu* polymerase, from a cosmid clone and ligated individually into pBluescriptII KS+ for sequence analysis. Fragments with the correct sequence were excised with their appropriate restriction enzymes and both ligated, together, into *Xba*I and *Hind*III digested pKC1139[132], a shuttle vector containing an apramycin resistance gene and the temperature-sensitive *Streptomyces* origin of replication from pSG5, to produce partial in-frame gene deletion plasmid pARGΔKR11, containing a 3.7kbp fragment spanning *monKR11*, with 33aa residues deleted.

3.7.2 Conjugation and Mutant Selection.

Delivery vector, pARGΔKR11, was introduced into *S. cinnamonensis* [Bulgarian Strain A519] ΔBII by conjugation with *E. coli* ET12567/pUZ8002[133] transformed with pARGΔKR11 by electroporation. Standard conjugation procedures were utilised as described in Kieser 2000. Apr^R transconjugants were picked, patched onto apramycin plates and cultivated at 40ºC (the non-permissive temperature for the pSG5-based replicon). Thus, only single-crossover mutants, in which pARGΔKR11 had integrated into the chromosome, would produce colonies. One of these Apr^R colonies was picked into TSB (5ml) and cultivated over 12 rounds of propagation, in order to allow for the second crossover to occur. Serial

dilutions of the final culture were plated without antibiotics and grown at 30ºC. 96 colonies were picked and patched, in parallel, onto antibiotic-free plates and Apr-containing plates. Putative 2nd crossover mutants were selected as being Apr^S, indicating excision of pARGΔKR11. Seven such putative mutants were obtained and cultivated under standard SM16-1 production conditions. Five of the selected had reverted to the original ΔBII mutant, and two mutants, *S. cinnamonensis* A519 [ΔBII, ΔKR11], were obtained. Genomic DNA was purified from these mutants and, using primers designed each side of the putative deletion site, the deletion was confirmed by analytical PCR.

3.8 Site-directed Mutagenesis of *monKR11*

3.8.1 Construction of mutant delivery plasmid pKR11Y150F

The QuikChange II Mutagenesis kit (obtained from Stratagene, UK) was utilised according to the manufacturer's instructions. Primers kr111 [5'-GCTCTCCGGATCCGGGTCGTACAGCGTCTCCAGG-3'] and kr112 [5'-CGCCTTCTAGAACAAGCACTACTGGGTGGAGCCGCC-3'] were used to clone a 2.2kbp *Bam*HI-*Xba*I chromosomal fragment of *S. cinnamonensis* [Bulg. Str. A519] ΔBII, spanning *monKR11*, using PCR-amplification with *Pfu* polymerase with a cloned cosmid template. This was digested appropriately and ligated into pUC19 for sequencing. (N.B. Owing to the large size of the fragment, a sequencing primer was designed to sequence the central section). A clone with the correct sequence was selected for mutant strand synthesis. Primers kr113 [5'-CCAGCAGGGCGCC{TTC}GGTGCGGCCAACCACTTCCTCGACG-3'] and kr114 [5'-CGTCGAGGAAGTGGTTGGCCGCACC{GAA}GGCGCCCTGCTGG-3'], with the latter being the reverse complement of the former and the Tyr→Phe mutation indicated in brackets, were used to amplify the clone, using *Pfu*-Turbo. The methylated, template DNA was then digested with *Dpn*I for 3 hours. The XL-10 Gold Ultracompetent Cells (supplied with the kit) were then transformed with this mixture, plated onto 2TY plates [with carbenicillin, XGal, IPTG, for Blue/White selection] and grown overnight at 37ºC. White colonies were picked into 2TY medium, grown overnight at 37ºC, and the

DNA purified for sequencing. A clone containing the desired mutation was selected, and the BamHI-XbaI mutant fragment excised and ligated into pKC1139, as in 3.7.1., to produce mutant delivery plasmid pKR11Y150F.

3.8.2 Conjugation and Mutant Selection.

The method used here was identical to that used for the in-frame deletion (detailed in 3.7.2) and, thus, will not be repeated. Three putative mutants were obtained. To confirm the mutations, primers were designed each side of the putative site of mutation, and the 0.5kbp *Bam*HI-*Nde*I fragment cloned from the genomic DNA by PCR, and ligated into pBluescriptII KS+ for sequence analysis.

4. Mass Spectrometry of Putative Triepoxides

All low-resolution studies were carried out by according to the normal LCMS method (2.3), with specific MS programs created as necessary.

High-resolution studies were carried out by direct infusion into a 'Finnigan LTQ Orbitrap™ Hybrid Mass Spectrometer'.

5. Retrobiosynthetic Analyses

All chemical structures were created with, and their stereochemistry checked by, *CS ChemDraw Ultra* Version 6.0.

Appendix

Table A1 ^{1}H NMR Chemical Shifts for C9-*epi*-monensin A in $CDCl_3$

Position	δ ppm	Position	δ ppm
1	-	21	3.88
2	2.62	22	1.43
3	3.99	23	1.45
4	2.02	24	1.48
5	4.67*	25	-
6	2.22	26	3.29, 4.10
7	3.88	2’	1.22
8	1.73, 1.94	4’	0.84
9	-	6’	0.95
10	1.73, 2.12	12’	1.49
11	2.16, 2.34	16’	1.51, 1.58
12	-	16’’	0.92
13	3.60	18’	0.90
14	1.62, 1.85	22’	0.81
15	1.43, 2.25	24’	0.96
16	-	C3-OMe	3.49
17	3.93		
18	2.27		
19	1.50, 1.69		
20	4.42		
	*Monensin A 4.02		

Table A2 ^{13}C-NMR Chemical Shifts for C9-*epi*-monensin A in $CDCl_3$

Position	δ ppm	Position	δ ppm
1	Not determined	21	74.5
2	42.0	22	Not determined
3	75.5	23	Not determined
4	38.5	24	Not determined
5	65.0	25	Not determined
6	35.0	26	65.5
7	71.0	2’	7.5
8	32.5	4’	11.5
9	Not determined	6’	12.0
10	39.0	12’	Not determined
11	32.5	16’	Not determined
12	Not determined	16’’	7.5
13	82.0	18’	13.0
14	26.0	22’	16.5
15	29.0	24’	16.0
16	Not determined	C3-OMe	50.5
17	84.5		
18	34.5		
19	34.0		
20	76.0		

Carbon shifts were determined solely from HSQC experiments. Those labelled “Not determined” are either quarternary carbons or unclear in the spectrum.

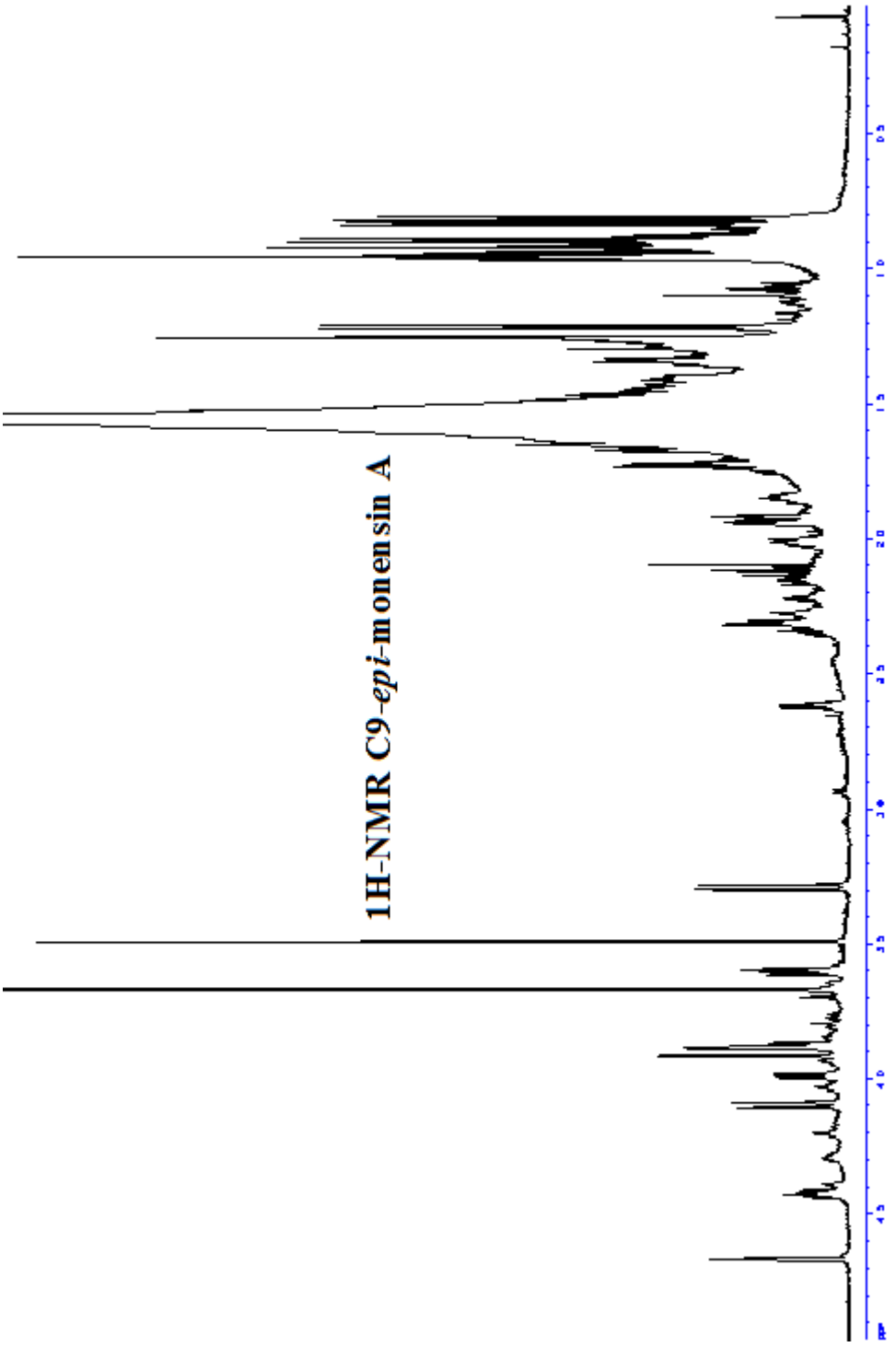

Figure A1 ^{1}H-NMR of C9-*epi*-monensin A

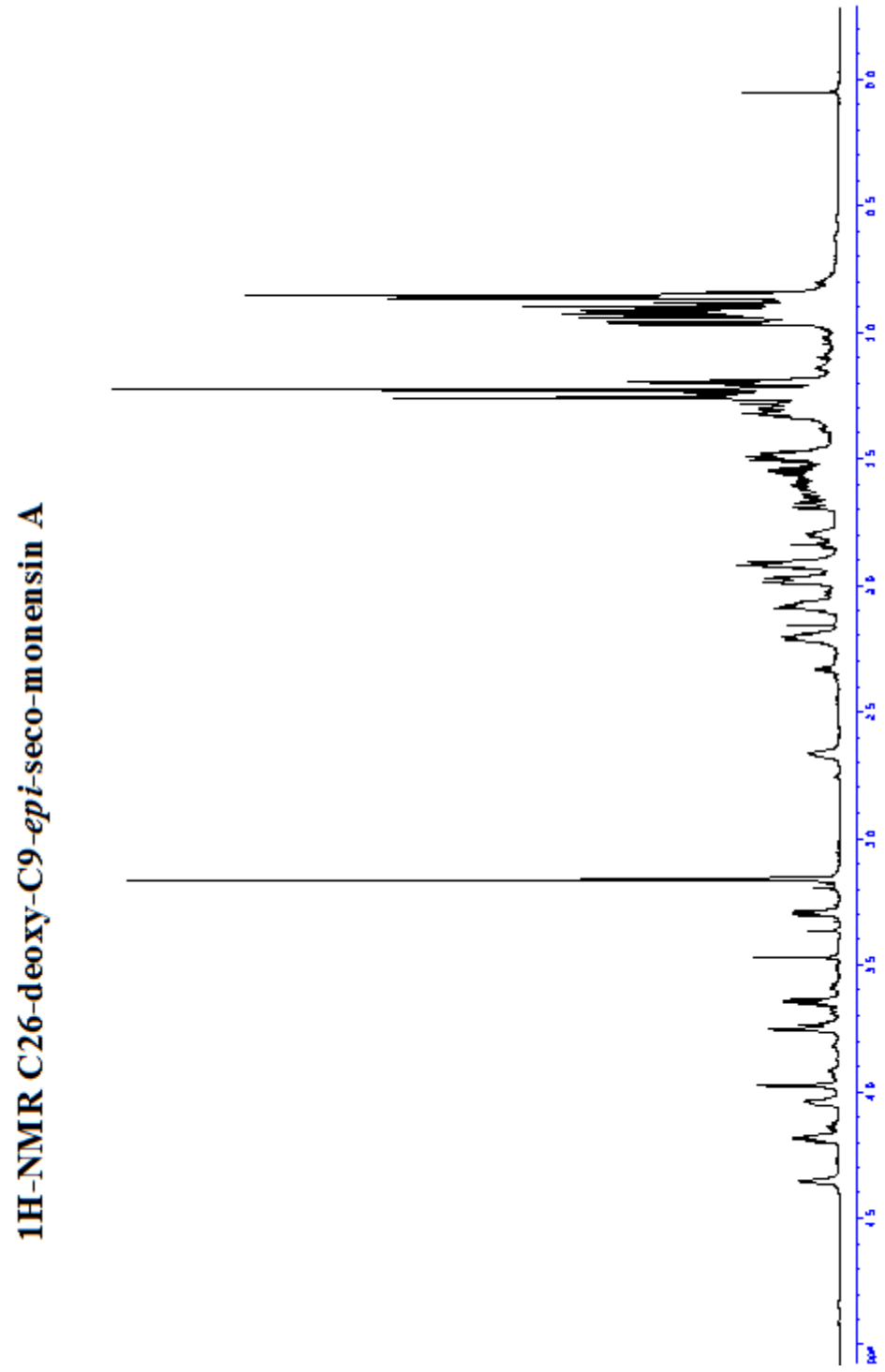

Figure A2 [1]H-NMR of open E-ring analogue of C9-*epi*-monensin A

References.

1. T. Yasumoto, *Chem. Rec*. **2001**, *1*(3), 228
2. S. Smith, *Faseb J*. **1994**, *8*(15), 1248
3. J. Staunton, K.J. Weissman, *Nat. Prod. Rep*. **2001**, *18*, 380
4. B.S. Moore, C. Hertweck, *Nat. Prod. Rep.* **2002**, *19*(1), 70
5. O. Ghisalba, H. Fuhrer, W.J. Richter, S. Moss, *J. Antibiot.* **1981**, *34*(1), 58
6. a) J. Cortes, S.F. Haydock, G.A. Roberts, D.J. Bevitt, P.F. Leadlay, *Nature* **1990**, *348*(6297), 176; b) S. Donadio, M.J. Staver, J.B. McAlpine, S.J. Swanson, L. Katz, *Science* **1991**, *252*(5006), 675; c) S. Donadio, L. Katz, *Gene* **1992**, *111*(1), 51
7. C.J. Dutton, B.J. Banks, C.B. Cooper, *Nat. Prod. Rep.* **1995**, *12*(2), 165
8. B.C. Pressman, *Ann. Rev. Biochem*. **1976**, *45*, 501
9. a) F.A.A. Paz, P.J. Gates, D.J. Fowler, A.R. Gallimore, B.M. Harvey, N.P. Lopes, C.B.W. Stark, J. Staunton, J. Klinowski, J.B. Spencer, *Acta Crystal. - Sec. E*, **2003**, *59*(11), M1050-M1052; b) W.L. Duax, G.D. Smith, P.D. Strong, *J. Am. Chem. Soc.* **1980**, *102*(22), 6725; c)W.K. Lutz, F.K. Winkler, J.D. Dunitz, *Helv. Chim. Acta*. **1971**, *54*(4), 1103
10. B.C. Pressman, M. Fahim, *Ann. Rev. Pharmacol. Toxicol*. **1982**, *22*, 465
11. J.B. Russell, A.J. Houlihan, *FEMS Microbiol. Rev*. **2003**, *27*, 65
12. a) P. Story, A. Doube, *New Zealand Medical Journal*, **2004**, *117*(1190); b)N. Sharma, A. Bhalla, S. Varma, S. Jain, S. Singh, *Emergency Medicine J*. **2005**, *22*(12), 880
13. W.H. Park, E.S. Kim, B.K. Kim, Y.Y. Lee, *Int. J. Oncol*. **2003**, *23*(1), 197
14. M.S. Shaik, O. Ikediobi, V.D. Turnage, J. McSween, N. Kanikkannan, M. Singh, *J Pharm Pharmacol*. **2001**, *53*(5), 617
15. A. Agtarap, J.W. Chamberlin, M. Pinkerton, T. Steinrauf, *J. Am. Chem. Soc.* **1967**, *89*(22), 5737
16. LE Day, JW Chamberlin, EZ Gordee, S Chen, M Gorman, RL Hamill, T Ness, RE Weeks, R Stroshane, *Antimicrob. Agents. Chemother*. **1973**, *4*, 410
17. G.R. Sood, J.A. Robinson, A.A. Ajaz, *J. Chem. Soc. Chem. Comm.* **1984**, *21*, 1421
18. a) AA Ajaz, JA Robinson, *Chem. Comm.* **1983**, *12*, 679; b) AA Ajaz, JA Robinson, DL Turner, *J. Chem. Soc. Perkin. Trans. I* **1987**, *27*

19. J.W. Westley, R.H. Evans, G. Harvey, R.G. Pitcher, D.L. Pruess, *J. Antibiotics* **1974**, *27*, 288
20. DE Cane, WD Celmer, JW Westley*, J. Am. Chem. Soc*. **1983**, *105*, 3594
21. C.A. Townsend, A. Basak, *Tetrahedron*, **1991**, *47*(14/15), 2591
22. Z.A. Hughes-Thomas, C.B.W. Stark, I.U. Bohm, J. Staunton, P.F. Leadlay, *Angew. Chemie. Int. Ed. Eng.* **2003**, *42*(37), 4475
23. P.F. Leadlay, J. Staunton, M. Oliynyk, C. Bisang, J. Cortes, E. Frost, Z.A Hughes-Thomas, M.A. Jones, S.G. Kendrew, J.B. Lester, P.F. Long, H.A.I McArthur, E.L McCormick, Z Oliynyk, CBW Stark, CJ Wilkinson, *J. Ind. Microbiol. Biotech*. 2001, 27, 360
24. a) M.L. Heathcote, J. Staunton, P.F. Leadlay, Chem. Biol. 2001, 8(2), 207; b) B.S. Kim, T.A. Cropp, B.J. Beck, D.H. Sherman, K.A. Reynolds, *J. Biol. Chem*. **2002**, *277*(50), 48028
25. A.R. Gallimore, **2004** *unpublished data*
26. M.A. Jones, *Postdoctoral Report I*, Dept. of Biochemistry, University of Cambridge, **2000**
27. Z.A. Hughes-Thomas, *PhD Thesis*, University of Cambridge, **2002**
28. A. Kuliopulos, G.P. Mullen, L. Xue, A.S. Mildvan*, Biochemistry*, **1991**, *30*, 3169
29. a) SW Kim, S Cha, H Cho, J Kim, N Ha, M Cho, S Joo, KK Kim, KY Choi, B Oh, *Biochemistry,* **1997**, *36*, 14030-14036; b) H Cho, G Choi, KY Choi, B Oh*, Biochemistry*, **1998**, *37*, 8325-8330
30. CM Holman, WF Benisek, *Biochemistry*, **1995**, *34*, 14245-14253
31. a) Z.R. Wu, S. Ebrahimian, M.E. Zawrotny, L.D. Thornburg, G.C. Perez-Alvarado, P. Brothers, R.M. Pollack, M.F. Summers, *Science*, **1997**, *276*, 415-418; b)L.D. Thornburg, F. Hénot, D.P. Bash, D.C. Hawkinson, S.D. Bartel, R.M. Pollack, *Biochemistry*, **1998**, *37*, 10499
32. G. Müller-Newen, W. Stoffel, *Biochemistry*, **1993**, *32*, 11405
33. J. Kennedy, K. Auclair, S.G. Kendrew, C. Park, J.C. Vederas, Hutchinson CR, *Science* **1999**, *284*(5418), 1368
34. D.S. Holmes, J.A. Sherrigham, U.C. Dyer, S.T. Russell, J.A. Robinson, *Helv. Chim. Acta* **1990,** *73*(2), 239

35. A. Bhatt, C.B.W. Stark, B.M. Harvey, A.R. Gallimore, Y.A. Demydchuk, J.B. Spencer, J. Staunton, P.F. Leadlay, *Angew. Chem. Int. Ed. Eng*. **2005**, *44*(43), 7075
36. A. Bhatt*, Postdoctoral report*, Dept. of Biochemistry, University of Cambridge, **2002**.
37. a) N.P. Lopes, C.B.W. Stark, H. Hong, P.J. Gates, J. Staunton, *Rap. Comm. Mass. Spec*. **2002**, *16*(5), 414; b)N.P. Lopes, C.B.W. Stark, P.J. Gates**,** J. Staunton, *Analyst*, **2002**, *127*(4), 503
38. S. Pospisil, P. Sedmera, J. Vokoun, Z. Vanek, M. Budesinsky, *J. Antibiot*. **1987**, *40*(4), 555
39. P.J. Gates, University of Bristol, UK, *personal communication*
40. a) AA Ajaz, JA Robinson, DL Turner, *J. Chem. Soc. Perkin. Trans. I* **1987**, 27; b)J.A. Robinson, D.L. Turner, *J. Chem. Soc, Chem. Comm*. **1982**, *3*, 148; c)A. Nagatsu, R. Tanaka**,** H. Mizukami, Y. Ogihara, J. Sakakibara,, *Tetrahedron* **2001**, 57(16), 3369
41. F. Perron, K.F. Albizati, *Chem. Rev*. **1989**, *89*, 1617
42. R.E. Ireland, D. Häbich, , D.W. Norbeck, *J. Am. Chem. Soc*. **1985**, *107*(11), 3271
43. M. Hebrant, Y. Pointud, J. Juillard, *J. Phys. Chem*. **1991**, *95*(9), 3653
44. J.E. Baldwin, *J. Chem. Soc. Chem. Comm.* **1976**, *11*, 734
45. a) I. Paterson, I. Boddy, I. Mason, *Tetrahedron Lett*. **1987**, *28*, 5205; b) S. Schreiber, T. Sammakai, B. Hulin, G. Schulte, *J. Am. Chem. Soc*. **1986**, *108*, 2106
46. H. Kinashi, N. Otake, H. Yonehara, S. Sato, Y. Saito, *Tet. Lett*. **1973**, *14*(49), 4955
47. J.W. Westley, J.F. Blount, R.H. Evans, C.M. Liu, *J. Antibiot*. **1977**, *30*(7), 610
48. B.M. Harvey, M.A. Jones, Z.A. Hughes-Thomas, R.M. Goss, M.L. Heathcote, V.M. Bolanos-Garcia, W. Kroutil, J. Staunton, P.F. Leadlay, *ChemBioChem*, **2005,** accepted
49. Y. Sun, X. Zhou, H. Dong, G. Tu, M. Wang, B. Wang, Z. Deng, *Chem. Biol*. **2003**, *10*(5), 431
50. T.L. Bullock, W.D. Clarkson, H.M. Kent, M. Stewart, *J. Mol. Biol*. **1996**, *260*(3), 422

51. T. Lundqvist, J. Rice, C.N. Hodge, G.S. Basarab, J. Pierce, Y. Lindqvist, *Structure*, **1994**, *2*(10), 937
52. M. Arand, B.M. Hallberg, J. Zou, T. Bergfors, F. Oesch, J. van der Werf, J.A.M. de Bont, T.A. Jones, S.L. Mowbray, *EMBO J.* **2003**, *22*(11), 2583
53. E.J. De Vries, D.B. Janssen, *Curr. Opin. Biotech*. **2003**, *14*, 414
54. a) R.N. Armstrong, *CRC Crit. Rev. Biochem.* **1987**, *22*, 39; b)M.A. Argiriadi, C. Morisseau, B.D. Hammock, D.W. Christianson, *Proc. Nat. Acad. Sci. USA* **1999**, *96*, 10637
55. M. Arand, A. Cronin, F. Oesch, S.L. Mowbray, T.A. Jones, *Drug Metab. Rev*. **1993**, *35*(4), 365
56. K.H. Hopmann, B.M. Hallberg, F. Himo, *J. Am. Chem. Soc.* **2005**, *127*(41), 14339
57. S. Donaldio, M.J. Staver, J.B. McAlpine, S.J. Swanson, L. Katz, *Science* **1991**, *252*, 675
58. R. Reid, M. Piagentini, E. Rodriguez, G. Ashley, N. Viswanathan, J. Carney, D.V. Santi, C.R. Hutchinson, R. McDaniel, *Biochemistry* **2003**, *42*(1), 72
59. L. Tang, L. Chung, J.R. Carney, C.M. Starks, P. Licari, L. Katz, *J. Antibiot*. **2005**, *58*(3), 178
60. a) A. Baerga-Ortiz, B. Popovic, A.P. Siskos, H.M. O'Hare, D. Spiteller, M.G. Williams, N. Campillo, J.B. Spencer, P.F. Leadlay, *Chem. Biol*. **2006**, *13*(3), 277; b)H.M. O'Hare, A. Baerga-Ortiz, B. Popovic, J.B. Spencer, P.F. Leadlay, *Chem. Biol*. **2006**, *13*(3), 287
61. M. Bierman, R. Logan, K. O'Brien, E.T. Seno, R.N. Rao, B.E. Schoner, *Gene* **1992**, *116*(1), 43
62. G. Muth, B. Nussbaumer, W. Wohlleben, A. Puhler, *Mol. Gener. Gen*. **1989**, *219*(3), 341
63. M.L. Souto, C.P. Manriquez, M. Norte, J.J. Fernandez, *Tetrahedron* **2002**, *58*, 8119
64. Y. Shimizu, H.-N. Chou, H. Bando, G. Van Duyne, J.C. Clardy, *J. A. Chem. Soc.* **1986**, *108*, 514
65. Y.Y. Lin, M. Risk, S.M. Ray, D. VanEngen, J. Clardy, J. Golik, J.C. James, K. Nakanishi, *J. Am. Chem. Soc*. **1981**, *103*, 6773
66. Y. Shimizu, *Pure Appl. Chem*. **1982**, *54*, 1973
67. T. Yasumoto, *Proc. Japan Acad. Ser. B*. **2005**, *81*(2), 43

68. B. Kirkpatrick, L.E. Fleming, D. Squicciarini, L.C. Backer, R. Clark, W. Abraham, J. Benson, Y.S. Cheng, D. Johnson, R. Pierce, J. Zaias, G.D. Bossart, D.G. Baden, *Harmful Algae* **2004**, *3*, 99
69. W.A. Catterall, *Physiol. Rev*. **1992**, *72*, S15
70. S-H. Wang, G.K. Wang, *Cell. Signal*. **2003**, *15*, 151
71. M.A. Poli, S.M. Musser, R.W. Dickey, P.P. Eilers, S. Hall, *Toxicon* **2000**, *38*, 981
72. T. Yasumoto, I. Nakajima, R. Bagnis, R. Adachi, *Jpn. Soc. Sci. Fish* **1977**, *43*, 1021
73. T. Yasumoto, *Proc. Japan Acad Ser. B* **2005**, *81*(2), 43
74. a) M. Murata, A.M. Legrand, T. Yasumoto, *Tet. Lett*. **1989**, *30*(29), 3793; b) M. Murata, A.M. Legrand, Y. Ishibashi, T. Yasumoto, *J. Am. Chem. Soc*. **1989**, *111*(24), 8929; c) M. Satake, A. Morohashi, H. Oguri, T. Oishi, M. Hirama, N. Harada, T. Yasumoto, *J. Am. Chem. Soc.* **1997**, *119*, 11325
75. M. Satake, M. Murata, T. Yasumoto, *Tet. Lett*. **1993**, *34*(12), 1975
76. R.J.Lewis, J. Vernoux, I.M. Brereton, *J. Am. Chem. Soc*. **1998**, *120*, 5914
77. T. Yasumoto, T. Igarashi, A.-M. Legrand, P.Cruchet, M. Chinain, T. Fujita, H. Naoki, *J. Am. Chem. Soc*. **2000**, *122*, 4988
78. R.J. Lewis, M. Sellin, M.A. Poli, R.S. Norton, J.K. MacLeod, M.M. Sheil, *Toxicon* **1991**, *29*(9), 1115
79. R.C. Hogg, R.J. Lewis, D.J. Adams, *Neurosci. Lett*. **1998**, *252*, 103
80. R.J. Lewis, *Toxicon* **1992**, *30*(2), 207
81. R.E. Gawley, K.S. Rein, G. Jeglitsch, D.J. Adams, E.A. Theodorakis, J. Tiebes, K.C. Nicolau, D.G. Baden, *Chem. Biol*. **1995**, *2*, 533
82. a) D.F. Bocian, H.M. Pickett, T.C. Rounds, H.L. Strauss, *J. Am. Chem. Soc*. **1975**, *97*(4), 687; b) G. Favini, *J. Mol. Struct*. **1983**, *93*, 139
83. R.E. Gawley, K.S. Rein, M. Kinoshita, D.G. Baden, *Toxicon* **1992**, *30*(7), 780
84. K.S. Rein, B. Lynn, R.E. Gawley, D.G. Baden, *J. Org. Chem*. **1994**, *59*, 2107
85. M. Murata, A.-M. Legrand, P.J. Scheuer, T. Yasumoto, *Tet. Lett*. **1992**, *33*(4), 525
86. M.L. Candenas, F.M. Pinto, C.G. Cintado, E.Q. Morales, I. Brouard, M.T. Díaz, M. Rico, E. Rodríguez, R.M. Rodríguez, R. Pérez, R.L. Pérez, J.D. Martín, *Tetrahedron*, **2002**, *58*, 1921

87. H. Nagai, K. Torigoe, M. Satake, M. Murata, T. Yasumoto, *J. Am. Chem. Soc*. **1992**, *114*, 1102

88. H. Nagai, Y. Mikami, K. Yazawa, T. Gonoi, T. Yasumoto, *J. Antibiot*. **1993**, *46*(3), 520

89. A. Morohashi, M. Satake, H. Nagai, Y. Oshima, T. Yasumoto, *Tetrahedron* **2000**, *56*, 8995

90. a) M. Satake, M. Murata, T. Yasumoto, *J. Am. Chem. Soc*. **1993**, *115*, 361; b) A. Morohashi, M. Sataki, T. Yasumoto, *Tet. Lett*. **1998**, *39*, 97

91. a) T. Yasumoto, M. Murata, *Chem. Rev*. **1993**, *93*, 1897; b) M. Ito, F. Suzuki-Toyota, K. Toshimori, H. Fuwa, K. Tachibana, M. Satake, M. Sasaki, *Toxicon*, **2003**, *42*, 733

92. a) M. Murata, M. Kumagai, J.S. Lee, T. Yasumoto, *Tet. Lett*. **1987**, *28*(47), 5869; b) M. Satake, K. Terasawa, Y. Kadowaki, T. Yasumoto, *Tet. Lett*. **1996**, *37*(33), 5955; c) H. Takahashi, T. Kusumi, Y. Kan, M. Satake, T. Yasumoto, *Tet. Lett*. **1996**, *37*(39), 7087

93. K. Eiki, M. Satake, K. Koike, T. Ogata, T. Mitsuya, Y. Oshima, *Fish. Sci*. **2005**, *71*, 633

94. P. Ciminiello, C. Dell'Aversano, E. Fattorusso, M. Forino, S. Magno, F. Guerrini, R. Pistocchi, L. Boni, *Toxicon*, **2003**, *42*, 7

95. M.L. Souto, J.J. Fernández, J.M. Franco, B. Paz, L.V. Gil, M. Norte*, J. Nat. Prod*. **2005**, *68*, 420

96. P. Ciminiello, E. Fattorusso, M. Forino, S. Magno, R. Viviani, *Tet. Lett*. **1998**, *39*, 8897

97. T. Aune, R. Sorby, T. Yasumoto, H. Ramstad, T. Landsverk, *Toxicon*, **2002**, *40*, 77

98. L.A. de la Rosa, A. Alfonso, N. Vilarino, M.R. Vieytes, L.M. Botana, *Biochem. Pharm.* **2001**, *61*, 827

99. L.A. de la Rosa, A. Alfonso, N. Vilarino, M.R. Vieytes, T, Yasumoto, L.M. Botana, *Cell. Signal*. **2001**, *13*, 711

100. A. Alfonso, L.A. de la Rosa, M.R. Vieytes, T, Yasumoto, L.M. Botana, *Biochem. Pharm*. **2003**, *65*, 193

101. A. Perez-Gomez, A. Ferrero-Gutierrez, A. Novelli, J.M. Franco, B. Paz, M.T. Fernandez-Sanchez, *Toxicol. Sci*. **2006**, *90*(1) 68

102. M. Satake, M. Shoji, Y. Oshima, H. Naoki, T. Fujita, T. Yasumoto, *Tet. Lett*. **2002**, *43*, 5829

103. M. Satake, Y. Tanaka, Y. Ishikura, Y. Oshima, H. Naoki, T. Yasumoto, *Tet. Lett*. **2005**, *46*, 3537

104. A.V.K. Prasad, Y. Shimizu, *J. Am. Chem. Soc*. **1989**, *111*, 6476

105. A.J. Bourdelais, S. Campbell, H. Jacocks, J. Naar, J.L.C. Wright, J. Carsi, D.G. Baden, *Cell. Mol. Neurobiol*. **2004**, *24*(4), 553

106. A.R. Gallimore, J.B. Spencer, *Angew. Chem. Int. Ed. Eng*. **2006**, *45*(27), 4406

107. a) H.-N. Chou, Y. Shimizu, *J. Am. Chem .Soc.* **1987**, *109*, 2184 b) M.S. Lee, G,-w Qin, K. Nakanishi, M.G. Zagorski, *J. Am. Chem. Soc.* **1989**, *111*, 6234

108. a) Y. Shimizu, *Natural Toxins: Animal, plant and microbial* (Ed.: J.B. Harris), Clarendon Press, Oxford, **1986**, p. 123; b) K. Nakanishi, *Toxicon* **1985**, *23*, 473

109. a) M. Murata, M. Izumikawa, K. Tachibana, T. Fujita, H. Naoki, *J. Am. Chem. Soc.* **1998**, *120*, 147; b) M. Izumikawa, M. Murata, K. Tachibana, T. Fujita, H. Naoki, *Eur. J. Biochem.* **2000**, *267*, 5179

110. H,-N, Chou, Y. Shimizu, G. Van Duyne, J. Clardy, *Tet. Lett.* **1985**, *26*, 2865

111. U. Koert, *Synthesis* **1995**, 115

112. N. Hayashi, K. Fujiwara, A. Murai, *Tetrahedron* **1997**, *53*(37), 12425

113. a) K.C. Nicolaou, C.V.C. Prasad, P.K. Somers, C.-K. Hwang, *J. Am. Chem. Soc.* **1989**, *111*, 5330; b) K.C. Nicolaou, C.V.C. Prasad, P.K. Somers, C.-K. Hwang, *J. Am. Chem. Soc.* **1989**, *111*, 5335

114. K. Fujiwara, N. Hayashi, T. Tokiwano, A. Murai, *Heterocycles* **1999**, *50*(1), 561

115. J.C. Valentine, F.E. McDonald, W.A. Neiwert, K.I. Hardcastle, *J. Am. Chem. Soc.* **2005**, *127*(13), 4586

116. F.E. McDonald, F. Bravo, X. Wang, X. Wei, M. Toganoh, J.R. Rodriguez, B. Do, W.A. Neiwert, K.I. Hardcastle, *J. Org. Chem.* **2002**, *67*, 2515

117. J. Giner, *J. Org. Chem.* **2005**, *70*, 721

118. L. Tang, S. Ward, L. Chung, J.R. Carney, Y. Li, R. Reid, L. Katz, *J. Am. Chem. Soc.* **2004**, *126*(1), 46

119. A.R. Gallimore, C.B.W. Stark, A. Bhatt, B.M. Harvey, Y. Demudchuk, V. Bolanos-Garcia, D.J. Fowler, J. Staunton, P.F. Leadlay, J.B. Spencer, *Chem. Biol.* **2006**, *13*(4), 453

120. K.D. Janda, C.G. Shevlin, R.A. Lerner, *Science* **1993**, *259*, 490

121. J.W. Westley, J.F. Blount, R.H. Evans, A. Stemple, J. Berger, *J. Antibiot.* **1974**, *27*, 597

122. a) S.B. Freedman, R.J. Miller, D.M. Miller, D.R. Tindall, *Proc. Natl. Acad. Sci. USA* **1984**, *81*(14), 4582; b) V. Morales-Tlalpan, L. Vaca, *Toxicon* **2002**, *40*, 493

123. M. Taglialatela, L.M.T. Canzoniero, A. Fatatis, G.D. Renzo, T. Yasumoto, L. Annunziato*, Biochim. Biophys. Acta* **1990**, *1026*, 126

124. a) M. Murata, T. Iwashita, S. Matsunaga, A. Yokoyama, M. Sasaki, T. Yasumoto*, J. Am. Chem. Soc*. **1992**, *114*, 6594; b) M. Murata, H. Naoki, T. Iwashita, S. Matsunaga, M. Sasaki, A. Yokoyama, T. Yasumoto, *J. Am. Chem. Soc*. **1993**, *115*, 2060

125. M. Murata, H. Naoki, S. Matsunaga, M. Satake, T. Yasumoto, *J. Am. Chem. Chem. Soc.* **1994**, *116*, 7098

126. M. Satake, S. Ishida, T. Yasumoto, M. Murata, H. Utsumi, T. Hinomoto, *J. Am. Chem. Soc*. **1995**, *117*, 7019

127. W. Zheng, J.A. DeMattei, J.-P. Wu, J.J.-W. Duan, L.R. Cook, H. Oinuma, Y. Kishi, J. Am. Chem. *Soc*. **1996**, *118*, 7946

128. a) M. Sasaki, N. Matsumori, T. Maruyama, T. Nonomura, M. Murata, K. Tachibana, T. Yasumoto, *Angew. Chem. Int. Ed. Eng*. **1996**, *35*(15), 1672; b) T. Nonomura, M. Sasaki, N. Matsumori, K. Tachibana, T. Yasumoto, *Angew. Chem. Int. Ed. Eng*. **1996**, *35*(15), 1675

129. K.C. Nicolau, S.A. Snyder*, Angew. Chem. Int. Ed. Eng*. **2005**, *44*, 1012

130. Y. Hayasaka, R. Shimofuri, S. Yamamoto, M. Satake, Y. Oshima*, Abstracts for the Annual Meeting of the Japanese Society of Fisheries Science*, March 31-April 4, **2005**, Tokyo

131. Takeshi Yasumoto, Prof. emeritus, Tohoku Univ. **2005**, *personal communication*

132. T. Kieser, M.J. Bibb, M.J. Buttner, K.F. Chater, D.A. Hopwood, *Practical Streptomyces Genetics*, John Innes Foundation, Norwich, **2000**

133. M.S.B. Paget, L. Chamberlin, A. Atrih, S.J. Foster, M.J. Buttner, *J. Bacteriology* **1999**, *181*, 204